CHALMERS
UNIVERSITY OF TECHNOLOGY

The 200 m timber tower

A study of building geometry and construction feasibility

Master's thesis in Structural Engineering and Building Technology

LIEN TRINH
HONG ZHANG

DEPARTMENT OF ARCHITECTURE AND CIVIL ENGINEERING

CHALMERS UNIVERSITY OF TECHNOLOGY
Gothenburg, Sweden 2021
www.chalmers.se

MASTER'S THESIS ACEX30

The 200 m timber tower

A study of building geometry and construction feasibility

Master's Thesis in Structural Engineering and Building Technology

LIEN TRINH
HONG ZHANG

Department of Architecture and Civil Engineering
Division of Structural Engineering
Research Group for Lightweight Structures
CHALMERS UNIVERSITY OF TECHNOLOGY
Göteborg, Sweden 2021

The 200 m timber tower
A study of building geometry and construction feasibility

Master's Thesis in Structural Engineering

LIEN TRINH

HONG ZHANG

Examensarbete ACEX30
Institutionen för arkitektur och samhällsbyggnadsteknik
Chalmers tekniska högskola, 2021

Department of Architecture and Civil Engineering
Division of Structural Engineering
Research Group for Lightweight Structures
Chalmers University of Technology
SE-412 96 Göteborg
Sweden
Telephone: + 46 (0)31-772 1000

Cover: The design of the 200 m timber tower

Department of Architecture and Civil Engineering
Göteborg, Sweden, 2021

The 200 m timber tower

A study of building geometry and construction feasibility

Master's thesis in Structural Engineering and Building Technology

LIEN TRINH

HONG ZHANG

Department of Architecture and Civil Engineering
Division of Structural Engineering
Research Group for Lightweight Structures
Chalmers University of Technology

ABSTRACT

There are a lot of building materials used in the building sector such as concrete, steel and timber, each with its own advantages and disadvantages. For a long time, timber has not been seen as a common material for advanced structures in civil engineering field and architecture field. With the continuous development of engineered wood products, timber has nowadays become a more common building material used for multi-floor buildings.

The 20th century witnessed a construction boom in tall buildings worldwide. So far, the knowledge of how to build a high-rise building with a timber structure is still limited. The current world's tallest timber building is Mjöstornet in Norway, with a height of 85m, which is only about one-tenth of the world's highest building Burj Khalifa in Dubai.

The main objective of this report is to study and evaluate different building geometries with main concerns about economy, environment aspect and structural performance of a 200m timber building. The building site is assumed to be 30m x 30m and is in Gothenburg with the ground condition of solid rock.

The study divided into two main steps and was mostly performed in Grasshopper and Karamba 3D. In the first step two concepts were selected through an evaluation based on the results of deflection, rental area and building mass of various concepts. In the second evaluation several criterions were added such as dynamic performance, base support force and building mass per rental area ratio to find a promising concept.

The final proposal is a diagrid structure in hyperboloid form and was chosen through comprehensive evaluation. This geometry has significantly better performance regarding dynamic performance compared to all other diagrid structures in convex form and traditional braced frame structure that has been studied, though providing much less rentable areas.

Key words: Acceleration, Aerodynamics, Burj Khalifa, Dynamics, Grasshopper, Karamba3D, Lateral deflection, Mjöstornet, Tall timber buildings, Timber, Timber connections, Rental area, Stiffness, Wind load.

Contents

Preface

The topic of tall buildings and skyscrapers is very popular in the field of architecture and engineering. There is always a demand to research new methods and innovative processes to build taller and more environmentally friendly. As future structural engineers, we would like to contribute what we have investigated to the constant development of the construction industry.

This master thesis is our work in the master's program Structural Engineering and Building Technology during spring term 2021. The project put a focus on the possibility of building a 200m tower in timber and the feasibility of constructing it. The project is being carried out at the research group for Lightweight Structures at the Department of Architecture and Civil Engineering, Chalmers University of Technology, Sweden. Structural engineers from the firm VBK are the initiators of this project, who came up with this topic and have been involved in the entire project.

During this period, we have enriched ourselves with new knowledge that we can use in the future, and we were very happy to work in this project. Due to the outbreak of Covid-19 most of the work has been done from home. We are grateful to VBK who provided us with workstations and computer software for us to work from home.

First and foremost, we want to thank our supervisors Andreas Lindelöf, Felicia Flink and Johan Örnborg, structural engineers from VBK, for their engagement in guiding us and giving us positive support despite their busy schedule. We also want to give our thanks to our supervisor and examinator from Chalmers, Robert Jockwer, for his informative advice during the entire project.

Gothenburg, August 2021

Lien Trinh and Hong Zhang

1 Introduction

The world we live in is developing, with society constantly changing and new demands emerging. The population in the world is increasing but the available land area that can be built on is decreasing. In order to maximize the use of land in densely urbanized areas, high-rise buildings were constructed. The 20th century witnessed a construction boom in tall buildings worldwide. Traditionally concrete and steel are the dominating building materials in the construction of high-rise buildings. However, in the recent years sustainable development is an important aspect in the construction industry and therefore using timber as the main structural material has been a tendency in modern buildings.

1.1 Background

The number of tall buildings with a height of over 200 meters completed between 2000-2020 is 1384, 5 times more than what completed under the period 1885-2000 (Al-Kodmany, 2020). The average height of the world's top 100 highest buildings has been increasing in the recent years, approaching 400m in 2020 (CTBUH, 2021). With the continuing urbanization, building skyscrapers and high-rise buildings is still the upcoming trend in the construction industry.

The prevailing building materials in high-rise building construction, i.e. concrete, steel and composites or combinations thereof, are not environmentally friendly. Despite the production with new technologies making them less harmful to the environment than before, emissions of carbon dioxide are still at a high level. Especially for tall buildings, with the rise in the height, the dimensions of structural elements increase dramatically because of the large self-weight of the building, meaning that the emission of carbon dioxide per rental floor can be even higher (SOM, 2013). In comparison with other materials, timber is both renewable and is formed through an ecological cycle that absorbs carbon dioxide from the air, making it a more sustainable substitution for concrete and steel. In addition, the high strength-mass ratio in timber also decreases the loads to the foundation and in this way saves the foundation materials (Svenskt trä, n.d.).

A lot of research and practice has been done regarding timber buildings. The appearance of engineered timber products, such as cross-laminated timber (CLT) and glued laminated timber (glulam), which to a large degree enhance the strength of timber and remedy the weakness arising from defects and anisotropy, increased the usage of timber in building construction. However, the usage of timber is still mostly limited to low-rise buildings nowadays, as a secondary structural element such as floor or combined or as a supplement to other main materials. Due to its low stiffness and strength, the resistance to horizontal load is relatively low compared to steel and concrete. Timber also has a low density and mass that makes it more challenging to build higher due to the problem of poor dynamic performance. So far, the knowledge of how a tall timber tower performs is still limited. At this time the tallest timber building in the world is Mjöstornet, located in Norway. It has a height of 85m and is far from comparable to the world's highest building, Burj Khalifa in Dubai, with a height of 828 m, almost 10 times higher than the highest timber tower. (Abrahamsen, 2017)

1.2 Aim

The aim of this project is to find the appropriate geometrical form with an applicable structural system for a 200 m tall timber tower with regards to structural stiffness and ease of construction. The design should not only fulfill criteria for lateral deformation and dynamic criteria but also provide as much rental area as possible.

1.3 Scope and limitation

The study is limited to the structural behavior in service limit state (SLS), although the dimensions of the main structural elements will be estimated in ultimate limit state (ULS). Furthermore, the following assumptions and simplifications are made:

- The location is chosen to be in central Gothenburg and the environmental data in Gothenburg is applied throughout the project when needed. Terrain category IV according to SS-EN 1991-1-4 is assumed.
- The entire building will be designed for commercial use as offices.
- Floor slabs and their properties are selected from the existing products in the market that may fulfill the requirement for serviceability. No deeper investigation will be done about this.
- The footprint area is limited to be 30m by 30m and the core is 10m by 10m. The estimation of sizes is chosen based on experience without check of architectural requirements.
- Only superstructure above the ground will be studied, i.e. the connection between upper structure and foundation will be given as boundary conditions. The foundation will not be incorporated.
- Long-term effects will be discussed only.

1.4 Method

The analysis was conducted in Rhino 3D and Grasshopper 3D and its plugin program Karamba 3D. Following steps were carried out for this project:

1. Literature study. Theories and previous study about slender buildings, geometries, timber as building material, structural systems and relevant standards and guidelines were studied.
2. General geometry study. In this early stage a series of volume geometries were generated, based on literature study and design workflow. These geometries were analyzed as shell elements by finite element analysis (FEA). The geometries were then assessed, and three geometrical forms were selected for further structural study.
3. Structural study. Based on earlier literature study of stabilizing systems, the selected concepts from the geometry study were further modelled in structural systems. The optimization of controlling parameters such as angles and sizes

were done with regards to static and dynamic performance and compared to the traditional braced frame structure.

4. Suggestions for feasible connections at critical places were given and roughly designed based on the loads on nodes from the former step.

2 Theoretical framework

This section consists of general knowledge and information of high-rise buildings, stabilizing systems and their structural behavior, design of geometries and their modifications, the effect of wind load on a tall building. The theory study of this project also includes information on timber as a building material and its connections. The design process and standards that were applied are also presented in this section. Theories and discussions presented in this section are the basis of further study.

2.1 Definition of a high-rise, timber building

The initial step is to define what a high-rise timber building is. The aim of this project is to investigate the structure of a 200 m timber tower. Although the height of the tower has been determined, it is still supposed to be high in the view of structural design in order to make the study meaningful. On the other hand, a clear definition of timber building in the view of the application of material is important since timber is usually used in combination with other materials, especially in high-rise buildings.

2.1.1 Definition of highness of timber building

There is no exact definition of what a "high-rise" building is because the definition varies from one culture and context to another. According to Council on Tall Buildings and Urban Habitat (CTBUH), there are three requirements for a building to be classified as "high": Height relative to context, proportions and building technology (Al-Kodmany, 2020). Buildings that have a height in the range of 50 to 300 m are considered as tall buildings. Meanwhile, supertall buildings should have a height of 300 to 600 m and buildings with a height surpassing 600m are called mega-tall buildings (CTBUH).

Height relative to context means how the building is in comparison to the surrounding buildings in a certain place. For example, a 14-story building is not considered as a tall building in a highly urbanized city such as Hong Kong or Chicago but in a provincial city it may be higher than the urban norm and still be referred to as a tall building (Al-Kodmany, 2020).

However, from the structural point of view, it is the absolute height rather than the relative height that makes sense for the design such as an overall height or a height to minimum plan dimension. The taller a building is, the larger the wind load impact on the building. This means that with the rise in height, the wind load increases dramatically.

CTBUH mentioned that that even if a building is very tall but has a large footprint, it is still not considered as a high building due to its proportions. Some buildings are not that high but are very slender and still give a vibe of tall building. In structural design, the proportion is usually measured as "slenderness". The slenderness ratio (SR) of a building is defined as in Figure 2.1.

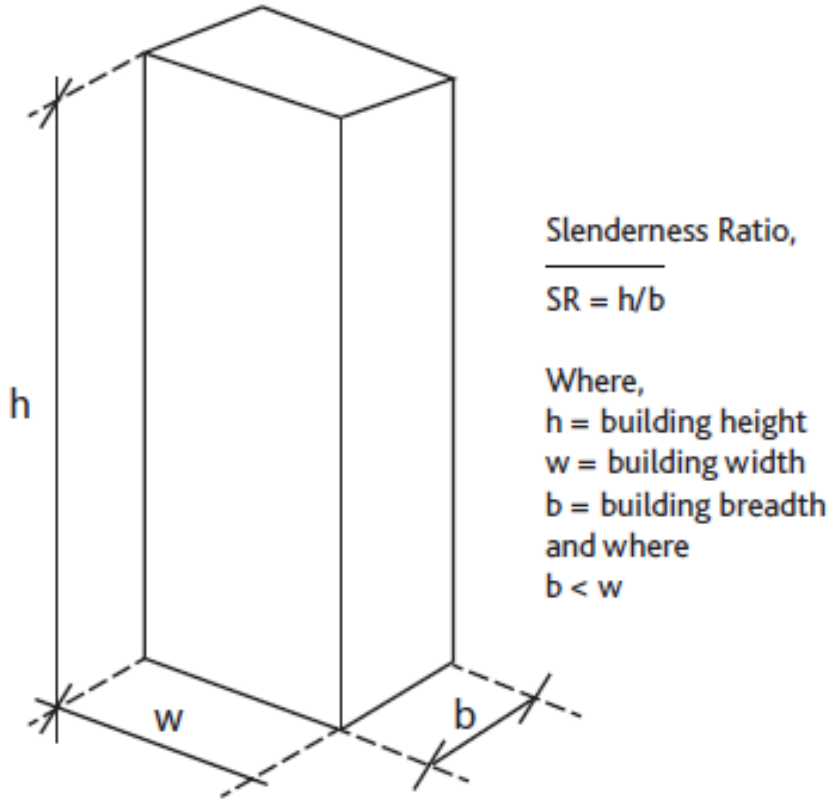

Figure 2.1 Definition of slenderness ratio (MPA & fib,2014)

The slenderness ratio is a basic proportion of the structure and influences the structural behavior of a high building significantly (Awida, 2011). For a slenderness ratio larger than h/8 the requirements on dynamic performance can be dominant during the design process. Slenderness ratios around h/6 or less are more appropriate and more common in tall buildings (MPA & fib, 2014).

The last criterion, high building technology in terms of e.g., structural system and material, was stated as weakest by CTBUH (Al-Kodmany, 2020). By this, they meant a building with which height-related technologies might be suggested to be high. For example, a building with specific vertical transport technology can still be categorized as a tall building. The number of floors is a bad measurement for a tall building because the dimension of floor-to-floor height varies with the building's function. Therefore, a building of 14 or more stories or higher than 50 m is a threshold for a tall building. There exists an obvious gap between the slenderness ratio of highest building in prevailing building materials such as concrete and that in timber. The existing highest timber building, Mjöstornet, cannot even be classified as a slender building with a slenderness ratio larger than 1:10 according to the general classification regardless of building materials.

At the initial stage of the project, it is important to decide the slenderness ratio for the 200 m timber tower. A few examples of the slenderness ratio from the existing tall buildings were studied. Figure 2.2 shows the width height ratios of some popular tall buildings and the highest timber tower.

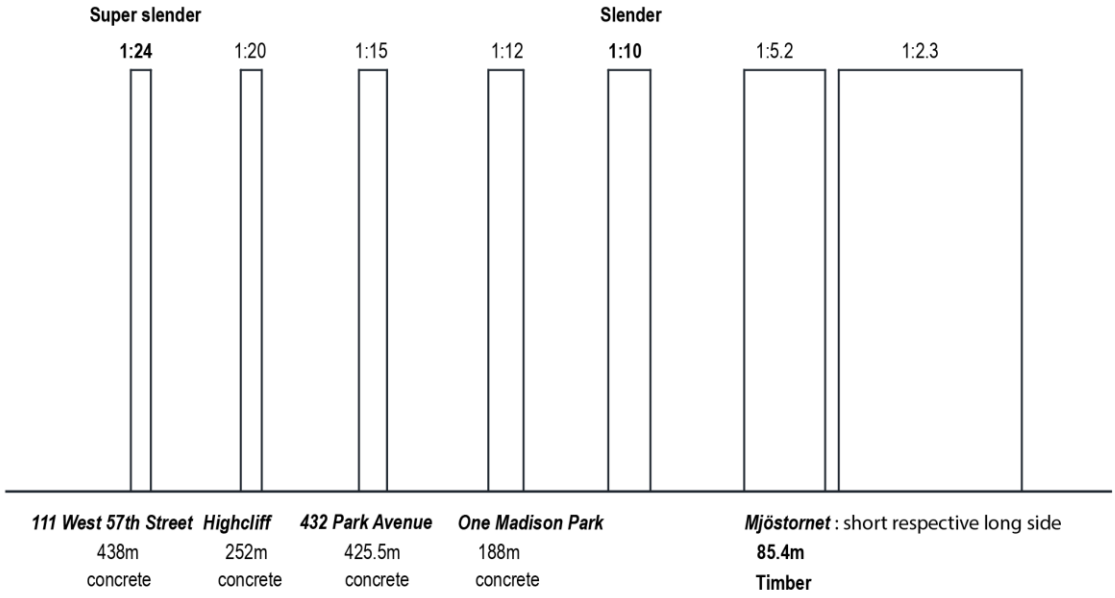

Figure 2.2 Slenderness ratio of high- rise buildings in concrete and that of Mjöstornet

2.1.2 Definition of timber building

Tall buildings can be divided into four categories according to the building materials that are utilized for the main vertical and horizontal load-bearing structural elements: concrete, steel, composite and mixed-structure buildings. The "main" structural elements refer to the primary structural members, where the secondary structural elements like the floor would not be considered in classification of a tall building with regards to structural materials. According to CTBUH a steel-framed tall building with concrete slabs resting on steel beams should be called a steel building rather than mixed. Furthermore, a building is defined as single-material when a single material makes up 85% or more of the height or the floor area of the building. (Foster et al., 2016).

To extend this classification criteria to cover timber buildings, when more than 85% of the height or floor area of the primary structures are constructed of any kind of timber the building can be referred to as a single-material timber building. The light weight of timber is one of the properties that contributes to the poor dynamic performance. It is common to supplement the structure with extra mass by using concrete floor slabs for better dynamic behavior. For example, the prefabricated wooden decks were replaced by concrete decks for floor 12-18 on the top part of the building in Mjöstornet to fulfill the requirements on acceleration (Abrahamsen, 2017). As stated before, regardless of the concrete slabs the building can be still classified as a timber building, though the diaphragm action and the mass contributed from the floor are very important for the global structural behaviour.

Traditional carpentry wooden connections are not commonly used in modern timber buildings, especially in high-rise buildings. For these weakest points, steel connection components such as plates and dowel are generally applied. Therefore, it is reasonable that the material used for timber joints are not included in the classification criteria. (Foster et al., 2017). Another general arrangement in timber buildings is that the lowest floors, often up to the first or second floor, are built in concrete. In this case the whole building should be regarded as mixed structure and the height of the upper section consisting of only timber can be regarded as the height of single-material timber structure. For better understanding several examples of schemes are presented in Figure 2.3.

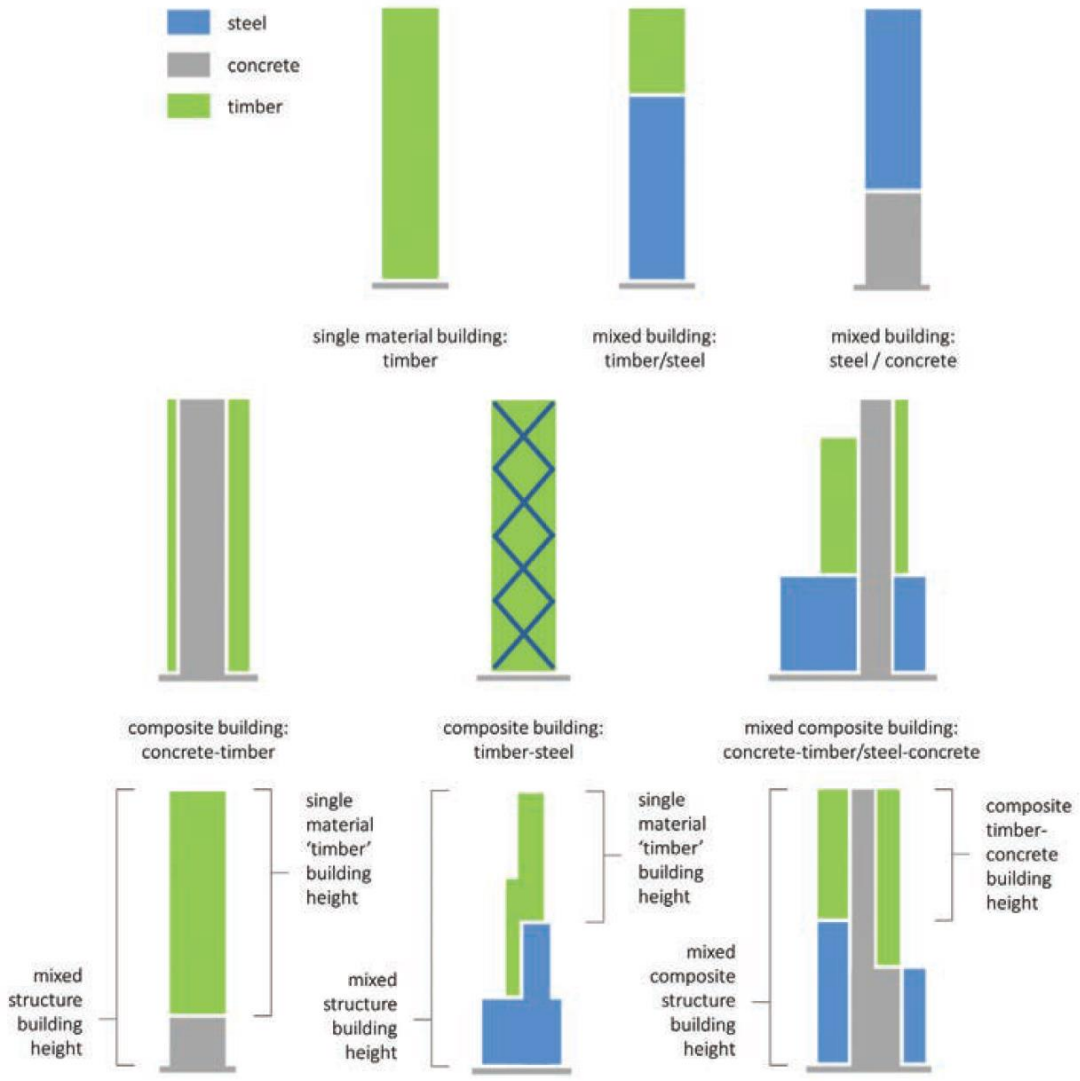

Figure 2.3 Examples of building typology by structural material (Foster et al. 2017)

2.1.3 Summary

In this project, 200 m is aimed to be the height of the single-material timber building. The footprint is assumed to be 30m x 30m and the prescribed slenderness ratio 6.6 is the starting point for the design, which is not slender according to general classification criteria. However, considering the material properties for timber a height of 200 m and a slenderness ratio of 6.66 can be challenging and worth exploring. Steel connections and concrete floors slabs will not influence the fact that the building is a timber building as long as the primary structural elements, such as columns, beams and load-bearing walls are in timber. The application of concrete in flooring system will also not influence the classification of the building. However, from a sustainability perspective the concrete slabs will be introduced only as necessary when the mass of wooden decks is not enough to fulfill dynamic criteria.

2.2 Considerations regarding structural design for high-rise buildings

The structural considerations for a high-rise building are in principle involved in the design process for a low-rise building as well. However, some of the factors might be more critical and require more attention when it comes to design for high-rise buildings.

2.2.1 Lateral resisting stiffness and strength

With increasing height of a building, the load acting on the surface of the building increase exponentially. Apart from this, the cantilever arm from the tip to ground gets longer and high-rise buildings are usually very slender. The higher the building will be, the more dominant the lateral loads are in the design process, in relation to gravity loads. The overturning moment at the base increases by a power of 2 and the sway at the tip increases by a power of 4 when the height of the building increases. The limit of the maximum lateral displacement and the interstory displacement (relative displacement between adjacent stories) are of great importance regarding not only comfort demands but also requirements related relating to for example façade cladding and placement of partition walls.

For a low-rise building in steel up to 10 stories, the design of structural elements designed for gravity loads only are adequate to resist lateral loads. For a building higher than 10 stories the sizes of the structural elements in the stabilizing system need to be enlarged to increase the global stiffness of the structure to satisfy the horizontal deflection control. (Balendtra, 1993). In the design of the 300 m tall timber building Oakwood Tower, the design was governed by the lateral stabilizing system. (Ramage et al., 2017).

It was also pointed out that the strength and the stiffness of the connections in the timber structures plays a key role in the structural behavior and a minor movement in the connection can weaken the global stiffness significantly. (Ramage et al., 2017).

Some ways to improve the lateral stiffness are:

- Increase the material stiffness parameters E and G
- Increase the size of the structural elements
- Increase geometrical stiffness and make use of the depth of the building, for example, place the stabilizing elements around the perimeter of the structure

Despite this a careful designed form of the building and reduction of the loads can improve the lateral deflection of the structure.

The net lifting forces in structural elements occurs when the tensile forces caused by overturning due to horizontal loads exceed gravity load. The design and construction for structural elements in tension are more complex and difficult. For concrete structures, the net uplifting force is not so common because of the high weight of concrete (SOM, 2013). Due to the light-weight nature of timber the occurrence of a net uplifting force is more probable. It is important to lead as much of the vertical load into the stabilizing system in the perimeter as possible to make use of the self-weight to resist overturning moments. (Ramage, 2017). In the design of the prototype building in the same research conducted by SOM, the concrete joints were adopted to provide enough ballast to avoid tensions (SOM, 2013).

2.2.2 Dynamic behavior

When the building is exposed to time-dependent loading such as wind loads and seismic loads, dynamics need to be investigated in detail. For buildings located in seismic zones, seismic actions can be critical. These loads are dominant cross a certain spectrum of frequencies. How a structure behaves under these loads depends on its natural frequency and damping ratios. (Ramage et al., 2017). When the structural frequency coincides with the frequency of the loading, the deflection of the structure will be amplified to the fullest. For a building located in a seismic zone, the seismic actions are more critical. Due to the low stiffness the natural frequency of a tall and slender building is usually low, and the performance of the structure can be influenced more by wind turbulence than by earthquakes. (Balendra, 1993).

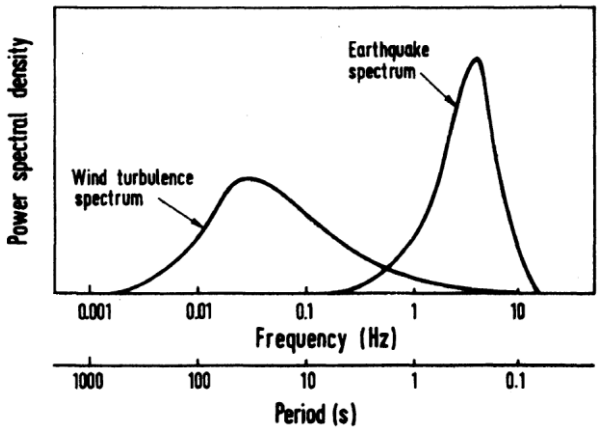

Figure 2.4 Example frequencies of wind turbulence and earthquake (Balendra, 1993).

In a dynamic problem the structure is subjected to both external dynamic loads such as wind loads and inertia forces which act opposite the external forces, both of which vary over time. The acceleration in correspondence to the inertia forces are:

$$f(z,t) = m(z) \cdot \ddot{v}(z,t) \qquad (2.1)$$

where:

$f(z,t)$	is the inertia force at height z and time t
$m(z)$	is the mass of the structure at height z
$\ddot{v}(z,t)$	is the acceleration of the structure at height z and time t

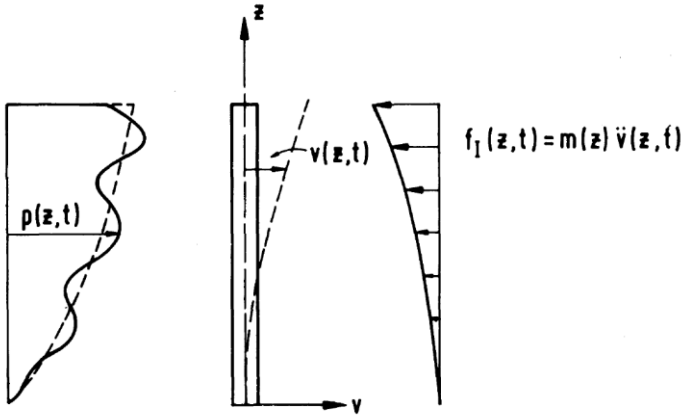

Figure 2.5 The structure subjected to dynamic loadings (Balendra, 1993).

For the structural system:

$$m\ddot{v} + c\dot{v} + kv = P(t) \qquad (2.2)$$

where:

m	is the mass
c	is the vicious damping coefficient
k	is the lateral stiffness
v	is the lateral displacement
$P(t)$	is the lateral loading

The mass, damping coefficient, lateral stiffness and the structural response of lateral displacement are key factors in the dynamic problem of a building. Larger mass, lateral stiffness and damping are favorable when it comes to the dynamic behavior.

2.2.3 Gravity resisting system

The gravity weights can help resist the uplifting force due to the overturning moment. One of the considerations in designing gravity resisting system in relation to the lateral load resistance is to transfer as much of the gravity loads through the stabilizing system as possible. Long spans connecting the core to the perimeter structures without interior columns and walls are desired. The challenge lies in the design of the floor slabs with large spans while still meeting requirements regarding dynamic issues. The depth of the floor might be quite large. The fixed connections between floor elements and the adjacent stabilizing system can make it possible for larger span. Another strategy is to widen the effective width of the core (SOM, 2013).

The uneven shortening of structural elements such as columns in the perimeter and the core walls, caused by the vertical loads, can cause problem in serviceability. This can lead to problems for floor finishing and cladding details. (MPA & fib, 2014).

2.3 Geometry and modification

This section describes how the shape of the building plays a significant role in the structural design and the effect of wind load on high buildings.

Due to the high speed of wind on the top of the tall building and the slender geometrical form, high-rise buildings are very subjected to wind load both in static and dynamic state. The wind force that a high-rise building subjected are along-wind, caused by the wind turbulences directly on the surfaces, and crosswind which can be induced by vortex shedding.

(a) (b)

Figure 2.6 The wind loads acting on a building (a) Wind flow (b) The resultant wind forces

During the structural design both the along-wind and crosswind should be taken into consideration and be designed for. For a supertall building the oscillations induced by vortex in the cross direction can be more critical (Alaghmandan & Elnimeiri, 2013). When the wind speed is low it is usually the along-wind which is dominant. While the wind speed increases the crosswind will become more and more critical and can dominate the structural behavior (Xie, 2014).

There are two general ways to improve the dynamic behavior of high-rise buildings. One is to optimize the building geometry to mitigate the wind loads from the source, and the other one is to choose proper structural system and improve the global stiffness during the structural design. (Alaghmandan & Elnimeiri, 2013). Since the geometry is very much dependent on the architectural design, the aerodynamic study is worth to be conducted at very beginning of the design.

2.3.1 Plan shape and corner modification

Buildings with square and rectangular plan section are common because they utilize the land most efficiently. However, symmetrical cross sections like square, rectangular, circular, or triangular are most susceptible to wind-induced vibration (Elbakheit, 2018). Corner modification is a very effective way to decrease the wind-induced loads on high-rise building. A rule of thumb is that the modified part should be at least 10% of the width of the building and in general the corner modification can contribute to reduce both along-wind and crosswind excitation (Xie, 2014).

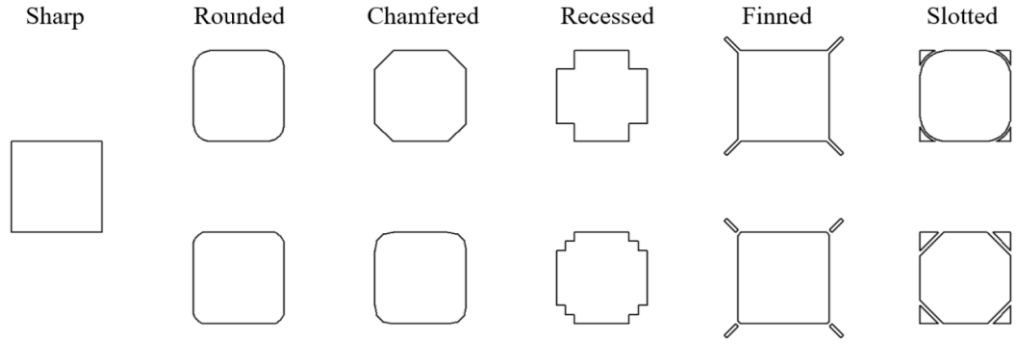

Figure 2.7 Examples of corner modification (Elshaer,2017)

Chamfer which is 10% of the width of the building can reduce 40% along-wind response and that of 30% in the cross direction compared to a building with square section without corner modification (Holmes,2001). Among chamfer, recession and roundness, roundness is the most effective way to improve the aerodynamic and dynamic response (Kawai, 1998).

2.3.2 Modification in elevation

Modification of the shapes in elevation can influence the architectural design, much more than local modification around the corners. Therefore, this process should be continuously involved in the architectural design of the building from the very beginning. Some common approaches are for example tapering, setback, twisting and opening in the building body. The common principle that makes all of these solutions work is that the change of the shape over the height make the frequency of the vortex shedding vary over the height as well to avoid the mutual excitation (Xie, 2014).

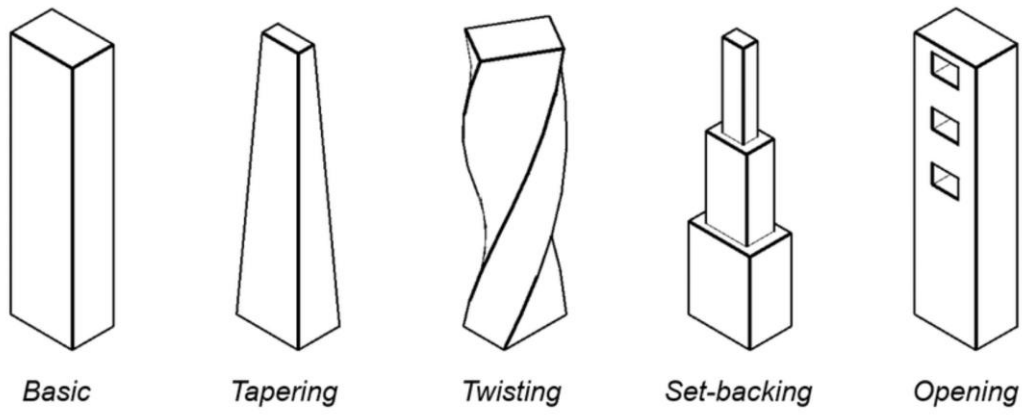

Figure 2.8 Example of form modification in elevation (Elshaer,2017)

2.3.2.1 Tapering and setback

Tapering means that the width of the floor plan section of the building gradually decreases over the height. Tapering is more effective in mitigating vortex shedding in the cross direction rather than the effect in the along-wind direction. But this might have a negative impact on the structure when the damping ratio is too low (Alaghmandan & Elnimeiri, 2013). This is because the narrowing to the top and the decrease in mass close to the tip can cause excessive acceleration, which is not expected with consideration to the comfort issue (Xie, 2014). Therefore, both effects need to be included. Setback involves a similar structural concept and principle as tapering and also the risk for increased acceleration.

2.3.2.2 Twisting

Twisting is another effective way to reduce wind effect. Xie (2014) showed that the effectivity increases with the increase twisting degrees. Considering the difficulty for façade cladding, 120 degrees with opening on the top can be an optimal choice.

2.3.2.3 Opening

Openings can help to reduce both the wind loads in the along-wind direction and vortex shedding. The opening can let the wind turbulence through the solid building body and release the surface pressure. Openings are commonly placed near the top of the building and the wind flow will be disrupted to improve the dynamic performance (Irwin, 2009).

2.3.3 Consideration regarding structural stiffness

Apart from the aerodynamic effect, the geometry of buildings can influence the structural stiffness as well. Geometries with circular sections have the same stiffness in all direction unlike geometries with square sections. Tapering or setback may improve the aerodynamic response but the decrease in the structural stiffness needs to be considered as well.

2.4 Structural systems for tall buildings

CTBUH describes four main types of structural systems for tall buildings: shear and frames system, interacting system, partial tubular systems and tubular systems. These can be further divided into interior and exterior structures, depending on which kind of primary lateral load resisting system a building has. Interior structures can be created by forming columns and beams in the core that are stiff enough to resist wind forces. The core is usually an elevator shaft in the middle of the building, saving a lot of open areas for each floor. Interior structures can be divided into rigid frames, shear wall hinged frames, shear wall or frame interacting systems and outrigger structures.

Interior structures have two common types of lateral load resisting system, moment-resisting frames and shear trusses or shear wall system. In exterior structures, the columns and beams instead of being inside the core are placed at the perimeter of the building and form a hollow, rigid tube that is as strong as the core but much lighter.

Exterior structures can be divided into tube structure, diagrid structure, space truss structures, super frames and exoskeleton structure (Ali & Moon, 2007).

2.4.1 Rigid frame

A rigid frame system is an interior structure with a moment-resisting frame. This system consists of horizontal girders and vertical columns that are rigidly connected together in a planar grid form, see Figure 2.9. The dimension of the columns in this system depends mostly on the gravity loads and vertical loads. However, to ensure the lateral stability of the building the dimensions of the horizontal girders depend on the stiffness of the frame. For a concrete construction in rigid frame, the most economical span is 8-9m (MPA & fib, 2014).

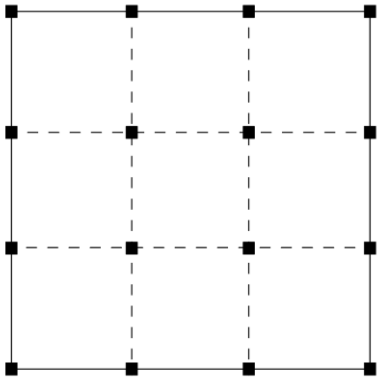

Figure 2.9 Typical plan of a frame structure,

2.4.2 Shear wall system

The whole system behaves like vertical cantilevers that are fixed at the base. It is common that shear walls are placed in the middle of the building as the service core. Concrete core and steel-framed core are two of the most common core systems (Fu, 2018). It can also be coupled shear walls which refers to more than two shear walls being connected by beams or slabs. The overall stiffness of the system exceeds the summation of individual stiffness (Ali & Moon, 2007).

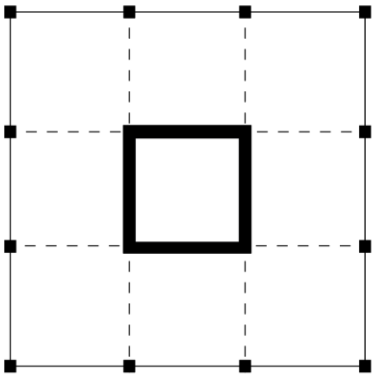

Figure 2.10 Typical plan of shear wall- hinged frame structure with core

2.4.3 Shear wall and frame interaction system

Shear wall and frame interactions system refers to the combination of two systems, the shear wall system, and the frame system. The frame can be a rigid frame or semi-rigid frame. One advantage of this system is that the large lateral displacement caused by moment deformation can be effectively restrained by the frame system in which the shear deformation dominates (Ali & Moon, 2007).

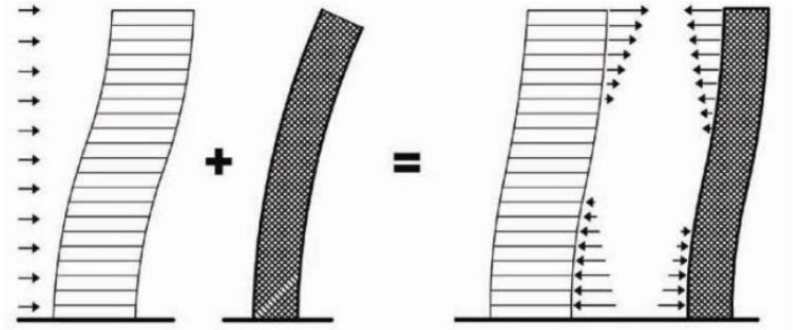

Figure 2.11 Combined effect of braced frame and core (Ali & Moon, 2007).

2.4.4 Outrigger system

The outrigger system has a core that behaves like a cantilever. By rigidly connecting the core and the exterior systems the overturning moment in the core can be decreased. Columns in the perimeter helps to resist the overturning moment by compression in the leeward and tension in the windward, see Figure 2.12.

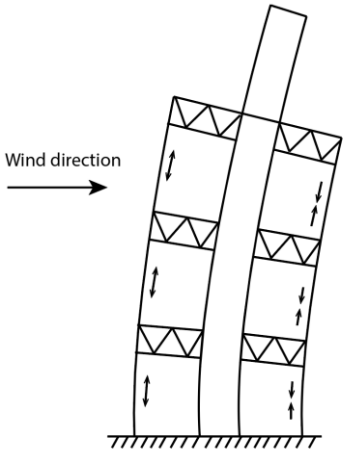

Figure 2.12 Outrigger system, with steel truss belt as outrigger

Two typical outriggers are steel outrigger consisting of truss system and concrete outrigger in form of deep beams or walls. Usually, the outrigger belt can take as high as one floor and another disadvantage is that the connection of the trusses to the core walls can be very complicated to ensure the effect (Fu, 2018).

2.4.5 Tube system

One type of exterior structure is the tube system. By designing the building as a hollow cantilever perpendicular to the ground it can resist lateral loads, making use of the full depth of the building and obtain maximum geometrical stiffness. There are four subcategories of this system: framed tube, braced tube, bundled tube and tube in tube.

2.4.5.1 Frame tube

The hollow cantilever can be constructed by placing the columns on the exterior of the buildings closely together and rigidly connected with deep spandrel beams. This results in a rigid frame that is dense and strong along the edges of the building. The typical distance between the columns is 1.5 - 4.5m (MPA & fib, 2014). By introducing bracing members, the columns in the perimeter can be more sparsely placed than the simple frame tube, called braced tube. Buildings in braced tube can reach up to 300m economically (MPA & fib, 2014).

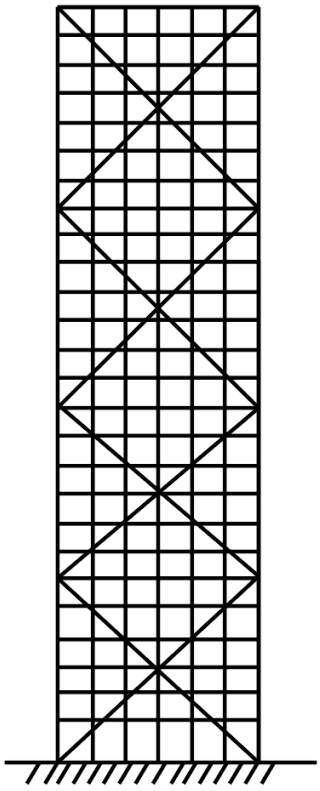

Figure 2.13 Elevation of a braced tube

The shear lag effect is a serious issue in frame tube system which can make the exterior tube not work as a true cantilever. The columns close to the corner are subjected to larger stresses than those in the middle of the span. The introduction of the diagonal braces can help to redistribute the stresses from higher stressed corner columns to the lower stressed inner columns. (Fu, 2018).

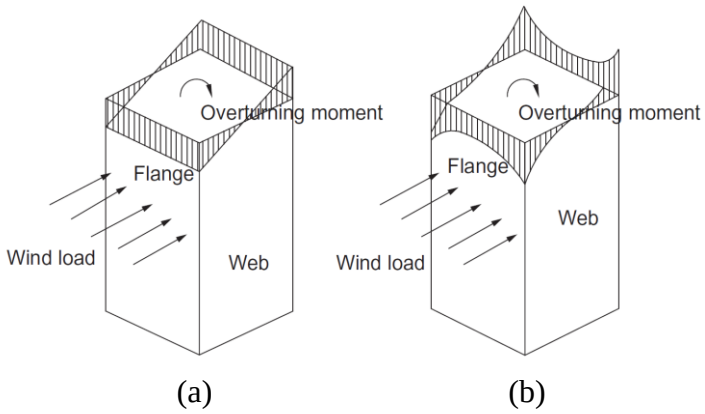

Figure 2.14 The illustration of shear lag effect in frame tube system (a) Frame tube works as a true cantilever; (b) The stresses in the corner columns are increased due to the shear lag effect. (Fu, 2018)

2.4.5.2 Bundled tube

A smaller tube system connected together as one unit is called bundled tube. By providing cross walls or cross frames in the building the strength and stiffness of the building increases, and it is possible to have wider column spacing in the tubular walls. To further enhance the stiffness trusses could be added. (Ali & Moon, 2007)

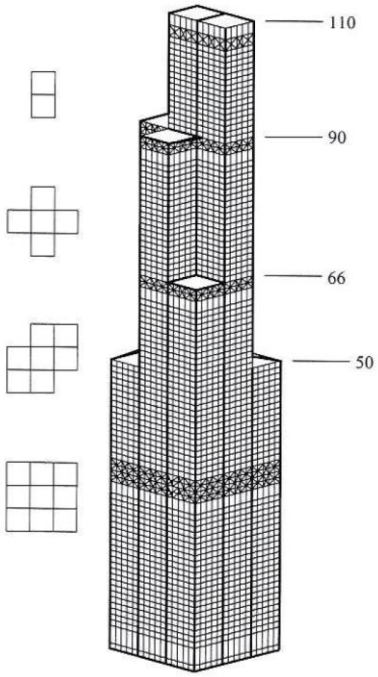

Figure 2.15 Illustration of bundled tube (Ali & Moon, 2007)

2.4.5.3 Tube in tube system

Combined with an interior tube, in forms of core, the structural stiffness of tube system can further increase. With a tube in tube system, the effective height of buildings can be approximately 80 stories (Ali & Moon, 2007).

2.4.5.4 Diagrid system

One structural system that is becoming popular is diagrid system. In a diagrid system most of the vertical columns are removed and given larger spacing. This system is structurally efficient as a tubular system. The diagonal components in a diagrid system can take both gravity loads and lateral loads because their triangulated arrangement is distributive and uniform. This system can resist the lateral shear by axial forces in the diagonal components, but one drawback is the complicated joints between diagonal members. Diagrid system on the façade can dominate the architectural expression. Therefore, good communication with the architects is important during the design process (Boake, 2014). Two very famous architectures in diagrid system are 30 St Mary Axe in London and Poly International Plaza in Beijing.

2.4.6 Spaces truss structure

Spaces truss structure is a modified version of braced tubes which also includes diagonals that connect the exterior to the interior. The distinction of a spaces truss structure is that some diagonals penetrate inside the building, while in a braced tube system the diagonals connecting the corner columns are located on the perimeter of the building. Space truss structure is mostly used in building with large span (Fu, 2018). One typical building utilizing a space truss system is the Bank of China Tower in Hong Kong.

2.4.7 Super frame structure

A super frame consists of mega columns and mega girders. This system is rigidly connected by multistory trusses at every 15 to 20 stories. “It is an ideal structure for super tall buildings” and it “resist lateral loads with minimum amount of structural material”. (Feng & Mita, 1995). Some examples of this system are the 56-storey tall Parque Central Complex towers in Venezuela and CITIC Tower in Beijing.

2.4.8 Exoskeleton

In exoskeleton structures the lateral-load resisting system is located outside the facade of the building. An example of this system is the Hotel de las Artes in Barcelona. One advantage of this system is that fire proofing is not a serious problem because the system is located outside the building line. However, thermal expansion, contraction and weather protection should still be considered. (Ali & Moon, 2007)

2.4.9 Classification and considerations regarding timber buildings

Fazlur Khan has developed and updated the diagrams of classification of structural systems for high-rise buildings in relation to the height regarding structural efficiency, for both steel and concrete constructions in 1969, 1972 and 1973. (Ali & Moon, 2011)

Supertall buildings with slenderness larger than 7 will perform very poor in resisting turning moment caused by the wind, especially for timber constructions. One potential solution for building high timber buildings is to put the stabilizing structural system on the façade, making use of the building depth to enhance the global stiffness, and at the same time try to lead as much gravity load to the exterior stabilizing system as possible. (Ramage, 2017). Taking away the interior columns and load-carrying walls can be one approach. The diagrams of exterior structures in Figure 2.16 shows also that the steel braced tube without interior columns can be built 50 stories higher than that with interior columns.

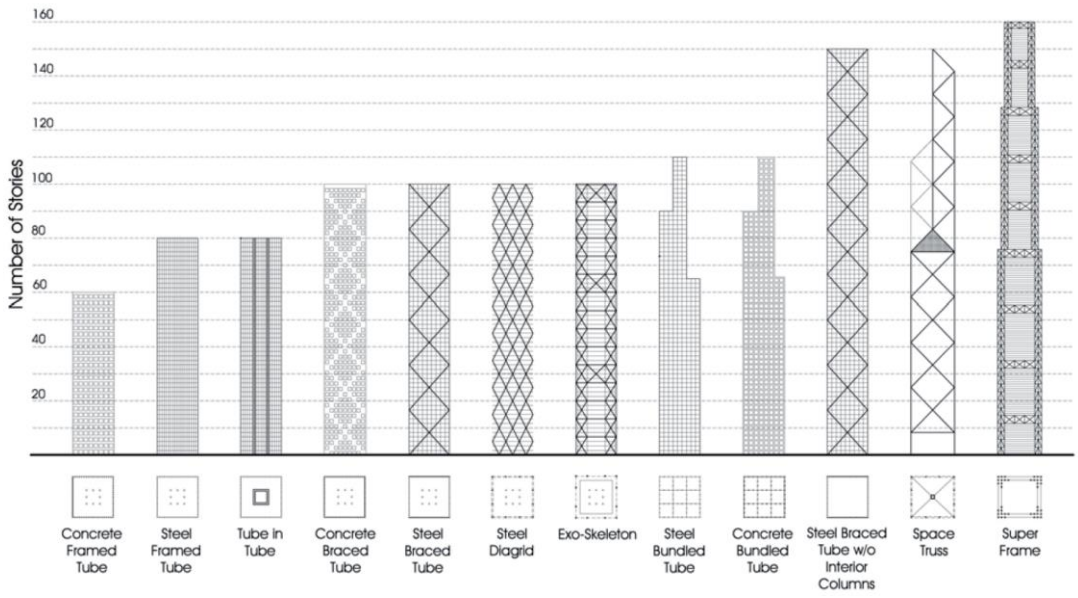

Figure 2.16 Exterior structures (Ali & Moon, 2011)

The exterior structures that can efficiently be built as high as 60 stories are tube structures, space truss and super frame for concrete and steel buildings. Such tube structures can be for example framed tube, braced tube, diagrid and bundled tube. Ramage (2017) argues that tubes, diagrid and mega-trusses could be considered for high-rise timber buildings.

2.5 Timber as a building material

In recent times, timber is one of the most common building materials in construction especially in buildings because it is environmentally friendly and has moderately high strength. Timber construction has variety in form and is very aesthetically pleasing with regards to architectural character. Despite all the advantages, timber is an anisotropic material which means it has different properties in different directions (Swedish Wood, 2016). It is also moisture dependent and is sensitive to rot and insects. Structural engineers always need to verify that the chosen timber materials, dimensions, and structural systems fulfil all the requirements regarding functionality, durability and maintenance. This section describes more about timber properties such as how it is affected by moisture and creep. Several recommended timber products and timber connections for a tall building are also introduced in this section.

2.5.1 Property of timber

2.5.1.1 Timber mechanical properties

In timber the effect of the natural characteristic such as knots, spiral grain, juvenile wood, and reaction wood decides its grade and strength (Swedish Wood, 2016). Timber is an anisotropic material which means that it has different properties in different directions. These directions are defined as longitudinal, tangential, and radial. In practice, there are two main directions which are important to consider in design: parallel to the grain and perpendicular to the grain.

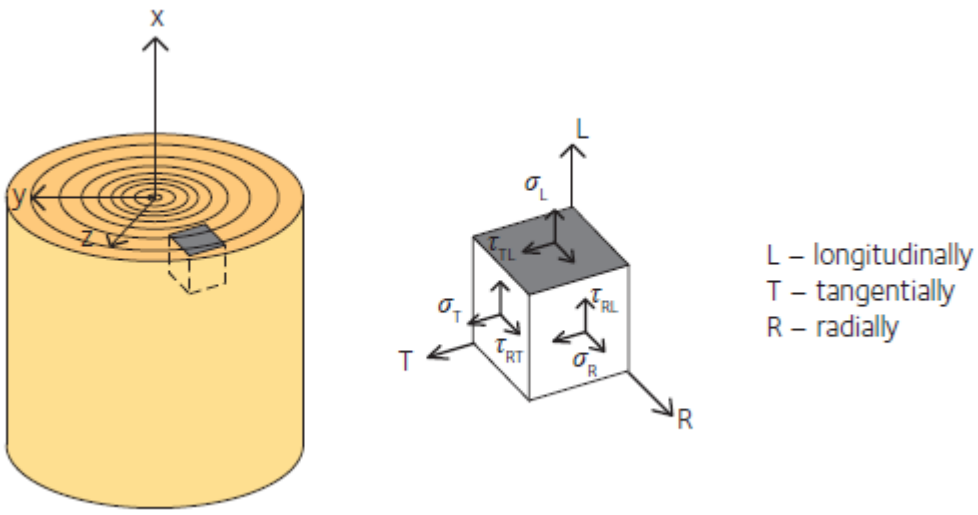

Figure 2.17 Three directions in wood. Figure 2.13 in Design of timber structures Volume 1 (Swedish Wood, 2016)

The strength of timber depends on the angle between the load and the grain direction, see Figure 2.18. Timber has its highest strength when subject to load parallel to its grain direction. The strength of wood in compression parallel to the grain is very high however when the load is too high the fibres start to buckle, and timber will have a ductile behaviour. In compression perpendicular to the grain the shape of the wood is crushed and deformed at low forces, therefore the strength of timber in this loading direction is very low. In tension perpendicular to the grain timber has its lowest strength. Timber has high strength in tension parallel to the grain but if failure occurs it will be very brittle.

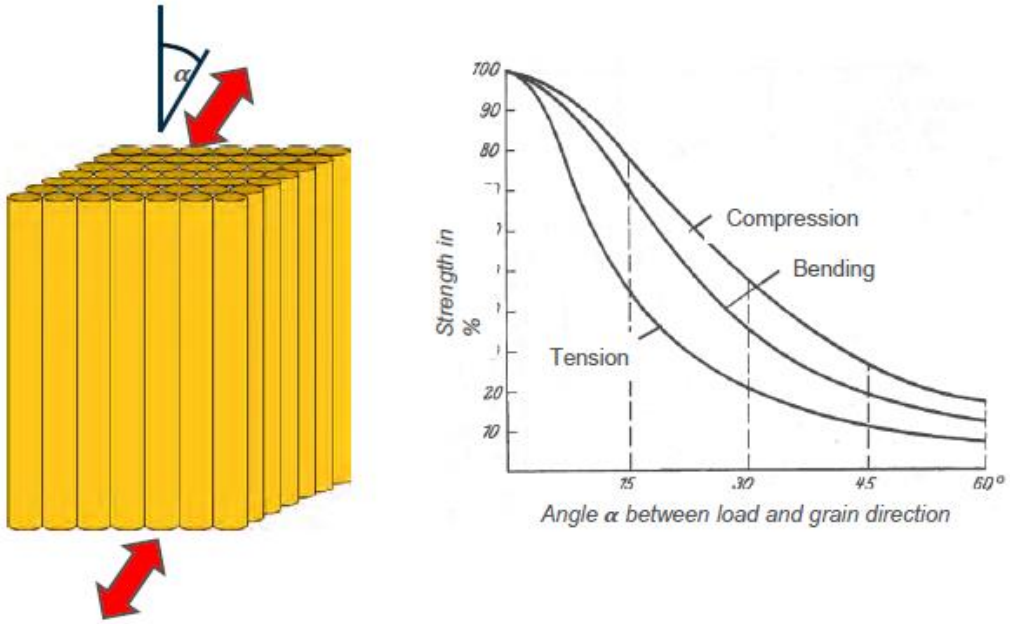

Figure 2.18 Strength in compression, bending and tension

Timber has a lot of advantages such as a high strength per weight ratio, it is a very light material compared to concrete and steel. In fact, the density of wood varies between 170 kg/m^3 to 1200 kg/m^3. Meanwhile the density of concrete is approximately 2400 kg/m^3 and the density of steel is around 7850 kg/m^3. The light weight of timber eases the transportation, construction and reduces the foundation work but also is a problem in building dynamics and vibration because the lower the mass, the lower the building's inertia and stiffness.

2.5.1.2 Influence of moisture

Timber is a hygroscopic material and is affected by the moisture content around it (Swedish Wood, 2016). Depending on the moisture content and environment, timber can either adsorb or desorb the moisture content. The strength of timber decreases with increasing moisture content, which is why timber needs to dry before being used as a building material, see Figure 2.19. Timber can be dried in a large kiln or solar kiln where humidity and moisture content can be controlled. If the moisture content is above the fiber saturation points (FSP) then the strength of timber is almost constant but if the moisture content is under FSP then the strength of timber increases with increasing moisture content. The compression strength of timber is most affected by the moisture content, meanwhile the tension strength of timber is almost

independent of the moisture content. Changes in moisture content in wood leads also to dimension change and the danger of being attack fungi attack may also increase.

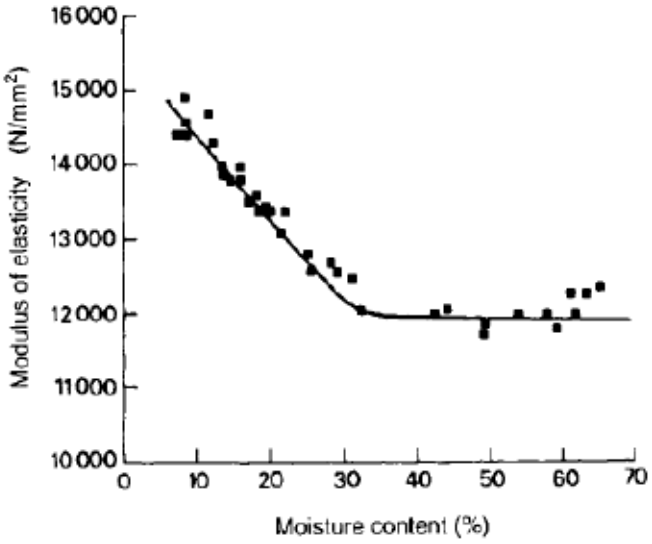

Figure 2.19 Modulus of elasticity of timber related to change of moisture content

2.5.1.3 Influence of creep

Creep is defined as the extra deformation increase with time under constant load (Swedish Wood, 2016). This time dependent deformation can be divided into three parts, elastic, delayed elastic and viscous deformation. The elastic deformation occurs directly after a load is applied to a structure. After that the deformation will grow slowly under a constant load, consisting of both delayed elastic and viscous deformation. The delayed elastic deformation is reversible in time while the viscous deformation is irreversible and remains the same under loading, see Figure 2.20. There are also some external factors that affects creep such as temperature, load direction, stiffness, knots, and moisture content.

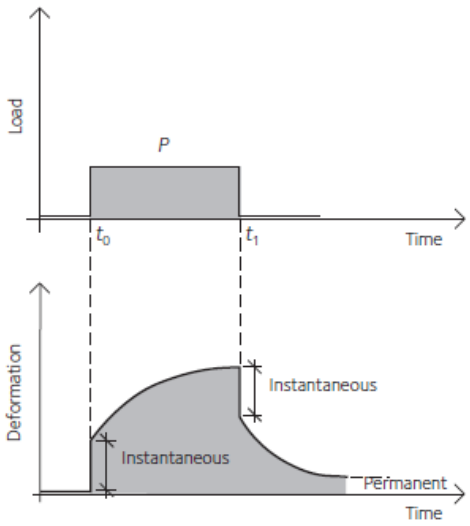

Figure 2.20 Creep curve. Loading and deformation over time. Figure 2.23 in Design of timber structures Volume 1 (Swedish Wood, 2016)

2.5.2 Wood product for tall buildings

There has been a huge development in the world of engineered wood products (EWP) to overcome the drawbacks of sawn timber. With EWP it is possible to produce almost all kind of shapes and sizes depending on the design demand (Swedish Wood, 2016). The largest disadvantage of sawn timber is its deviations such as knots, reaction wood and grain angle, but these deviations can be decreased with EWP. The problem with lack of old growth timber can be solved by using lower quality wood to produce EWP with desired quality. EWP are also less affected by moisture dependent deformation like shrinkage, and it is easier to control its strength and elasticity properties.

High buildings are subject to larger loads therefore the primary components are usually larger and have higher strength. A building consists of many parts and each part has different requirement in terms of strength and size. Depending on the application in buildings, a combination of timber products will be better. There are three common primary components for timber buildings: solid timber, glued laminated timber (glulam) and cross laminated timber (CLT).

Structural timber is also known as solid timber which normally is up to 6m long and 245 mm high. The strength grading of solid timber grades each timber into different strength class from C14 to C40. The number of the indicates the bending strength parallel to the grain of the timber. For example, C14 means that the timber product has a bending strength of 14MPa. In Sweden only C14 to C35 are available in the market. Solid timber can even be longer if finger jointing is applied.

Glulam is the oldest of the engineered wood products. Glulam is made of small timber laminates bonded together with adhesives and finger joints. All the lamination is oriented in the same direction and all grains are parallel to the longitudinal axis. Glulam can be homogeneous or consist of different strength graded lamellas which is called combined glulam. Due to the gluing process, it is possible to match the lamination quality to the level of design process and therefore glulam can have bigger dimensions and more shapes than solid timber. The largest available dimension of glulam in the market is 2m x 2m and 30m length.

Cross laminated timber is also called (CLT) and has lamellas oriented in different directions and often is used in stabilizing walls or slabs. Each layer of lamella in CLT is placed perpendicular to the layer above and below it. Depending on the demand and design the number of layers can be 3, 5 or 7. One important thing is the two outer layers of CLT always have the same direction and better strength. The dimension of CLT available can be up to 500 mm thick, 3 m wide and 24 m long.

Laminated veneer lumber or LVL is made of veneers which are usually 20 to 90 mm thick and made from spruce or pine and glued together either in perpendicular direction or in the same direction. LVL has high bending, tension, compression strength and has high stiffness and as well as shear strength. LVL is available in dimension up to maximum 3m wide and 24m long.

2.5.3 Connection in timber buildings

Timber elements need to be connected to each other to form a functional structural system. Timber connections affect the structural behavior of the structural system. There are three types of timber joints: traditional timber joints, dowel joints and glued joints. The stiffness of timber joints depends on the number of fasteners, density of the timber, the fasteners diameter and type of fasteners i.e. glue, nail, screw, bolt etc.

2.5.3.1 Dowel joints

This is the most common type of joint in timber (Swedish Wood, 2016). In dowel joints forces transfer through shear. Predrilled holes are required or not depending on the type of fastener and this might weaken the structure because of the reduction in the cross section. Dowels are divided in five subgroups including nails, screws, dowels, nails plates and bolts.

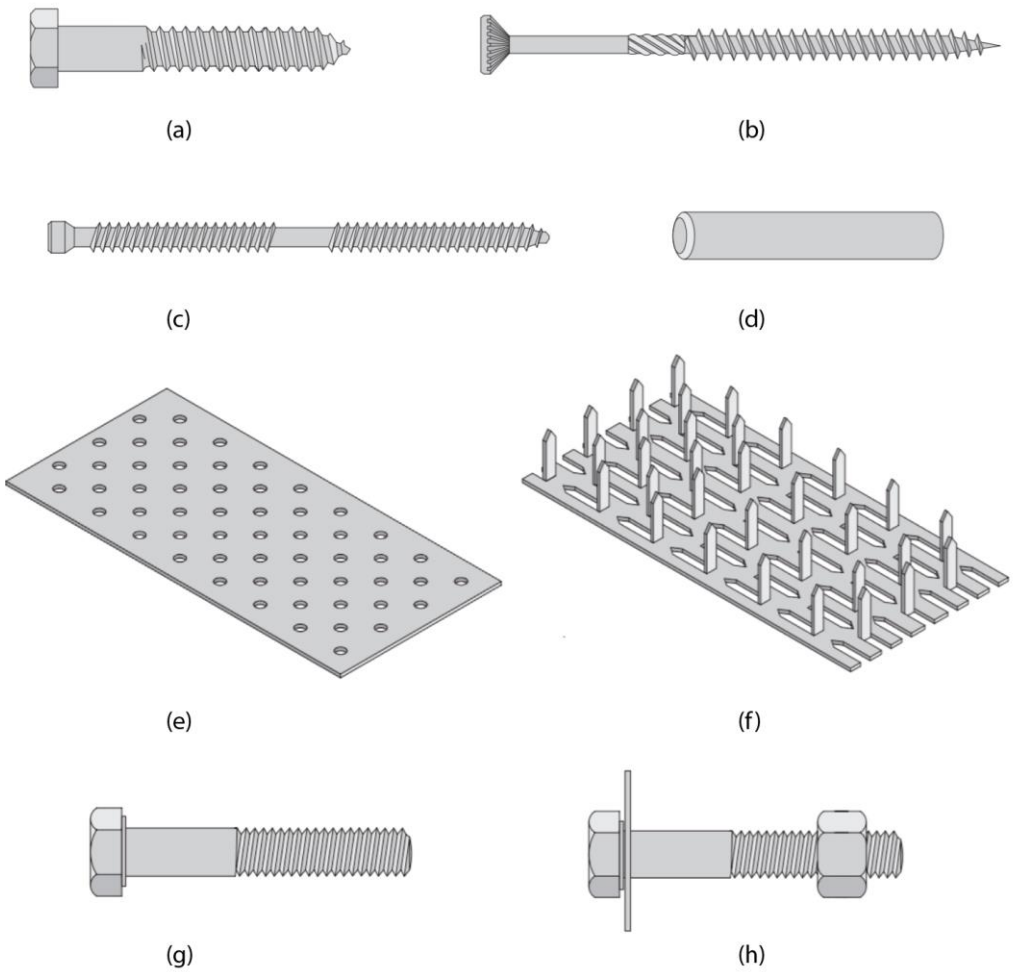

Figure 2.21 Different types of timber connections (a) Hexagon head wood screw, (pre-drilling required), (b) Countersunk head wood screw, (c) Double threaded wood screw, (d) Dowel, (e) Nail plate, (f) Punched metal plate fastener, (g) Bolt, (h) Bolt with washer and nut (Swedish Wood, 2016).

When a dowel joint is loaded it can fail in different modes, based on Johansen's yield theory. The assumptions in Johansen's theory are rigid-plastic behavior of fasteners in bending and rigid-plastic behavior of the timber in embedding. Rigid-plastic behavior means that neither lateral nor axial deformation takes place at low value of loading.

2.6 Other considerations

This section gives information about other consideration that are also important when working with timber material in buildings.

2.6.1 Fire safety

Fire escape and fire resistance are two important aspects to ensure safety in case of fire accidents. For the former one, proper design of escape stairs and path need to be included in early design of plan layout. For the latter one the structural elements and joints need to have adequate resistance during the resistance time. 90 minutes is usually the requirement, while 120 minutes can be required for more important elements. For Oakwood Tower all the primary structural elements like columns, beams and walls are designed to have a resistance time of 120 minutes (Ramage et al., 2017). Considering the height up to 200m, the resistance time of 120 minutes might be practical for this design.

For timber, a charring layer close to the surface will be formed due to exposure to the fire, which will contribute to insulate the cross section in the core. The burning rate should be regarded as constant (SIS, 2009). Fire resistance should be designed following the procedures in SS-EN1995-1-2 and SS-EN1991-1-2. The resistance time, the resulting capacity of the effective cross section and the temperature should be verified. The effective cross section can be calculated by the simplified method and be calculated by the initial cross section area subtracted by the effective charring depth. The charring depth can be calculated by expression 2.3:

$$d_f = d_{char,n} + k_0 d_0 \qquad (2.3)$$

where:

d_f	is the effective charring depth
$d_{char,n}$	is the design nominal charring depth
$k_0 d_0$	is the depth of the weakened layer

The values of k_0 and d_0 are given in Section 4.2.2 in SS-EN1995-1-2 and the calculation procedures for the nominal charring depth in 3.4.3. Since the fire design is not the focus in this project the design details will not be presented here. However, the fire design for structural elements is of great importance.

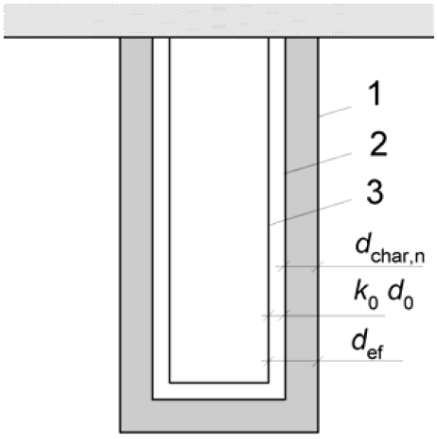

1: Initial surface of the structural member
2: Border for residual cross section
3: Border for effective cross section

Figure 2.22 Illustration of the residual cross section and effective cross section. Figure 4.1 in SS-EN1995-1-2 (SIS, 2009).

In strategy, mega structural members are better than a great number of elements of small size since the percentages of the remaining cross section are larger for structural members of large sizes, compared to those with small sizes, if the effective depth is the same for all. It was mentioned that the large sizes mega truss elements for the timber building Oakwood Tower have great significance in fire resistance (Ramage et al., 2017). With regards to the shape of the structural members a design principle applied in the timber tower research project led by SOM (2013) is to use simple shapes with high volume to surface ratio. A square cross section is preferred rather than rectangular. The design strategy for structural members regarding the fire safety can be to choose:

- Mega structural members
- Members with large volume to surface area ratio, for example, members in square cross section

Penetration and smoke control, sprinkle system, escape space etc. regarding fire safety should be included during the design process. Fire retardant paints and covering of the joints should be given consideration.

2.6.2 Sound and vibration issues of the floor

The low mass of timber can cause acoustic problems for wooden floor elements. CLT floor elements exist on the market which, when combined with sound insulation and sound absorption layers, can handle sound issues and satisfy sound requirements for residential housing and office buildings. The investigation to ensure that the floor slabs supported by the external structure and core walls without columns can fulfill the dynamic requirements are not included in this thesis, but by study of existing timber buildings and CLT products in the market, a span up to 10m is possible.

2.6.3 Daylight

A simple rule of thumb regarding the daylight in design is that the window area should be at least 10% of the floor areas (Boverket, 2019). In general, when the depth of the room, i.e., the distance from the windows to the deepest walls, is smaller than 5m, adequate daylight can be expected. In the range between 5m to 10m, the daylight can partly reach. Deeper than 10m, the condition of the daylight can be regarded as bad. (Ibrahim & Hyman, 2005). To simplify the analysis, a design with maximum depth of 10m was considered as acceptable in this thesis.

2.6.4 Vertical transportation

Transportation within a high-rise building relies heavily on the vertical transportation system consisting of elevator and stairs etc. A proper design of the number of elevators and what floor each of them can reach can greatly improve the efficiency of transportation. Calculation of the required number of lifts, lift speed and waiting time etc. by a lift specialist is required already in the early stage of the design process (MPA & fib, 2014).

In terms of accessibility, according to Boverket, the national board of housing, building, and planning of Sweden, the main rule is that for buildings with more than one floor there must exist one elevator that provides enough space for a person with wheelchair and assistant. For buildings with more than 4 floors, at least one rescue elevator that can fit stretchers is required. The required size for this kind of elevator is 1.1x2.1m. For buildings with more than 10 floors at least two such elevators are required. (Boverket, 2011). For office buildings, there might be additional requirement on the size of elevators with consideration to rush hours.

Turning Torso, the current tallest building in Sweden where most of the floors are used for residence and a few commercial usages, is provided with 5 elevators. In a previous investigation of the 200 m timber tower, various shapes of cores with 8 elevators and with minimum space of 2 m at the opening were studied. (Gyllensten & Modig, 2020). A core of approximately 10 m by 10 m should be feasible and was adopted in this thesis.

2.7 Structural design

The structural members should be designed both for ultimate limit state (ULS) and service limit state (SLS).

2.7.1 Design of the structure and the structural components in ULS

In the ultimate limit state, the structural components should be designed to provide sufficient capacity, verified according to Eurocode and EKS11. In Appendix E the relevant procedures can be found.

Some of the main ways to improve the structural performance in ultimate limit state are:

- Optimize the building geometry to reduce the loads acting on the building
- Optimize the geometry and structural systems to avoid shear lag for more evenly distributed stresses
- Optimize the building geometry and structural systems to make full use of the building depth to improve the global stiffness
- Optimize the cross section of structural components
- Use materials with higher strength
- Make use of the strength parallel to the grains which is usually the strongest direction for timber
- Avoid buckling of the structural components to ensure full use of structural resistance

2.7.2 Design of the structure and the structural components in SLS

In the design for service limit state the serviceability of the building should be controlled. The deformation and dynamic problem are two of the main issues that can cause damage of non-structural elements, comfort problems and difficulties in usability, appearance and so on.

2.7.2.1 Limitation for global deformation

Horizontal deformation is crucial for high-rise buildings. The horizontal displacement of the building and the relative story displacement can affect the façade cladding. This limitation needs to be confirmed with the façade engineers. In practice values between h/300 and h/500 have been used before (MPA & fib, 2014).

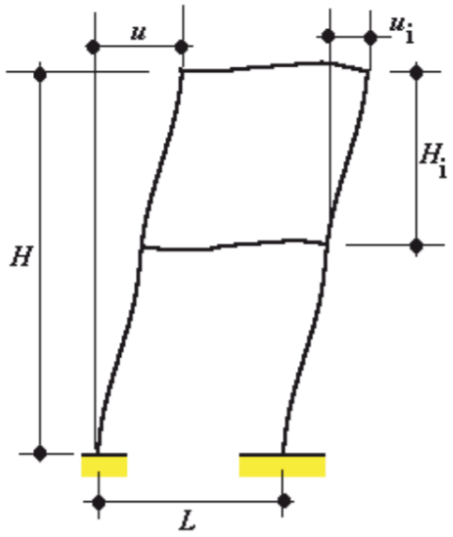

u: the maximum horizontal displacement of building
u_i: the horizontal displacement over one floor

Figure 2.23 Definition of horizontal displacement. Figure A1.2 in SS-EN1990. (SIS, 2002)

For the limitation h/500, the horizontal displacement of a building of 200 m should be limited to 400 mm, where for each floor it is about 6.5 mm.

The horizontal displacement of a building is a sum of that from bending deformation, shear deformation and deformation of joints.

The approaches to improve the structural behavior with regards to the global deformation are for example:

- Use stiffer material with higher modulus of elasticity and shear modulus
- Optimize building geometries and structural systems as mentioned before to improve ULS performance, to increase the global stiffness of the structure
- Stiffen joints and decrease joint slip
- Decrease the loads which trigger the horizontal displacements

2.7.2.2 Limitation for deflections for beams

Both the instantaneous and final deflections including creep for beams need to be controlled.

Table 2.1 Limitations for deflections for beams. Table 7.2 in SS-EN 1995.

	w_{inst}	$w_{net,fin}$	w_{fin}
Beam on two supports	ℓ/300 to ℓ/500	ℓ/250 to ℓ/350	ℓ/150 to ℓ/300
Cantilevering beams	ℓ/150 to ℓ/250	ℓ/125 to ℓ/175	ℓ/75 to ℓ/150

The verification should be conducted according to Eurocode. In this thesis the deflection of the individual structural components is not considered, and the focus is on the global behavior.

2.7.3 Dynamic design in SLS

The design and criteria to achieve satisfying vibration behaviors in the service limit state shall consider the receivers, which can be categorized as the structure, the building content, and the comfort of users. The detailed criteria are specified in the same international standards SS-ISO-10137 which is applicable for Swedish standards as well. Regarding the comfort of users, the peak acceleration is a very important variable, the users' sensibility to it varies with the frequency of the building. (SIS, 2008). The guidance for human response to wind-induced motions is attached in Appendix C in SS-ISO-10137.

Figure 2.24 shows the evaluation curves for wind-induced vibrations for buildings in horizontal directions for one-year return period, where curve 1 is for office buildings and curve 2 for residential buildings. The peak acceleration of the target floor should not exceed the evaluation curves in the structural direction (in along wind and cross wind directions) and in torsion. The peak acceleration in torsion should be recalculated to the translational torsional acceleration as $r \cdot A_\theta(t)$, where r is the distance to the torsional center and $A_\theta(t)$ is the angular acceleration in torsion. (SIS, 2008).

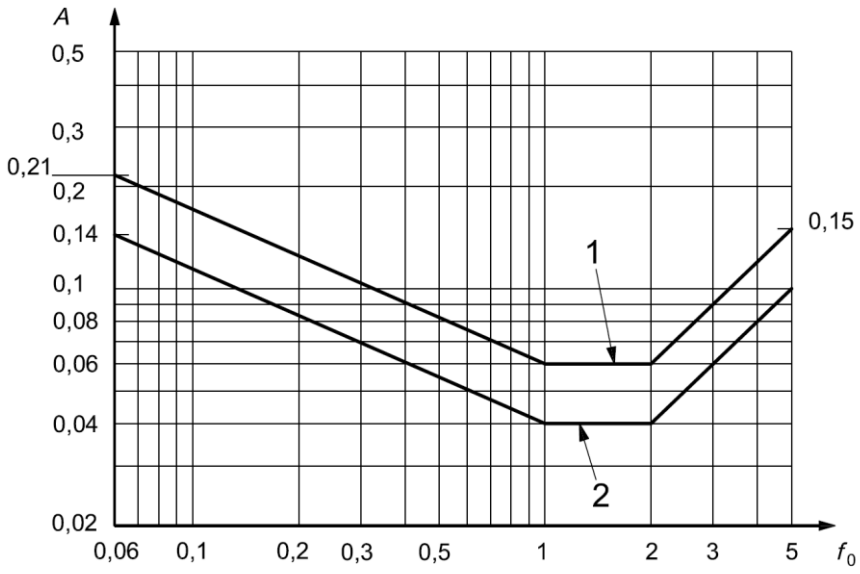

A: the peak acceleration m/s^2
f_0: the first natural frequency Hz

Figure 2.24 the evaluation curves for wind-induced vibrations. Curve 1 for office and curve 2 for residence. (SIS, 2008).

The wind velocity for 1 year return period can be determined by the following equation according to ISO 6897 (SIS,2008):

$$\upsilon T_a = 0.75\upsilon_{50}\sqrt{1 - 0.2ln(-ln(1 - \frac{1}{T_a}))} \qquad (2.3)$$

where:

T_a is the number of years, set to 1 year for the evaluation of comfort criteria

υ_{50} is the characteristic value of the reference wind velocity, given in *EKS11*

The peak acceleration can be determined by Equation (2.4) according to *EKS11*.

$$\ddot{X}_{max}(z) = k_p \cdot \sigma_{\ddot{X}}(z) \qquad (2.4)$$

where:

$\ddot{X}_{max}(z)$ is the peak acceleration, see Appendix F

k_p is the peak factor, calculated by expression (C.7) in Appendix B

$\sigma_{\ddot{X}}(z)$ is the standard deviation of the acceleration, calculated by expression (G.2) in Appendix F

The complete calculation procedure can be found in Appendix F. In the calculation for peak acceleration, the value for the mechanic damping of 9% was applied.

The mass, damping coefficient, lateral stiffness and the structural response of lateral displacement are key factors in the dynamic problem of a building. Larger mass, lateral stiffness and damping are favorable when it comes to the dynamic behavior. For improvement of the dynamic behaviour, the most efficient ways summarised by Gyllensten & Modig (2020) are:

- Increase mass when the eigenfrequency is smaller than 1Hz
- Introduce damping when the eigenfrequency is between 1Hz and 2Hz
- Increase the structural stiffness when the eigenfrequency is larger than 2Hz

3 Geometry study

In this section various volume geometries were modeled, and the structural behavior, consumed material and obtained rental area were compared, among which one promising alternative was selected for further study.

The research process is shown in Figure 3.1 below. The procedures labeled with dashed lines present the geometry generation method and geometries created for analysis. Those with solid lines stand for analysis conducted where those in red are finite element analysis.

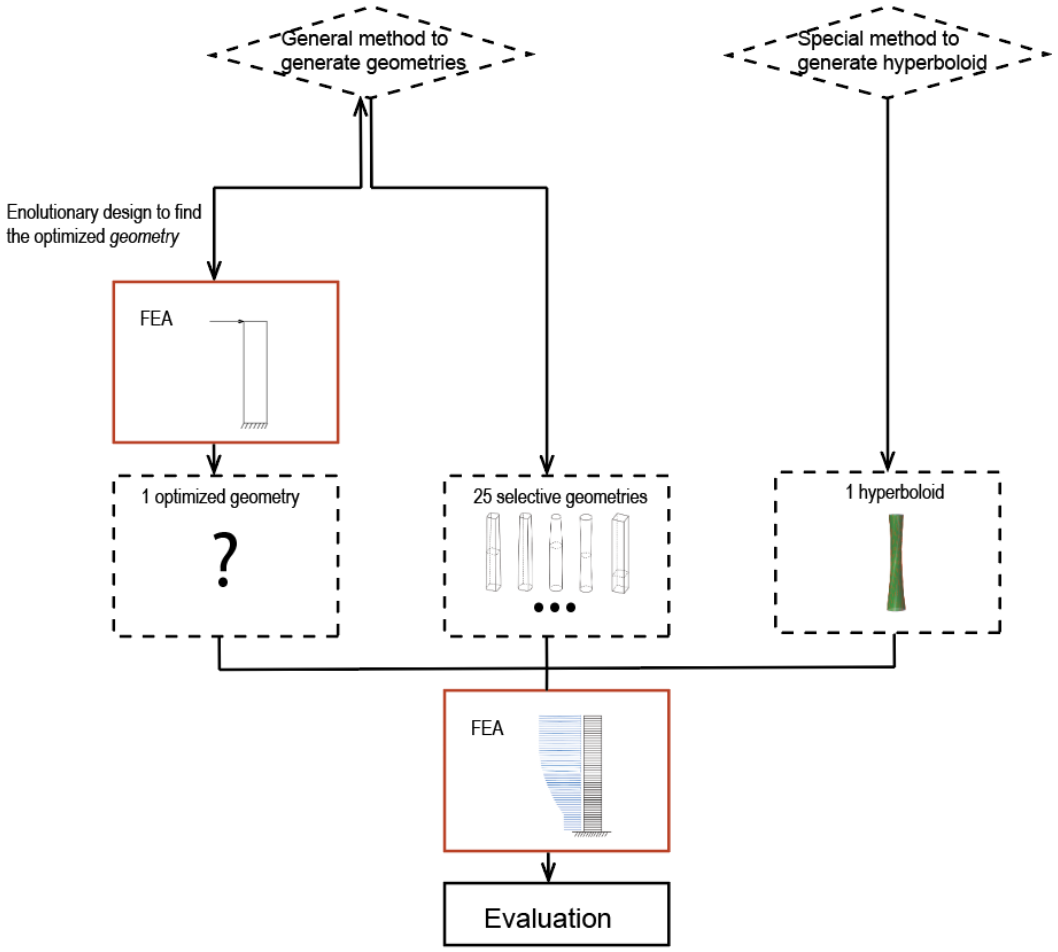

Figure 3.1 Work process for geometry study

The general method was applied to parametrically control all geometries expect the special hyperboloid, presented in Section 3.1. By this method countless geometries can be created and it is not possible to manually study all of them. By the optimization algorithm *Galapagos*, see in Section 3.4.1, with its evolutionary design, the inputs parameters that govern the shape can be optimized for minimum defection. Due to the large amounts of computation that occur during the evolutionary process, the structural model was simplified to have only one point load on the top edge, which differs from the real situation where the wind load is exponentially distributed over the height. The best solution that causes minimum tip displacement was kept for further study, see Section 3.4. Apart from this, 25 geometries combined with various

façade curvature and plan sections were manually selected for study to get a deeper and more intuitive understanding, see Section 3.5.

Hyperboloid geometry can in theory be a promising one due to the potential for straight load paths. It has surfaces that are doubly ruled and for each point on the surface there are always two crossing straight lines that lie on the curved surface. This was generated in its own special way and one applicable case was chosen, see Section 3.6.

Thereafter all these 27 geometries will be analyzed with FEM with distributed wind loads. The result will be compared and evaluated according to a series of criteria, see Section 3.7 and Section 3.8.

3.1 Parametric volume geometry

As discussed in Section 2.3, square plans with various roundness of corners were chosen to be investigated. Volume geometries were determined by the combination of shapes in plan and facade curvature.

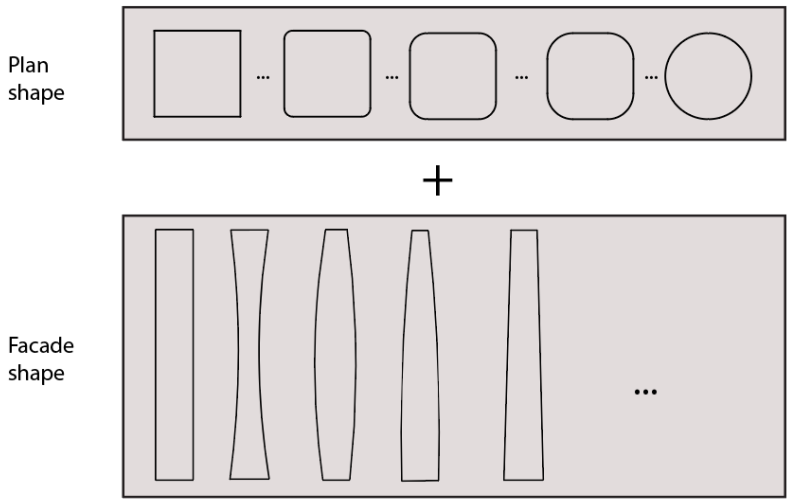

Figure 3.2 Geometries as combination of a plan shape and a facade contour, where the plan shape is chosen from squares with rounded corners. When the radius is equal to 15 the plan is circular. The facade contour is either hyperbolic or linear in the height direction.

Since the geometries are controlled by the parameters it is possible to make investigations into all potential geometries within the domain, rather than the predetermined geometries presented above. The controlling parameters and geometry-generating process are illustrated in Figure 3.3.

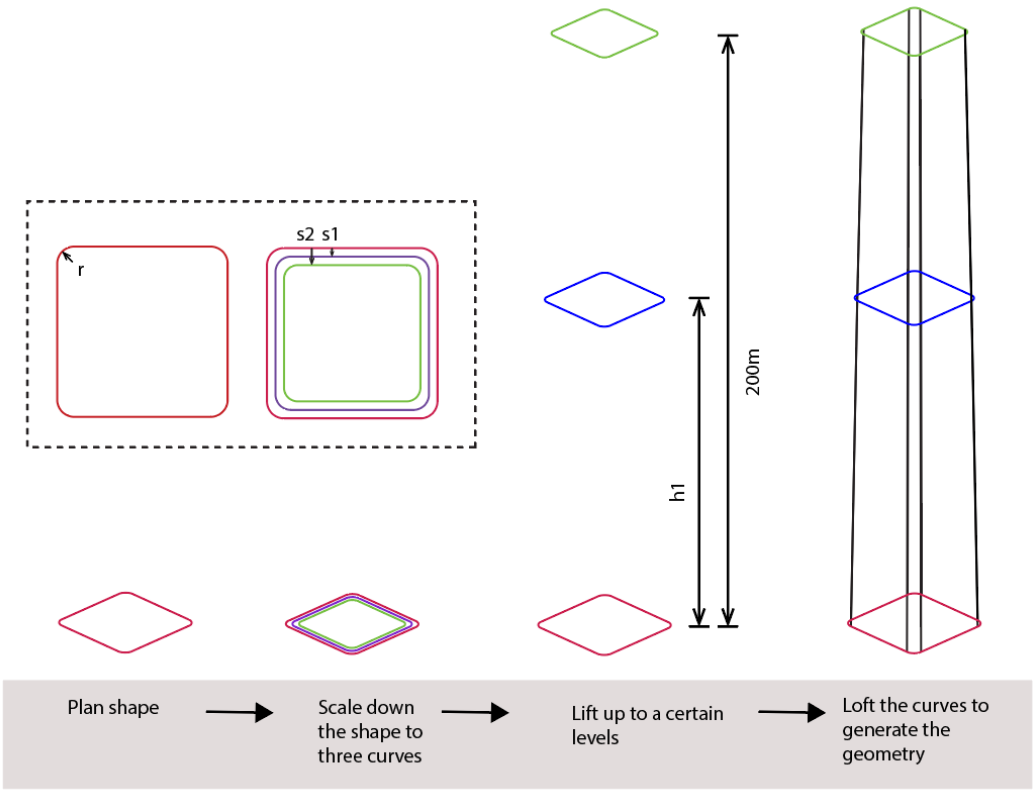

r: radius of the rounded corner
s1: scale of the in- between curve
s2: scale of the curve on the top
h1: height of the in- between curve

Figure 3.3 Parametrized geometry. The generation of the geometry is determined by four parameters: roundness of the corners, scales of upper two controlling curves and height of the curve in the middle.

Several examples are presented as follows:

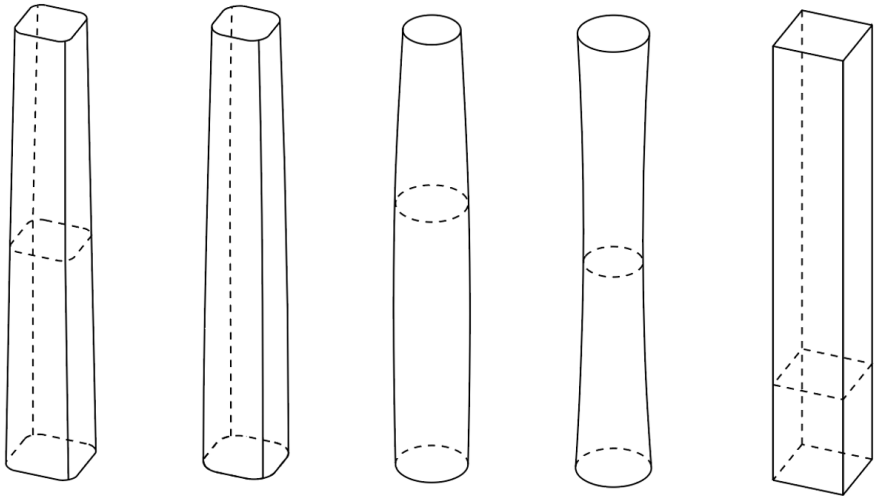

r: 6	r: 9	r: 15	r: 15	r: 0
s1:0.9	s1:1	s1:1	s1:0.83	s1:1
s2:0.8	s2:0.8	s2:0.8	s2:0.95	s2:1
h1:100	h1:0.01	h1:120	h1:52	h1:20

Figure 3.4 Several examples of geometries and the corresponding parameters

3.2 Structural model

Though in reality the structural behavior of a high-rise building, subjected to both gravity load and exponential distributed wind load, is quite complicated, several simplifications can be made in this early stage to simplify the evaluation.

3.2.1 Simplified structural model

As discussed in Section 2.4, the external system is supposed to resist the lateral load as a cantilever beam. The modelling of the complex stabilizing structure was simplified to a tubal structure. Also, in this early stage, the precise load and material properties are not essential, as long as different alternatives of geometries can be sufficiently compared to each other. For a cantilever beam with identical cross section along axis and constant stiffness EI, the lateral stiffness of the structure can be reflected to a great extent by the end deflection. In the present case when the stiffness varies over the height due to the various geometries and the wind load is not evenly or linearly distributed over the height, the structural behavior can be more complex. But the global stiffness can be still reflected by the maximum horizontal displacement at the top and/or the average horizontal displacement.

The wind loads act directly on the enveloping surfaces of the building by the wind pressure, varying from windward side to the leeward side. In this study it is the global structural behavior that is interesting rather than the local effect, therefore a resulting wind force on each diaphragm floor is sufficient to estimate the global structural response. Since the wind loads increase over height and the cross section of the building geometry varies, the interaction will be more complex. The result will be more reliable if the distributed wind forces over height can be more precisely estimated, rather than simplified as being uniformly distributed. The structural model was therefore simplified to a tubal shell structural connected by stiff floor slabs with distributed wind forces anchored at each floor level (see Figure 3.5(b)).

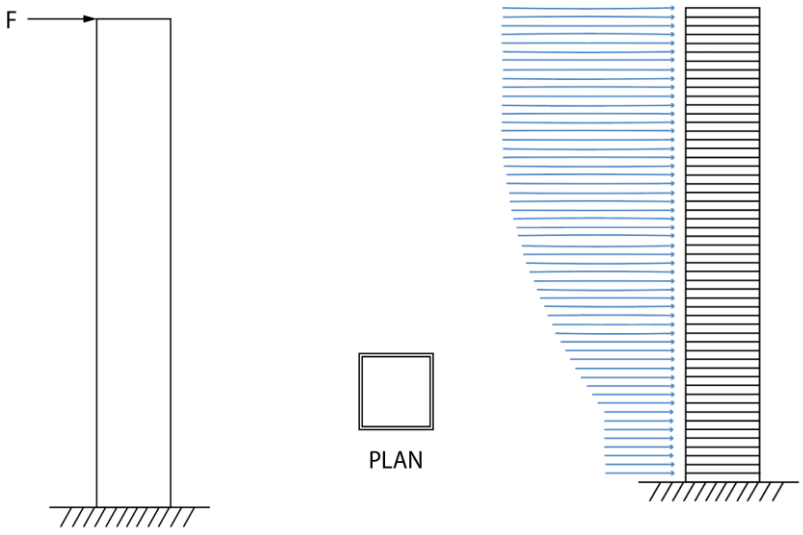

Figure 3.5 Simplified structural model. A tubal structure (of square cross section as an example here) subjected to (a) a lateral point load. (b) Distributed point loads on each floor. The structure is fixed at the base.

The evolutionary design requires significant computing resource because of the great number of models that need to go be run through. In order to avoid overly long computation times for this, the structure is further simplified to have a single point load applied on the top edge of the structure in the mass screening of parametric geometries during the evolutionary design, see Figure 3.5(a). By this all the other diaphragm floor slabs, except the one on the top where the point load acts on to efficiently activate the bending deformation, can be neglected and the number of meshes included will decrease dramatically, saving large amounts of computation time. Note that this model will only be used to get a single optimized geometry from the mass screening in the evolutionary design. The optimized geometry obtained from this process will thereafter be further analyzed with all other geometries according to the structural model with exponentially distributed wind forces, see Figure 3.5(b).

The influence of the simplification in evolutionary design has been controlled, see in Appendix C4. This simplification might be a good balance between the precision and computation efficiency.

3.2.2 Properties of elements

The slabs were assumed to be so rigid that the point load will be transferred axially to the flanges and be carried mainly by the bending of the tube, not by the deformation of the slabs themselves. In order to achieve this effect, a fictive slab with a very small thickness and large modulus of elasticity was adopted. The Poisson's constant of the slab was set to 0 to avoid the influence of transverse deformation.

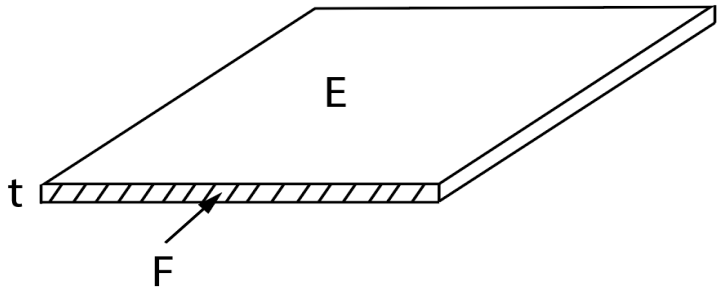

Figure 3.6 Floor slabs. If the thickness of the slab is small enough and the modulus of elasticity large enough, the bending stiffness EI can be sufficiently small compared to the axial stiffness E, so that the load can be regarded to be carried only by the axial resistance.

For the tubal structure, usage of isotropic material is sufficient to evaluate geometries, though for a truss or frame structure the stiffness in different directions can differ. Since both shear deformation and lateral bending deformation are involved the relative bending stiffness and shear stiffness may influence how the structure behaves globally. There is uncertainty as to what extent this will affect these slender geometries, where bending dominates. The equivalent membrane Young's modulus and shear modulus for diagrid trusses with given angles and sizes of truss members were applied in this study, by using "diagrid structure equivalent elastic orthotropic membrane method" (Shi & Zhang, 2019).

The equivalent membrane modulus for trusses can be calculated from:

$$E = \frac{2E_d A_d sin^3\theta}{bt} \quad (3.1)$$

$$G = \frac{2E_d A_d cos^3\theta tg\theta}{bt} \quad (3.2)$$

where:

E	is the equivalent modulus of elasticity
G	is the equivalent Shear modulus
E_d	is the axial modulus of elasticity the truss beam
A_d	is the area of cross section of the truss beam
b	is the width shown in Figure 3.7
θ	is the angle of diagrid element, shown in Figure 3.7
t	is the equivalent thickness of the membrane element

The angle and height h, see Figure 3.7, for calculation are assumed to be 65 degrees and the height over two floors approximate 6.4m. The cross section of the truss element is assumed to be 1m^2. Note that the actual equivalent Young's modulus and shear modulus varies after the design of truss system. The relative bending respective shear stiffness is affected dominantly by the angles of diagrids.

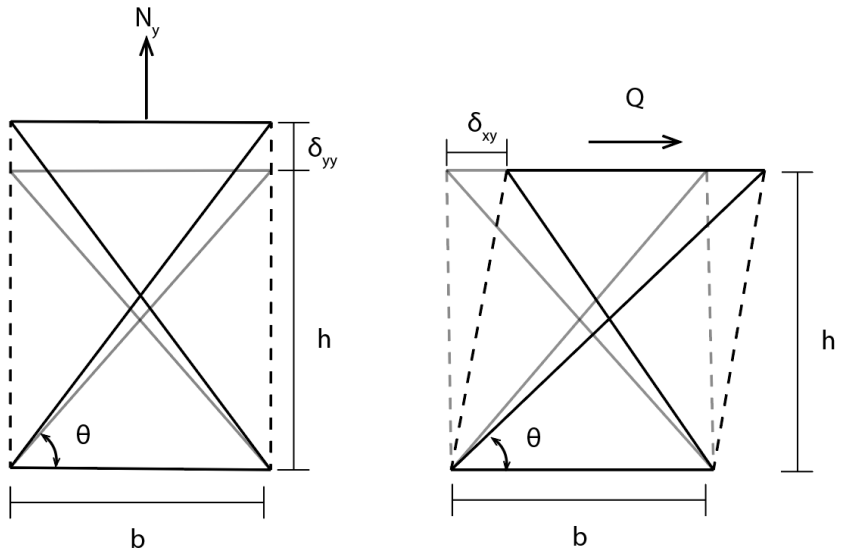

Figure 3.7 Illustration of deformation of diagrid element and equivalent membrane element. (a) Axial deformation (b)Shear deformation (Shi &Zhang, 2019)

3.2.3 Load

Only wind loads were included in structural models for geometry study.

The wind loads applied on the top was calculated according to *EN 1991-1-4*. The wind force acting on a structure can be calculated by the expression:

$$F_w = c_s c_d \cdot c_f \cdot q_p(z_e) \cdot A_f \qquad (3.3)$$

By discretization:

$$F_w = c_s c_d \cdot \sum c_f \cdot q_p(z_e) A_{ref} \qquad (3.4)$$

where:

$c_s c_d$ is the structure factor, set to 1 in this study
c_f is the force coefficient, see Appendix A
$q_p(z_e)$ is the peak velocity pressure at reference height z_e, see Figure 3.8
A_f is the reference area of the structure or structure element, see Figure 3.9

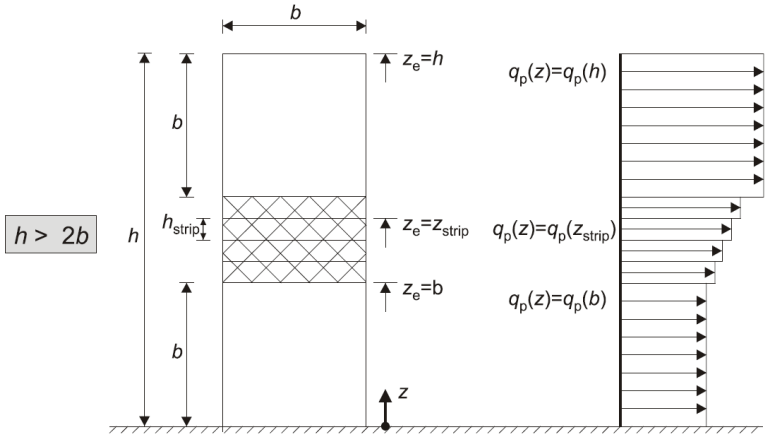

Figure 3.8 Distribution of $q_p(z_e)$ over height

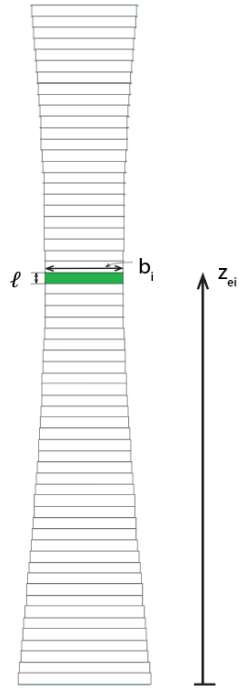

Figure 3.9 Illustration of discretization of the reference area.

It was observed that the force coefficient and the reference area differ with regards to varying geometries. When the discretization method is applied to handle the peak velocity pressure that varies over height, the distribution of peak velocity and discretized strip area, as seen in Figure 3.9, together will cause different effect on wind forces on different geometries. For building in form of cylinder the peak velocity pressure can affect even the force coefficient, meaning that the force coefficient varies in height. To simplify the calculation this effect was ignored, and force coefficient was calculated with a constant building width 30m. Apart from this the structural factor was set to 1 for all geometries. The detailed calculation of wind loads can be found in Appendix B.

The calculation of the force coefficient with regards to different cross sections was conducted in line with *EN 1991-1-4*, see Appendix A, with mentioned simplifications. The following values was adopted for wind load calculation.

Figure 3.1 Force coefficient for modifications of cross section

Cross section: roundness radius of corners r	Force coefficient c_f
0-3(square with sharp ends)	1.4
3-6	1
6-14	0.7
14-15 (circle)	0.5

In the calculation with only one individual point load on the top end for evolutionary design, the magnitude of point load was calculated as:

$$F_w = c_f \cdot c_{Af} \cdot F_b \qquad (3.5)$$

where:

F_b is a basic wind load

c_f is the force coefficient defined in *EN 1991-1-4*

c_{Af} is the ratio of the reference area to that of a benchmark reference area, i.e., 30m x 200m

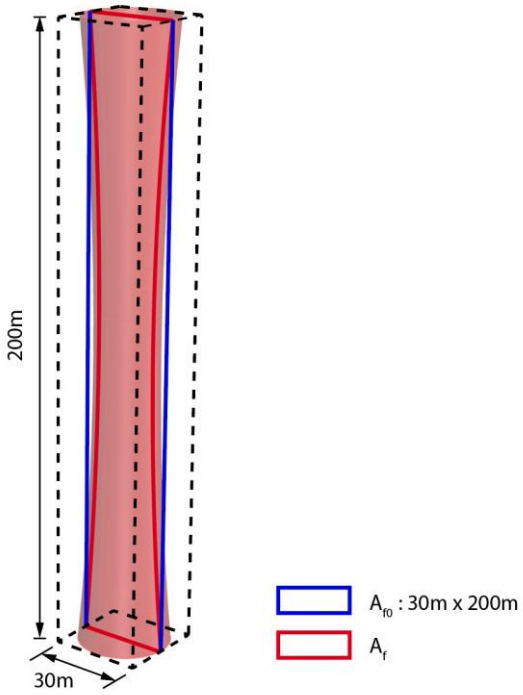

Figure 3.10 Illustration of the reference area of a structure and the benchmark reference area

c_{Af} is defined as:

$$c_{Af} = \frac{A_f}{A_{f0}} \qquad (3.6)$$

where A_f is the actual reference value while A_{f0} is the benchmark reference area of a building with dimension 30m x 30m x 200m, i.e., 6000m^2, see Figure 3.10 above.

3.3 Finite element models for the general analysis

The parametric geometric models built in Grasshopper were then further developed and assembled to finite element models with the help *of Karamba 3D*. A convergence study was conducted. The models were verified by comparison to hand calculations.

3.3.1 Structural elements

The structure includes a tubal structure and slab elements. Both are modeled as shell elements in FEM models as seen in Figure 3.11.

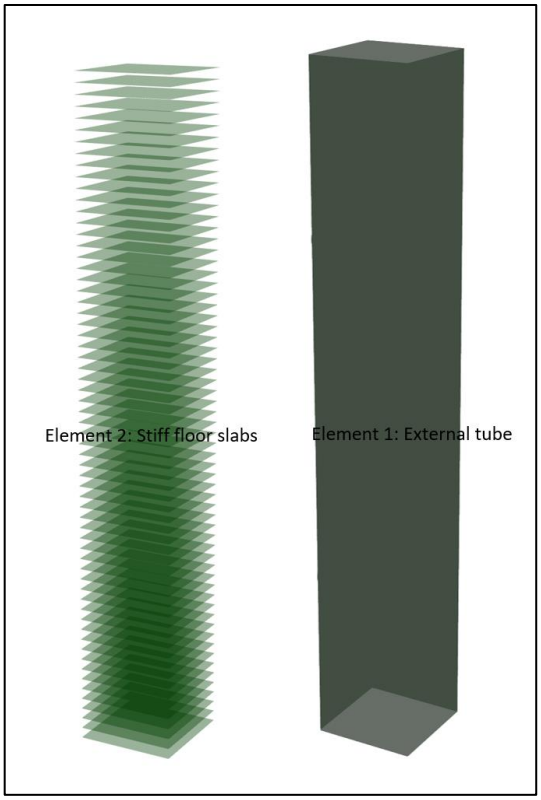

Figure 3.11 Structural elements in FE model for the geometry analysis

The features of both the tubal structure and slabs were modeled in line with the principles described in Section 3.2.2. Theoretically the stiffness of Element 2 (top slab/floor slabs) should be infinite large. However, excessively large values of this can lead to unreliable results due to numerical errors in the FE calculation.

Cross sections and material properties for respective structural elements shown in Table 3.2 were applied showing a reliable structural response.

Table 3.2 Cross sections and materials for structural elements

Element 1 :External tubal structure	
Cross section	Shell constant [50 cm]
Material	E: 10480MPa G: 2278MPa
Element 2: Slab(s)	
Cross section	Shell constant [1 cm]
Material	E: 105000MPa G: 52500MPa

3.3.2 Boundary condition

The boundary conditions are presented as follows in Figure 3.12:

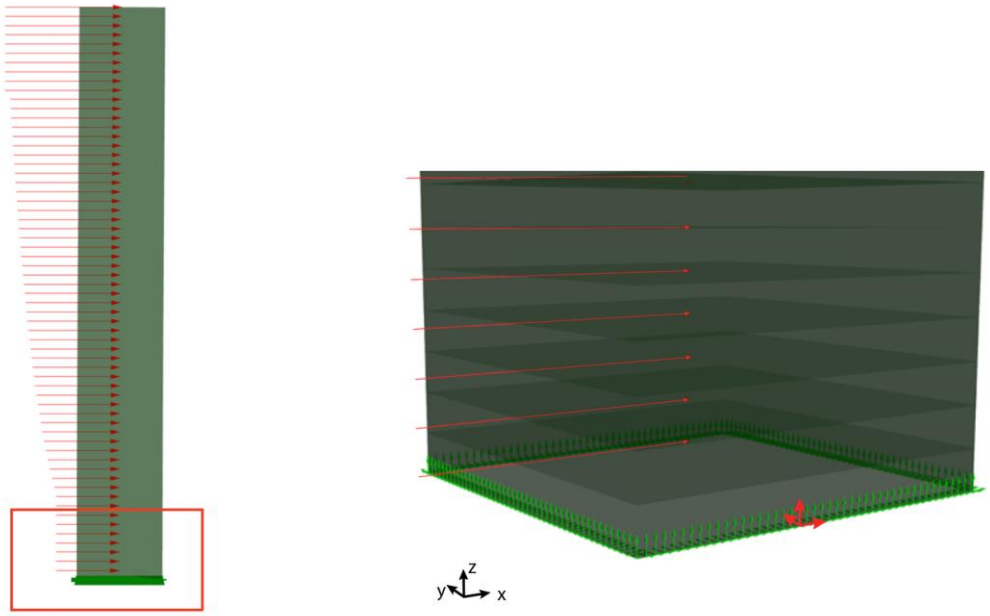

Figure 3.12 Support conditions where nodes on the bottom are fixed in x-, y- and z-direction.

The nodes on the bottom are constrained from displacement in all x-, y- and z-directions.

3.3.3 Loads

The loads acting along the x direction and in diagonal were considered. The magnitude of the load was assigned as described in Section 3.2.3. Since element 2, i.e., the roof slab on the top/floor slabs were constructed to behave like a rigid body by assigning an appropriate material, the concentrated loads can be transferred to the shell element uniformly. This was examined by the results where no evident local deformation was observed. The translation of the nodes included in the same slabs are the same. Therefore, the introduction of a single point load on the top edge/each floor slab in the FE model can be sufficient to simulate the global deformations.

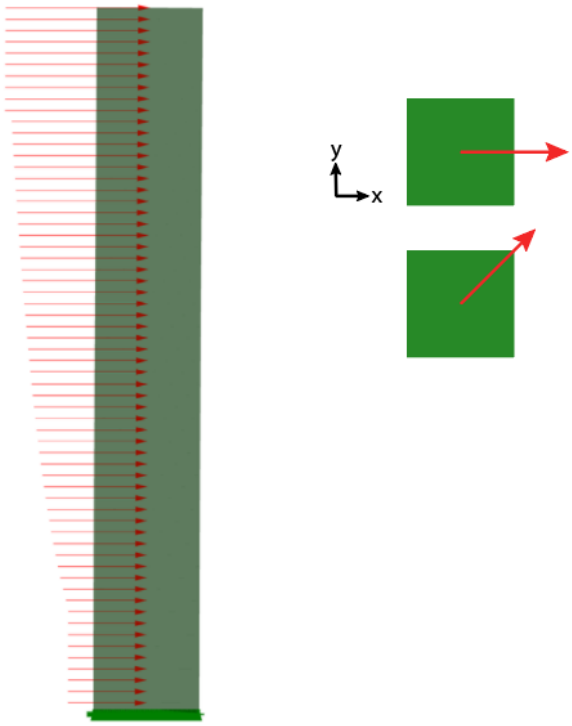

Figure 3.13 Loads applied in FEM model

3.3.4 Mesh

The quality of the mesh is important in the FE analysis, affecting not only the speed of the calculation process, but also the precision of the result. In Karamba 3D, interaction between different parts of the model is based on the common nodes. In order for the model to perform globally as a whole, it is essential that the tube and the slabs are rigidly connected by common nodes. Therefore, the peripherical nodes on the tubal element located at each floor level should be included in the nodes for slabs as well.

The shell elements for the tube and slabs were converted to meshes by the component *mesh breps*, making it possible to mesh from given points, common nodes that sit at the connection of elements. The size of meshes are mainly controlled by mesh resolution where 1m was used.

Meshes for the tubal structural were generated by *Mesh Surface* which can precisely control the number of quad elements in each local direction. A convergence study for the models with the top slab and the tubal structure was carried out and can be seen in Appendix C2., showed that a mesh size of 1m is sufficient for this type of structure.

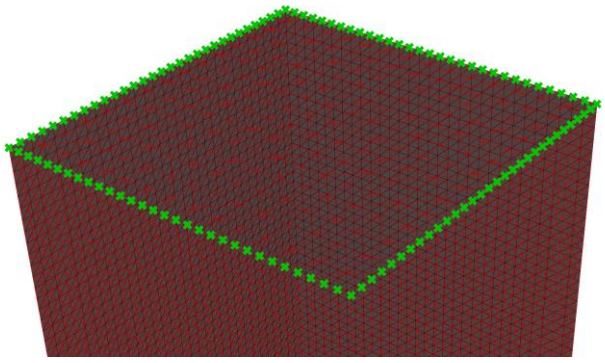

Figure 3.14 Example of common nodes for the top slab and the tubal structure. The same arrangement was used for other slab elements as well to ensure good interaction between them

3.3.5 Verification of FE models

From the results it was observed that the displacements for all the nodes on the top slab are identical, meaning that the slab works as a rigid body as expected. The FE models was verified by comparing end displacement to hand calculation of displacement of cantilever beam with both circular and square constant cross section, subjected to a point load. The verification shows that the result of deflection from hand calculation is slightly smaller than that from FEA. This can be explained by the fact that in hand calculation only bending deformation and not shear deformation was included. The deviation is smaller than 5% for both cases and can be regarded as within tolerance, see Appendix C3.

3.4 Evolutionary design

The algometric component *Galapagos* in Grasshopper was run to get an optimized geometry.

3.4.1 Optimizing algorithm

Galapagos is a plug-in tool for generative design. There are two inputs that must be defined in order to run it:

The genome: variables that generate various objects for analysis
The fitness function: parameter that need to be optimized (maximized or minimized)

Figure 3.15 Evolutionary computation component from Grasshopper

In the present analysis the genomes are r, s1, s2 and h1, as shown in Figure 3.3 and the fitness target is the end horizontal displacement on the top.

There are two different optimizing algorithms inside *Galapagos*. They are evolutionary solver and annealing solver, where the former one was used. In this process genetic populations in the next generation are generated mainly from a given number "best" populations in the former generation. Settings of the evolutionary computation are presented in figure 3.16.

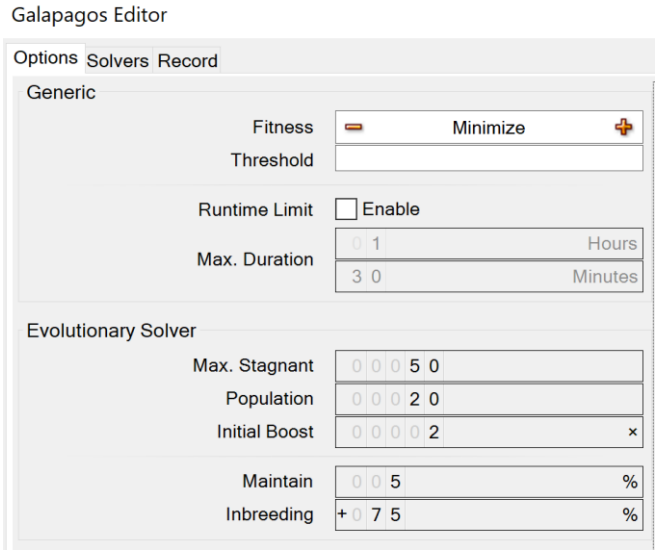

Figure 3.16 Settings for evolutionary computation in Galapagos

3.4.2 Description of the models used in geometry optimization

As mentioned before, the evolutionary design requires large computational resources. The FEM model for evolutionary design, shown in Figure 3.17, consists of one tubal structure (Element 1) and a rigid top slab (Element 2).

One single point load on the top (see Figure 3.18) was applied to save the computation time. Shape effect was included, and basic load value applied is 500kN. The final wind load included in calculation is according to equation (3.5).

One mistake would be that the loads in the diagonal direction, supposed to be the weak direction, was not included and in theory for the building with square section should have much worse structural performance with regards to lateral displacement. On the other hand, the wind acting on the structure is smaller in the diagonal direction as well and the effect of the shape factor was supposed to be included in the optimization process. Later analysis showed that for all geometries chosen for analysis, including the optimized one from evolutionary design presented in Figure 3.23, the horizontal displacement is not significantly larger when the structure is subjected to wind forces in diagonal direction than that in x direction when the same magnitude of wind forces was applied and the omission of this may not significantly influence the result from this section.

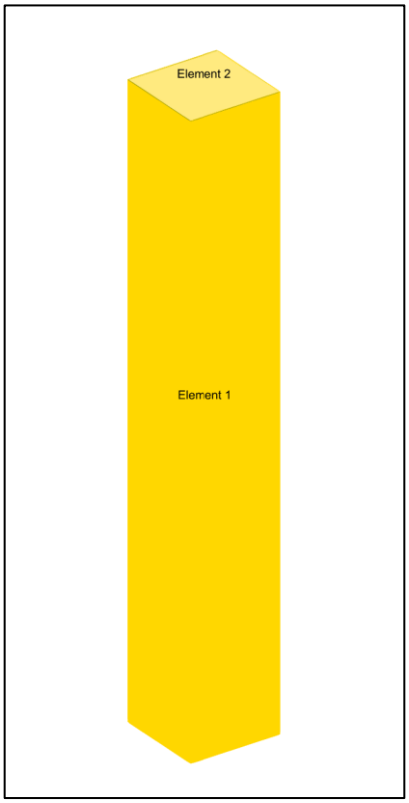

Figure 3.17 Structural elements in FEM model for evolutionary design

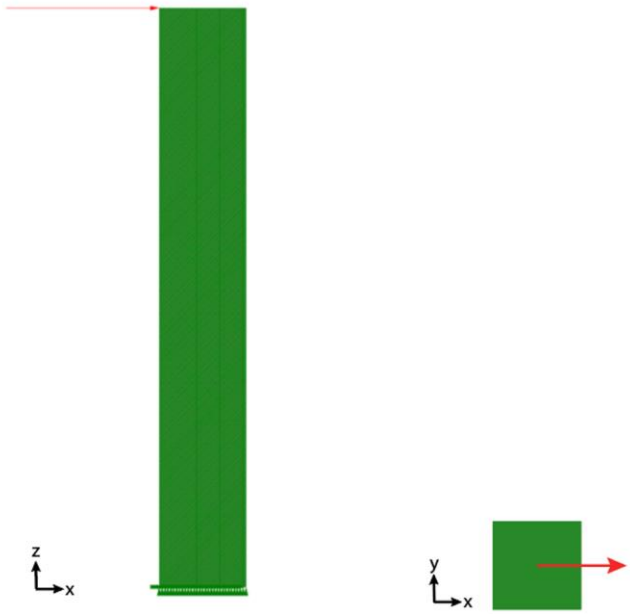

Figure 3.18 Loads in FEM model for evolutionary design

Due to the lack of the time to update and re-run the study of this part, the materials assigned for this part differ from those in the subsequent general analysis.

The material properties presented in Table 3.3 were applied. The material properties adopted for the tubal structure corresponds that of steel. This corresponds with a truss module with a size of approximate 1.6x1.6m and angles of 83 degrees. The assumed h, see in Figure 3.8, is height over 2 floors.

Figure 3.3 *Material properties for tubal structure and the top slab in evolutionary design*

Element 1 :Tube	
Cross section	Shell constant [50 cm]
Material	E: 210000MPa G: 80760MPa
Element 2: Slab	
Cross section	Shell constant [1 cm]
Material	E: $210 \cdot 10^{13}$ MPa G: $105 \cdot 10^{13}$ MPa

It is observed that the different assignment of material properties and loads influence the magnitude of deflections but the influence on the relative deflections between different geometries are quite minor, see Appendix C4. The result from this part can be regarded as reliable.

Unlike in the general analysis of all geometries, the tubal shell element was transformed to meshed by *mesh surface* while there is only one set of common nodes aligned with the connection curves between the top slab and the tube, by which the pattern of meshes will be more under control and regularly placed. The density of meshes is controlled by the number of quads elements in each local direction. The quads later were divided into triangular elements.

The corresponding mesh size is 1m for the tube. Convergence study can be found in Appendix D2.

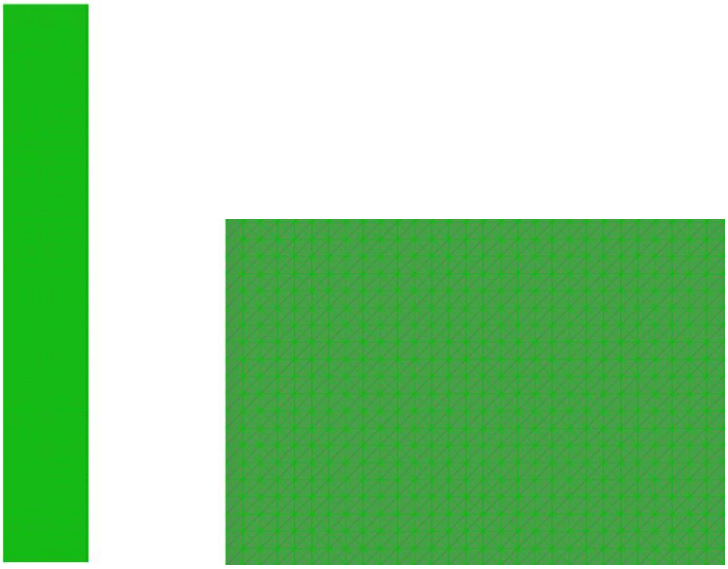

Figure 3.19 Mesh density: The mesh resolution was set to 1m

The mesh on the top slab was generated by *Mesh Breps* in order to incorporate the nodes on the top edge of the tube for rigid connection between them. A mesh size of 2m was deemed to be sufficient and therefore applied to further speed up the optimization process.

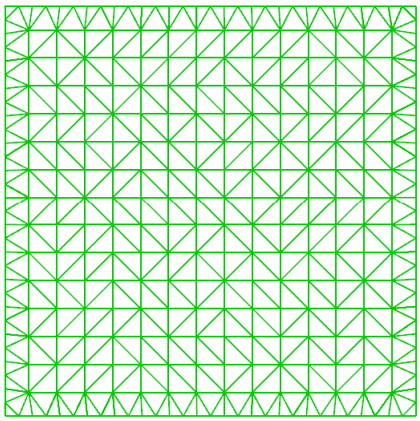

Figure 3.20 Mesh density of top slab. Mesh resolution 2m

3.4.3 Optimized geometry

A total of 11 generations were developed in *Galapagos* by the evolutionary solver.

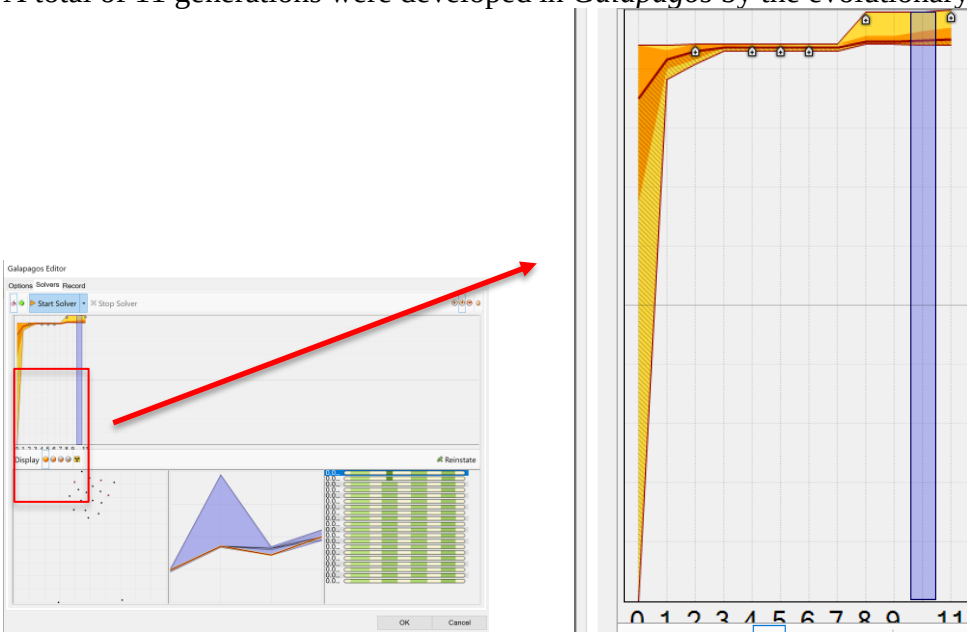

Figure 3.21 Fitness over generations

The fitness over generations in Figure 3.21 above showed that the fitness values among populations is approaching convergence already at generation 3. The genetic properties and the fitness are stable over generation 3- 7. In generation 8 the extreme fitness on the lower side drops dramatically while the rest of the fitness values among the same generation are still centralized. By checking the value and the visualized model in Rhino, the structure deforms in the opposite direction to the force load, which might come from the singularities, leading to invalid results. The fault source is of large probability due to the extreme large elastic modulus of the top slab.

The parameters r, s1, s2 and h are fluctuating around a specific converged value. The corresponding parameters and results after a careful mesh study are:

Table 3.4 Parameters and results for the optimized geometry from evolutionary design

Parameter				Result		
r [m]	s1 [-]	s2 [-]	h1 [m]	Displacement at top floor [m]	Average displacement of all floors [m]	Rental area [m^2]
6	1	0.8	44	0.001199	0.000457	48054

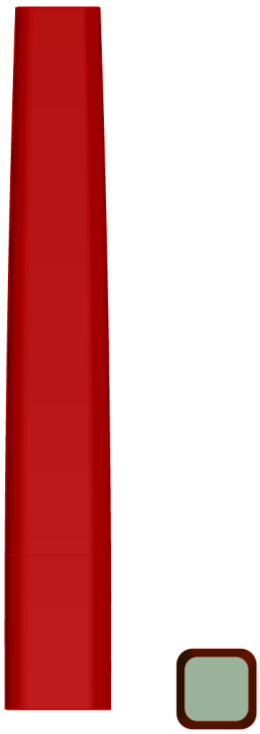

Figure 3.23 *The optimized geometry from evolutionary design*

The aim of this study is only to find optimized geometries through a mass screening of parametric geometries. For later comparison this optimized one will be further analyzed with the same material and loads and together with? all other geometries to ensure the comparability. Some of the examples extracted from different generations can be found in Appendix C5.

3.5 Typical geometries

A series of geometries were created in line with the method described in Section 3.1. These geometries are numbered in Figure 3.24 where those in the same column share the same façade shape and those in the same row have common plan section. Controlling parameters for these geometries can be found in Table 3.5 and the perspective view of the geometries can be found in Appendix C1.

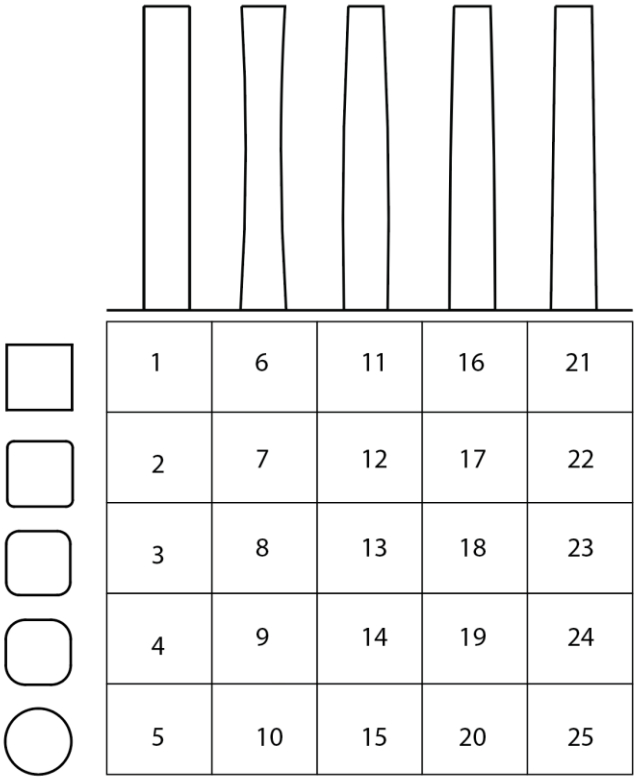

Figure 3.24 Numbering of representative typical geometries.

Table 3.5 Parameters for modelling of 25 typical geometries

	r	s1	s2	h1
Model 1	0	1	1	-
Model 2	3			
Model 3	6			
Model 4	9			
Model 5	15			
Model 6	0	0.83	0.95	52
Model 7	3			
Model 8	6			
Model 9	9			
Model 10	15			
Model 11	0	1	0.8	120
Model 12	3			
Model 13	6			
Model 14	9			
Model 15	15			

Model 16	0	1	0.8	0.01
Model 17	3			
Model 18	6			
Model 19	9			
Model 20	15			
Model 21	0	0.9	0.8	100
Model 22	3			
Model 23	6			
Model 24	9			
Model 25	15			

3.6 Hyperboloid

With the method for generation of geometries described in Section 3.1, most concave shapes will be included. However, there must be continuous straight line that connects the top and bottom plans for a concave shape to be a hyperboloid. In fact, a hyperboloid with a doubly ruled surface has two distinct lines in each point on the surface. It is not always ensured that hyperboloids are included in the analysis. Specifically for the evolutionary design presented in Section 3.4 because concave shapes have generally worse structural behavior with regards to the lateral displacement, which was optimized for, therefore some gene features such as smaller waist (smaller value of s2) might not be inherited and lost during the generations. To make sure that hyperboloid, which might be potentially structurally effective because of the straight load path down to the ground, will be included in the analysis, these geometries are generated as an individual family.

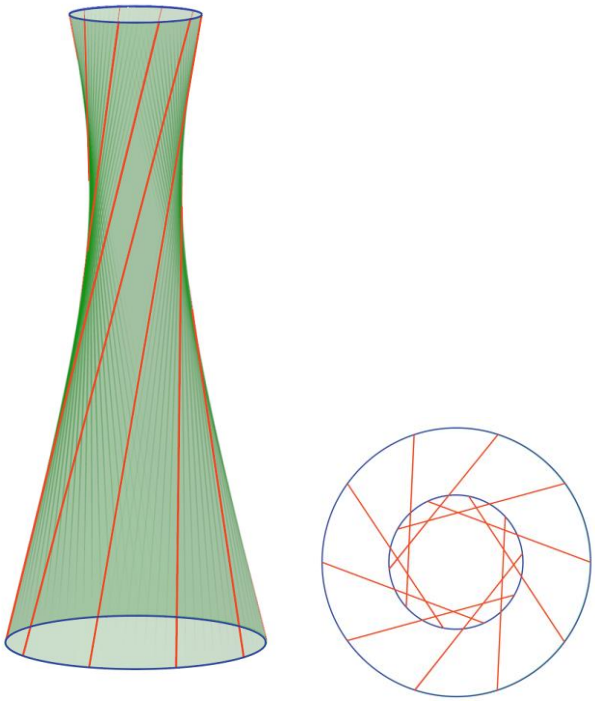

Figure 3.25 Example of geometry of hyperboloid and its continuous lines

Generation procedure:

1. Create a circle with radius of 15m, inscribed in the ground limitation of 30x30m.
2. Copy and move the circle to 200m in height (z-direction) and scale by a scale factor.
3. Rotate the circle generated in step 2 by a given degrees.
4. Divide both the circles into a given segments.
5. Connect the corresponding diving points of the two circles together.
6. Create lofted surface through the set of lines created in step 5.

The scale factor given in step 2 and the rotation degrees in step 3 are important with regards to how the geometries look like, for example, how small the waist will be. With the same circles on the ground plan and top plan, a larger rotation will result in a narrower waist.

One of the difficulties for hyperboloid buildings is the narrow waist and the curvature along façade, which may render some spaces on some floors unusable. With the space limitation for the design (30x30x200m), there are not many choices. The one selected for analysis has parameters:

Table 3.6 Parameters for the investigated hyperboloid geometry

Scale factor	0.8
Rotation	1.7

Figure 3.26 The selected hyperbolical geometry for further investigation

3.7 Result

The linear elastic FEA (Finite element analysis) was conducted. Compared to non-linear analysis the linear elastic analysis requires less computational resources.

The 25 geometries from Section 3.5, the geometry of hyperboloid from Section 3.4 and the optimized one out of evolutionary design from Section 3.3 are modelled with distributed wind loads and the results are presented here below.

3.7.1 Rental area

Within the group with the same façade contour, the rentable area drops with increasing floor plan radius as expected. The building of identical plans (façade featured with straight lines, model 1-5) provides most rentable space where the largest is 55000 m^2 and smallest with round plan 44000 m^2. The convex (model 11-15 and model 16-20) and the trapezoid (model 21-25) come after. The concave (model 6-10) provides observable less areas where even largest one in square plan provides less than 40000 m^2. The hyperboloid, as a special case of these, has only space for 22000 m^2. The optimized geometry obtained from evolutionary design is a special case for convex group, providing slight less than 50000 m^2.

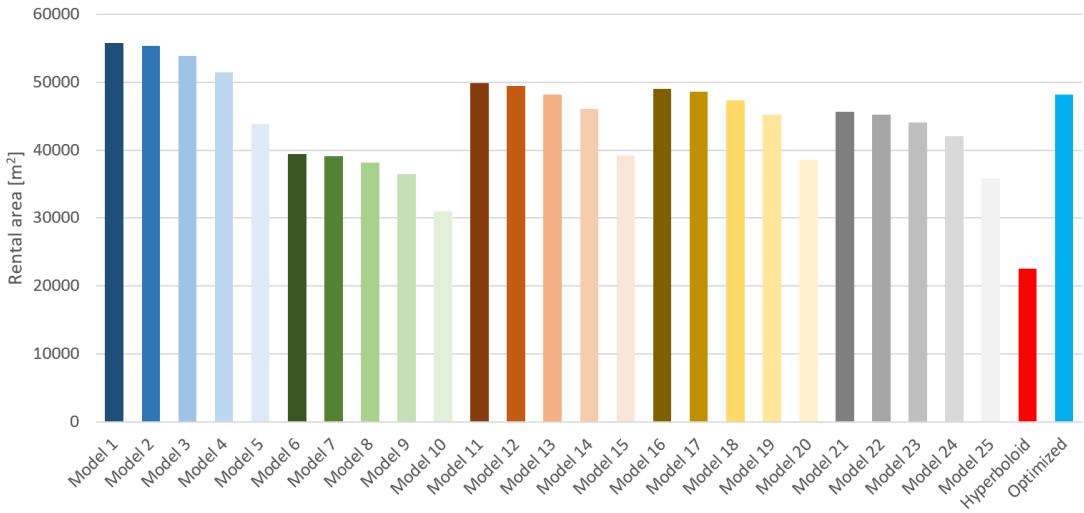

Figure 3.27 Rental area. The rental areas showed are only for comparison, communication areas such as service cores are included.

3.7.2 Mass and mass per area

The masses presented in this section is only a parameter to compare different geometries and are not related to consumption of building materials for the structure. The figure below shows that the mass of material decreases within each category when the corners are increasingly rounded. Between categories the straight shapes with constant section over height consumes most and concaves shapes least. The special case of concave geometries hyperboloid requires least material of all geometries, which is only 55% of that for the geometry 1, the straight square one. However, if the factor of the usable area is considered, the mass of material per rental area for hyperboloid stands on top of all, due to the dramatic drop in the enclosed space and areas. The optimized geometry from evolutionary design has a mass per unit area that is one of the lowest ones.

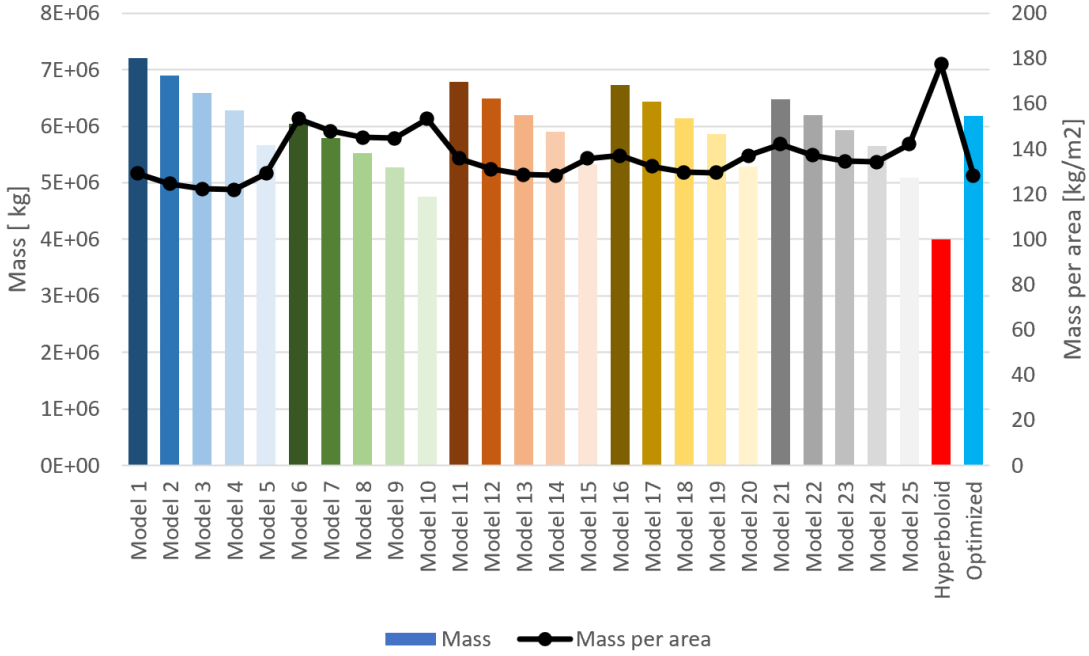

Figure 3.28 Mass of consumed timber and mass per rental area

3.7.3 Lateral displacement with consideration to structural stiffness, under equal loads

It is observed that geometries with square section are stiffest, decreasing with increased rounding of corners. Except for the concave geometries, those with facade curved inwards which has significantly lower stiffness, the differences in maximum displacement between those that share the same section are small compared to differences for those that have common façade curvature, which are approximate 0.06 m and 0.02 m. The hyperboloid performs by far the worst among all and the optimized one is one of those that has highest stiffness. The best one is the straight façade with square section.

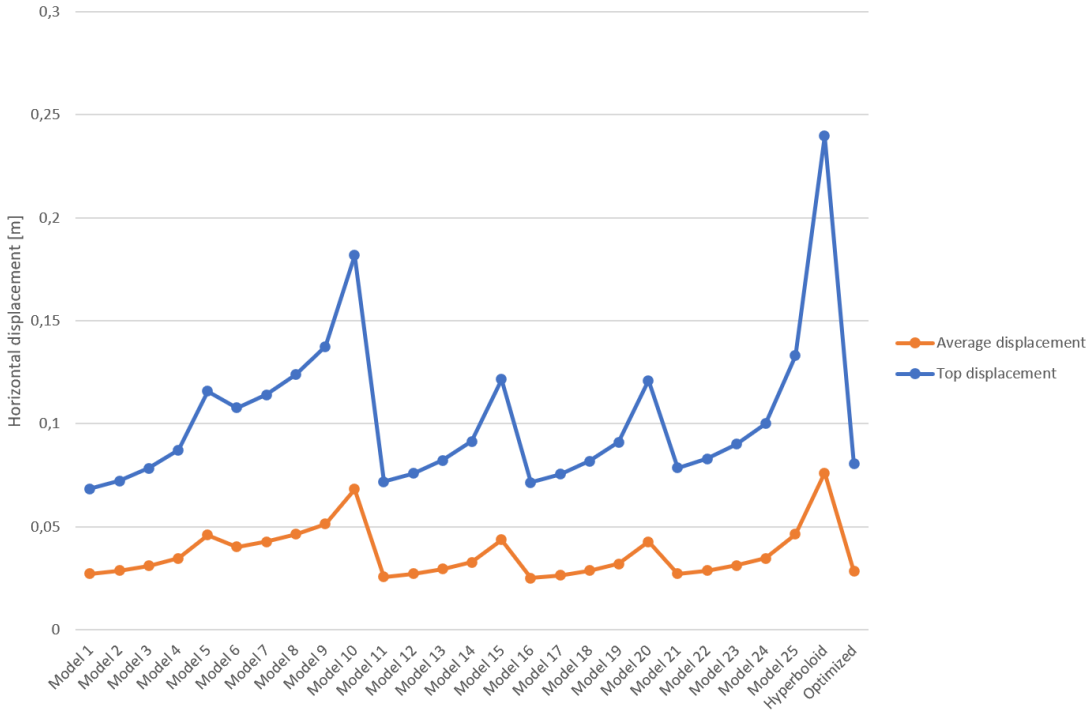

Figure 3.29 Lateral displacement with consideration to structural stiffness, under constant loads

The same trend can be observed with regards to the average displacement though there are some marginal changes in ranking. The best one is geometry 16 followed by geometry 11. The worst one is however still the hyperboloid one.

3.7.4 Lateral displacement with consideration to both structural stiffness and aerodynamics, under loads varying between geometries

The geometry has great impact on the wind loads that act on the structure as well. To include this effect, the lateral displacements of the geometries were studied with inclusion of force factors.

It is clearly observed that within each category the horizontal displacement decreases dramatically when the radius of roundness of corners increases from 0 to 6. The geometries have lowest horizontal displacements when the radius of the roundness of corners are 6 m and when the cross section is circular. Those with radius of 9 m are slightly higher than those of 6 m because of continuous decrease in second moment of area due to decrease of the plan area while the applied form factor is kept the same Compared between categories the concave geometries, models 6 - 10, see Figure 3.24, have obviously worse performance in lateral stiffness.

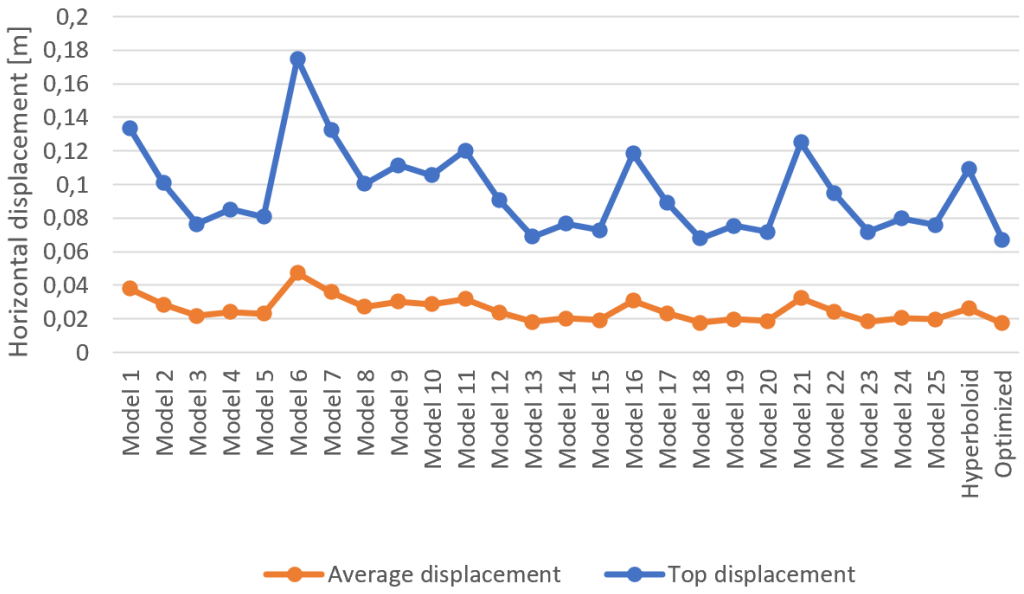

Figure 3.30 Lateral displacement

The optimized one has both smallest maximum displacement and average displacement and proved to be the best geometry regarding lateral deformation. The hyperboloid one is no longer at the bottom of the list. The worst ones are those with square section and this is because of the largest wind loads on these forms.

3.8 Evaluation

The different geometries are compared, evaluated, and selected for further structural analysis. Involved criteria for the evaluations are lateral displacement which reflect the structural stiffness and aerodynamic effect, total rental areas, footprint area, and ratios such mass per area, and stiffness per consumed material which reflects the material efficiency and structural efficiency.

3.8.1 Evaluation criteria

The evaluation criteria involved are:

- Rental area. The reason for and precondition of erecting skyscrapers is the scarcity of land resources. It is desired to get as much useful area as possible. Therefore, rental area is a very important criterion for preliminary design.
- Mass of consumed material per rental area. This parameter reflects the price for unit rental area. For the constructor, the economy and costing are of great importance. However, in terms of urban planning more usable area might be given priority rather than the unit cost.
- Stiffness per unit material. Stiffness per consumed material is an index to measure the material and structural efficiency. Since the structural stiffness is to a great extent reflected by the lateral displacement, reciprocally related, the multiplication of mass of consumed material and deflection with identical winds load is used to measure this.
- The displacements under various wind load including aerodynamic consideration can reflect lateral displacement of the structure in real cases.

The various criteria are compared to each other and weighing factors are obtained and presented as in Table 3.7.

Table 3.7 Evaluation criteria and weighing factors

Evaluation criteria		1	2	3	4	Total	Weighing factor
Rental area	1		2	1	1	4	17%
Mass of building material per rental area	2	2		1	1	4	17%
Multiplication of mass of building material and lateral displacement under constant wind loads	3	3	3		2	8	33%
Lateral displacement under wind loads varying with geometrical shapes	4	3	3	2		8	33%

Note: If a criterion is less important than another, it receives 1 point; If a criterion is of the same importance as another, it receives 2 points; If a criterion is more important than another, it receives 3 points.

3.8.2 Primary evaluation

The geometries with their performance were evaluated according to the weighed criteria presented in Table 3.7.

3.8.2.1 Rental area

The rental areas were normalized by dividing by that of geometry 1. The maximum normalized area is 1 for model 1 and the minimum one is 0.4 for the hyperboloid. Thereafter a scale between 1-5 was given to each according the normalized rental area, see Table C6.1 and Table C6.2 in Appendix C6.

3.8.2.2 Mass of building material per rental area

The mass of required building material per rental for each proposal is presented in Figure 3.28 in Section 3.7.2 above. The details about the normalization and scaling are presented in Table C6.3 and Table C6.4 in Appendix C6.

3.8.2.3 Structural stiffness per mass material

The structural stiffness per mass material can be reflected by the multiplication of mass of building material and lateral displacement under constant wind loads. The lateral displacement can be found Figure 3.29 in Section 3.7.3. Figure 3.31 shows this factor for all alternatives. The details on normalization and scaling are presented in Table C6.5 and Figure C6.6 in Appendix C6.

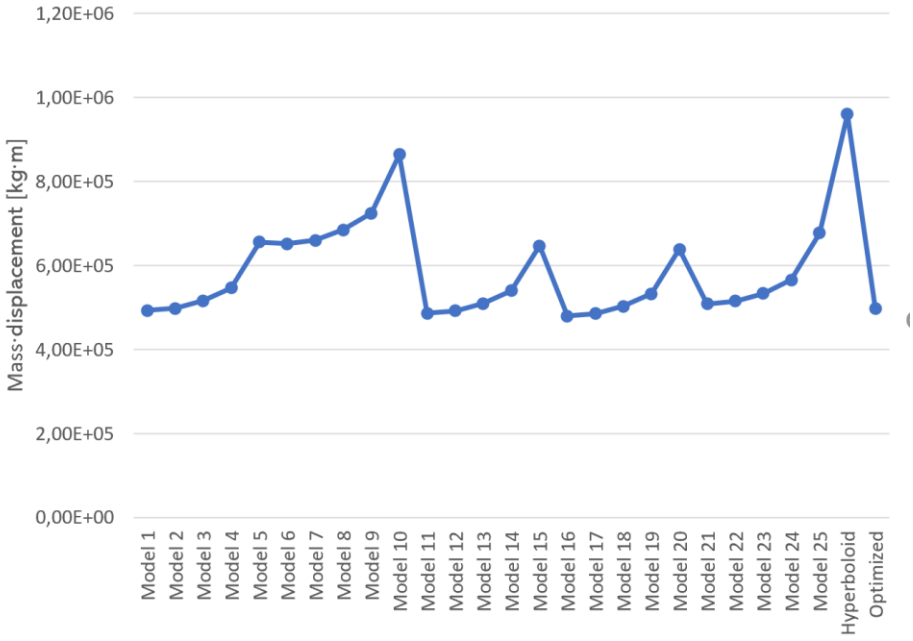

Figure 3.31 Structural stiffness related to unit mass of building materials

3.8.2.4 Lateral displacement

Lateral maximum displacement wind loads with aerodynamic effect included. The result of this for all alternatives is presented in Figure 3.30 in Section 3.7.4. In Table C6.7 and Table C6.8 in Appendix C6 the detailed information about the normalization and scaling for further evaluation can be found.

3.8.2.5 Evaluation

The primary evaluation for various geometries is presented in Table 3.8.

Table 3.8 Primary evaluation of the geometrical design

	Criteria 1 17%	Criteria 2 17%	Criteria 3 33%	Criteria 4 33%	
Model 1	5	5	5	3	4.66
Model 2	5	5	5	4	4.83
Model 3	5	5	5	5	5
Model 4	5	5	5	5	5
Model 5	4	5	4	5	4.5
Model 6	3	3	4	1	2.99
Model 7	3	3	4	2	3.16
Model 8	3	3	3	4	3.17
Model 9	3	3	3	3	3
Model 10	2	3	1	4	2.34
Model 11	5	4	5	3	4.33
Model 12	5	5	5	4	4.83
Model 13	4	5	5	5	4.83
Model 14	4	5	5	5	4.83
Model 15	3	4	4	5	4
Model 16	4	4	5	3	4.16
Model 17	4	5	5	4	4.66
Model 18	4	5	5	5	4.83
Model 19	4	5	5	5	4.83
Model 20	3	4	4	5	4
Model 21	4	4	5	3	4.16
Model 22	4	4	5	4	4.33
Model 23	4	4	5	5	4.5
Model 24	3	4	5	5	4.33
Model 25	2	4	3	5	3.5
Hyperboloid	1	1	1	3	1.34
Optimized	4	5	5	5	4.83

From the primary evaluation Geometry 3 and 4 are the best followed by geometries 2, 12, 13, 14, 18, 19 and the optimized one from evolutionary design. Geometry 3 and 4 have the best performance with regards to all the criteria while Geometry 18, 19 and the optimized geometry obtained from the evolutionary design has slightly lower points regarding the real area.

3.8.3 Secondary selection

All geometries that have highest scores from the primary evaluation have rounded corners. The façade is otherwise straight over height or curved outwards. Since geometry 13, 14, 18, 19 and the optimized one are of similar shape and are likely to have similar structural behavior, the optimized one which is subjected to smallest lateral displacement was selected to be further studies.

The straight one, geometry 3 and geometry 4 win the highest points because they have relatively good performance in all aspects, however, not best in any of them. Compared to these 5 convex ones, they have much larger rental areas. In terms of the urban development scarcity of urban land, it is likely to take a raised construction price due to more material consumption, to make full use of the land. Instead of geometry 3 and 4 with rounded corners, the geometry 1 with straight façade and rectangular section which uses the land to fullest, was selected. This one was chosen as a benchmark building for further comparison, designed with a traditional braced frame.

The hyperboloid one has not showed any advantage in any aspects in this part of geometry study with membrane structure. In theory this geometry should be of great efficiency due to the existing straight load path. However, when the slender structure is simplified to a membrane element, it is not guaranteed that the load will travel down through these straight lines as expected. On the other hand, another important criterion for a high-rise building that is not included in the evaluation process is the peak acceleration. Because of the widened top part, the hyperboloid is supposed to have good dynamic performance. It is therefore worth to take this shape further to the next step.

4 Stabilizing structure study

In this chapter the external tubal structure of the shell will be further transformed into a stabilizing structural system consisting of diagrid trusses or braced columns. For practical reasons, a core wall is introduced as well, which is necessary to carry the gravity load while to some degree contributing to the resistance to lateral load as well. The main parameters investigated are the size of modules and angles between elements in the truss system. Apart from the rental area, additional criteria for evaluation of alternatives are introduced, such as consumed timber material per floor area, lateral drifts which reflects structural stiffness, natural frequency and peak acceleration. To make different alternatives comparable, the lateral displacement at the top is kept at the similar level close to the requirement in SLS when selecting sizes of the cross section.

4.1 Geometries to investigate

From earlier study three geometries are taken into the further investigation. These are a traditional straight building in square plan that has most rental area, a tapered building with balanced result between rental area and lateral stiffness and a hyperboloid which might potentially provide the best results with regards to lateral stiffness because of the potential existence of straight load paths.

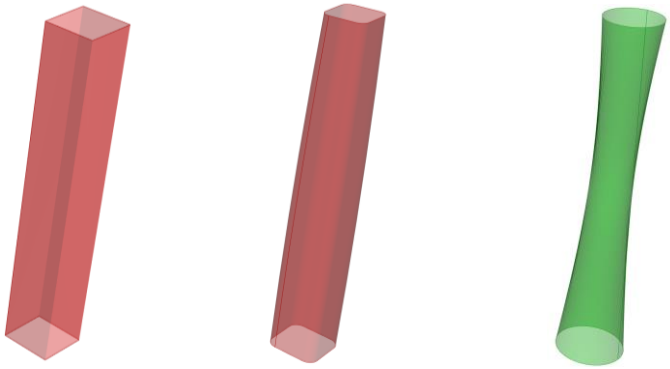

Figure 4.1 Geometries for structural study (a) Cuboid for benchmark structure in braced frame (b) Convex geometry (c) Hyperboloid

4.2 Structural models

4.2.1 Structural models

All models investigated in this stage consist of an external diagrid structure at the perimeter, a service core constructed as a wall structure and floor slabs. In a diagrid structural system, the triangular compositions are essential, making the structure stable. Therefore, beams that tie together diagrid trusses are included. Various wind loads calculated according to Eurocode act on each floor slab as a point load since the focus of this study is the global structural behavior.

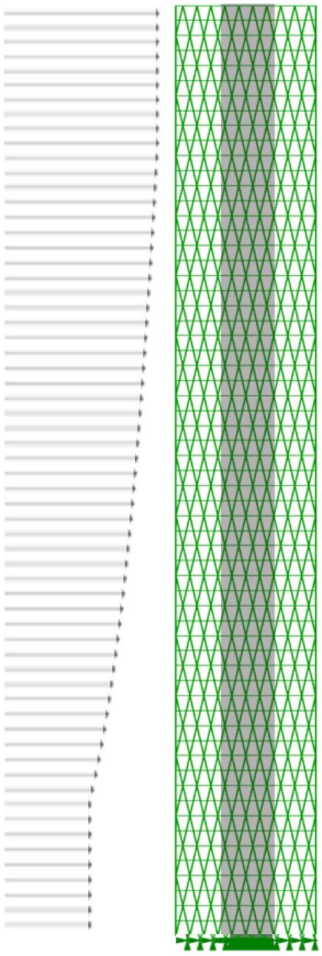

Figure 4.2 Structural model

4.2.2 Structural elements

4.2.2.1 Floor

In the building Mjöstornet the prefabricated wooden floor elements *Trä8* from manufacturer *Moelven* were used, designed for imposed load 2kN/m^2 with load carrying depth of 480 mm and 590 mm for the whole floor. The density of the *Trä8* is 172kg/m^3. (Moelven, n.d.). Martinsson has before produced wooden floor elements consisting of CLT glued together with glulam beams where full interaction between them can be considered. The maximum span for this is 12 m. A depth of 500 mm is required for a span of 10 m. (Sidén, 2017).

Table 4.1 Dimensions and tolerance of cassette floor element type MBK from Martinsson (Engelmark, 2005)

	Dimension [m]	[mm]
Length	2-12	±2
Width	0.3-2.4	±2
Depth	0.3-0.65	±2

Table 4.2 The characteristic Young's modulus and shear modulus for calculation for the two types of this kind of floor elements. (Engelmark, 2005)

Floor type	Shear modulus G [N/mm^2]	Elastic modulus E_x [N/mm^2]	Elastic modulus E_y [N/mm^2]
MB73	500	6200	6700
MB65	500	5200	7800

According to *Svenska Trä,* cassette floor elements with load-carrying depth of 510mm have a self-weight of 92kg/m2, corresponding to a density of 180kg/m^3, which is close to that of *Trä8.*

The total depth and weight of the floor elements consists of not only load-carrying part, but also sound isolation and covering. Apart from this, the dimensions and the load-carrying beams for the specific large span which need to fulfill the vibration criteria can not easily be estimated exactly. Moreover, the plan layout the partition walls will influence the total weight acting on the floors, regarded as distributed over the floors. In this project the density of the floor of 356kg/m^3 is assigned as material property. This may seem light but has been deemed acceptable for the purposes of the project. Considered the floor slabs as a whole where the floor composite will be placed in both two directions, the elastic modulus is regarded as isotropic to 6500MPa.

4.2.2.2 Core wall

Cross laminated timber of C30 grade timber is considered for use. The elastic modulus parallel and perpendicular to the grain are 12GPa and 0.4GPa, respectively. The elastic modulus of the whole composite varies due to the arrangement and thickness of each layer. A value of 7360 MPa was assumed in each direction.

Thickness of the load carrying part was preliminary estimated in ULS where the dead load of the main structure, snow load and imposed load are included. 50% of the gravity load was considered to be carried by the core wall since the intention is to let the external structure in the perimeter be relatively stiffer and carry the horizontal load. It is also beneficial to let the stabilizing structure carry as much gravity load as possible. In reality, the core wall will contribute a part of resistance to horizontal load. In all models the core walls are modelled as a shell element of 500 mm, which is larger than that estimated for only carrying 50% gravity load.

4.2.2.3 Truss and beam

Glued laminated timber of type GL30h was used. The cross sections of both the trusses and beams that tie them together were set to be square. Sizes included in the calculation were chosen by the built-in cross section optimization algorithm *OptCroSec* in Karamba 3D in ULS. Those floors within individual band of triangles are grouped together with regard to the dimensions of the trusses. Regarding beams, all beams for the stories were grouped together to be assigned with an identical cross section.

4.2.2.4 Material properties in finite element model

The material properties used in the modelling are listed below. Due to limitations of the software only one common strength value can be defined for timber in compression, tension and bending. The compression and bending strength for GL30h is 30MPa. However, the strength of 24MPa, which is the strength for tension, was assigned in the model. This will lead to the design always on the safe side and the utilization calculated by the program of trusses in compression 20% higher than it is supposed to be, which need to be revised to get a more precise estimation.

Table 4.3 Material used in the finite element model

Floor slab: Cassette floor composite					
E_1	E_2	G	Density	f_k	f_d
6500MPa	6500MPa	500MPa	358kg/m^3	24MPa	11.5MPa
Core wall: Cross laminated timber: CLT C30					
E_1	E_2	G	Density	f_k	f_d
7360MPa	7360MPa	750MPa	500kg/m^3	24MPa	11.5MPa
Truss & Beam: Glued laminated timber: GL30h					
E_1	E_2	G	Density	f_k	f_d
13600Pa	13600Pa	650	490kg/m^3	24MPa	11.5MPa

4.2.2.5 Joint

With consideration to making use of the axial stiffness of timber the connection is expected to not transfer bending moment, that is to say, as pinned joints. However, since the modelling of pinned joints is somewhat complicated, they are modelled as fixed in this study. It was concluded that the influence of how joints are modelled are quite minor in most cases when it comes to the tubal structure of diagrid (Gyllensten & Modig, 2020).

4.2.3 Boundary conditions

Fixed movement in all directions for the nodes on the ground, see Figure 4.2.

4.2.4 Loads

Self-weight, imposed load and wind loads are incorporated. Self-weight was calculated by the program from the user-given density of materials. Note that in Karamba 3D the gravitational acceleration is set as $10 m/s^2$. However, this is regarded as precise enough for engineering calculations (Preisinger, 2016).

The wind load was calculated according to Eurocode 1991-1-4 and the Swedish standard EKS11 and coded in the inbuilt Python component in Karamba 3D. The shape factor used for the wind calculation was simplified to use the same values drawn in Chapter 3.

According to EN 1991-1-4 and EKS11 the building is designed for office use and imposed for this category is $3 kN/m^2$. The reduction factor is chosen to 0.7. This is modelled as "shell load" on floor slabs where the load will be assigned evenly to all the nodes on the relevant shell element for slabs. It is observed that the imposed load is assigned to nodes on the boundary, in connection to adjacent elements, which differs from the real case.

4.3 Cross section optimization

The cross section of trusses will be optimized and designed in ultimate limit state. As mentioned before there are two cases that need to be checked:

- Compression in ULS where the imposed load is unfavorable
- Tension in ULS where the imposed load is favorable

The built-in optimization component *OptCroSec* was used, where the user is able to set the desired limit of maximum displacement and/or maximum utilization of structural elements. The algorithm is an iterative procedure and can automatically select the most appropriate cross sections of beams and shells. Cross sections in order from smallest to the largest is given by the user. The computing procedure for determining the appropriate cross section is as follows:

1. Start from the initial (smallest) cross section and compute the sectional forces at a number of points along all beams.
2. For each element or grouped element, select the first sufficient cross section from the user-defined cross section or the same material family.

3. The process stops if the largest cross section is not sufficient or the maximum step of iterations as an input is reached.

Since the compression is assumed to be more critical, the cross section was optimized first for the load case with imposed load as unfavorable and the maximum utilization was set to 1. In Karamba 3D the compressional and tensile utilization is determined by the ratio of the axial stress to the given material strength. As mentioned before, the compression strength is undervalued, the real strength is 20% higher than the given one, meaning that the utilization of the compression strength should be corrected by decreasing 20%.

After the preliminary optimization conducted by the algorithm *OptCroSec*, the capacity in bending respective compression in ULS, and the buckling were checked according to SS-EN1995-1, both with and without imposed loads for all trusses and columns. The dimensions of the design increases until it reaches the requirement.

4.4 The benchmark building

In order to have an intuitive understanding of how well the structure performs a braced frame structure with core walls is studied as a benchmark building for comparison.

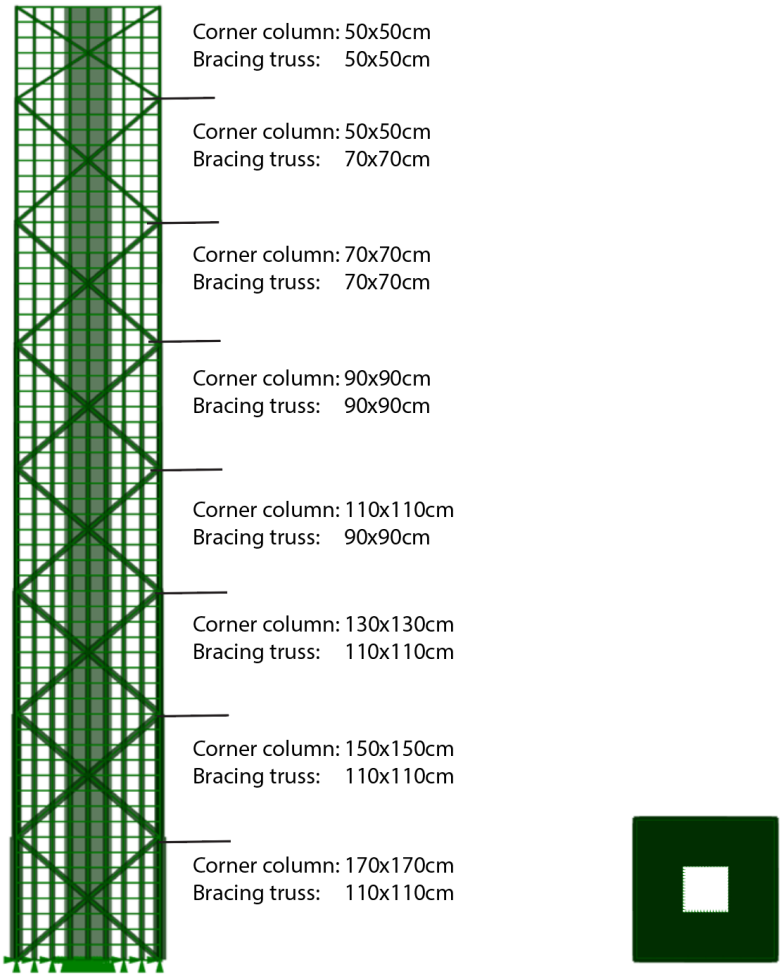

Figure 4.3 Traditional braced frame structure

The cross section of vertical columns between spans, corners columns and bracing trusses are optimized in the same way by *Optimize Cross Section* in ULS where cases both with and without imposed loads are checked. The corner columns are grouped over the same floors as the bracing members during the optimization while span columns are grouped within individual floor only.

Dimensions of the incorporated structural members and the mass are presented in Table 4.4 and the result of performance is summarized in Table 4.5

Table 4.4 Design of the structural members and the corresponding mass of timber

Structural parts	Size		Mass
Bracings	Floor	Dimension [cm]	935.7 tons
	1-8:	110x110	
	9-16:	110x110	
	17-24:	110x110	
	25-32:	90x90	
	33-40:	90x90	
	41-48:	70x70	
	49-56:	70x70	
	57-62:	50x50	
Corner columns	Floor	Dimension [cm]	494.6 tons
	1-8:	170x170	
	9-16:	150x150	
	17-24:	130x130	
	25-32:	110x110	
	33-40:	90x90	
	41-48:	70x70	
	49-56:	70x70	
	57-62:	50x50	
Span columns	Floor	Dimension [cm]	1953.6 tons
	1-19:	130x130	
	20-35:	110x110	
	36-46:	90x90	
	47-62:	70x70	
Floor	All floors	50 cm	8878.4 tons
Core wall	All floors	80 cm	3200 tons
Spandrel beam	All floors	30x30cm	333.4 tons

Table 4.5 Performance of the braced frame structure

Displacement [mm]	273
Natural frequency [Hz]	0.41
Peak acceleration of top floor [m/s^2]	0.08
Rental Area [m^2]	49600
Mass [tons]	18529.7
Base moment [kNm]	$1088 \cdot 10^3$
Base horizontal reaction force [kN]	9633

4.5 Convex geometry

The convex geometry model is illustrated in Figure 4.4. It has a core inside the building and the diagrid structure on edge of the building. The model's plan has a shape of a rounded square.

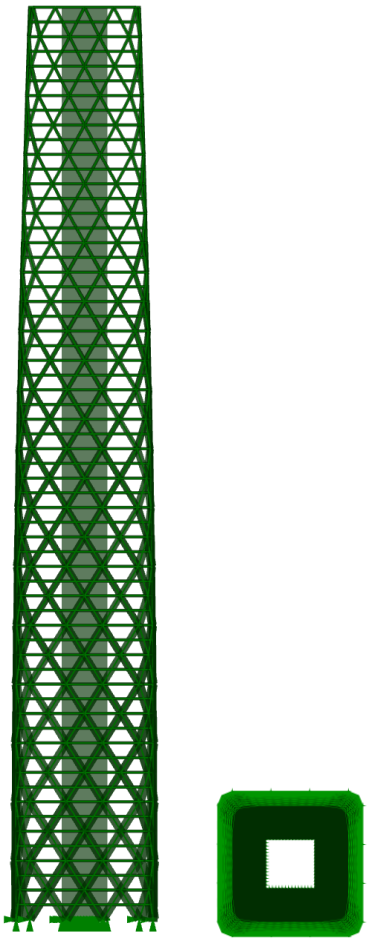

Figure 4.4 Diagrid structure of the convex building

4.5.1 Parameters

Triangle modules are the fundamental elements in a diagrid system, where the inclined columns carry both horizontal and vertical loads. The key parameters are the angle of inclination and the size of the triangular module, meaning how many floors there are within the height of the triangle.

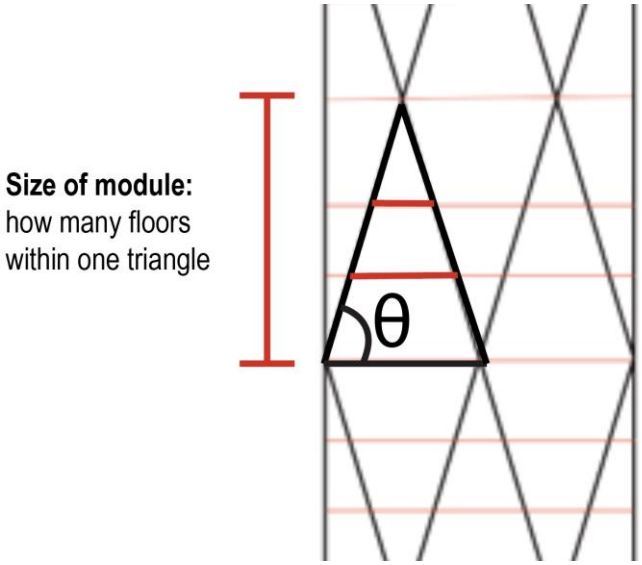

Figure 4.5 Studied parameters

Some of the combinations are not possible to build in reality. For example, while the angle can be as large as 85 degrees, small sizes will give insufficient space between joint points, especially when the size of trusses don't decrease to the same scale. An excessively dense truss configuration will decrease light transmission. On the contrary, when the trusses are too sparse, beams with too large spans will be required, which is neither economic to build nor structurally efficient.

After checking the models designed with optimized cross sections, some of the cases are presented for study of the influence of these two factors, see in Table 4.6. They are named by the angle followed by the size of modules. Since the façades are curved the angles vary in height.

Table 4.6 Truss patterns and the design of structural members

Patterns	**Properties**		**Dimensions**		
Name	**Angle [degree]**	**Size of module [number of floors]**	**Optimized cross section of truss elements for different floors**	**Thickness of core walls [cm]**	**Beam[cm]**
85deg-4	85°	4	1-32: 70x70cm 33-52: 55x55cm 52-62: 40x40cm	50cm	25x25cm
85deg-8	85°	8	1-32: 85x85cm 33-48: 70x70cm 49-62: 55x55cm	50cm	25x25cm
85deg-16	85°	16	1-32: 115x115cm 33-48: 85x85cm	50cm	40x40cm

			49-62:	70x70cm		
80deg-2	80˚	2	1-24: 25-46: 47-62:	70x70cm 55x55cm 40x40cm	50cm	25x25cm
80deg-4	80˚	4	1-24: 25-40: 41-56: 57-62:	85x85cm 70x70cm 55x55cm 40x40cm	50cm	25x25cm
80deg-8	80˚	8	1-8: 9-16: 17-32: 33-40: 41-56: 57-62:	130x130cm 115x115cm 100x100cm 85x85cm 70x70cm 55x55cm	50cm	25x25cm
75deg-1	75˚	1	1-8: 9-36: 37-58: 59-62:	70x70cm 55x55cm 40x40cm 25x25cm	50cm	55x55cm
75deg-2	75˚	2	1-12: 13-30: 31-48: 49-62:	85x85cm 70x70cm 55x55cm 40x40cm	50cm	25x25cm
75deg-4	75˚	4	1-16: 17-24: 25-32: 33-44: 45-60: 61-62:	115x115cm 100x100cm 85x85cm 70x70cm 55x55cm 40x40cm	50cm	25x25cm
70deg-1	70˚	1	1-6: 7-20: 21-40: 41-59: 60-62:	85x85cm 70x70cm 55x55cm 40x40cm 25x25cm	50cm	55x55cm
70deg-2	70	2	1-4: 5-14: 15-24: 25-34: 35-50: 51-62:	115x115cm 100x100cm 85x85cm 70x70cm 55x55cm 40x40cm	50cm	25x25cm
65deg-1	65˚	1	1-14: 15-26: 27-44: 45-58: 59-62:	85x85cm 70x70cm 55x55cm 40x40cm 25x25cm	50cm	55x55cm
65deg-2	65˚	2	1-4: 7-12: 17-20: 23-28:	130x130cm 115x115cm 100x100cm 85x85cm	50cm	25x25cm

			31-40: 70x70cm 37-50: 55x55cm 43-60: 40x40cm 57-62: 25x25cm		
59deg-1	59°	1	1-3: 115x115cm 9-14: 100x100cm 19-24: 85x85cm 27-32: 70x70cm 35-45: 55x55cm 45-56: 40x40cm 57-62: 25x25cm	50cm	70x70cm
59deg-2	59°	2	1-8: 145x145cm 5-16: 130x130cm 15-24: 115x115cm 21-28: 100x100cm 27-36: 85x85cm 33-44: 70x70cm 37-52: 55x55cm 43-62: 40x40cm	50cm	25x25cm

4.5.2 Results

The results for the listed patterns are compared and analyzed.

4.5.2.1 Lateral deflection

The maximum lateral displacement decreases as the angles decrease from 85 degrees to around 59 degrees. When the angle reaches 59 degrees and the size of triangular module is 1, the displacement approaches the lowest value of 122mm. It is also observed that the deformation pattern changes from obvious shear deformation to bending deformation when the angle decreases. When the angles drop down to 70 degrees almost pure bending deformations are observed.

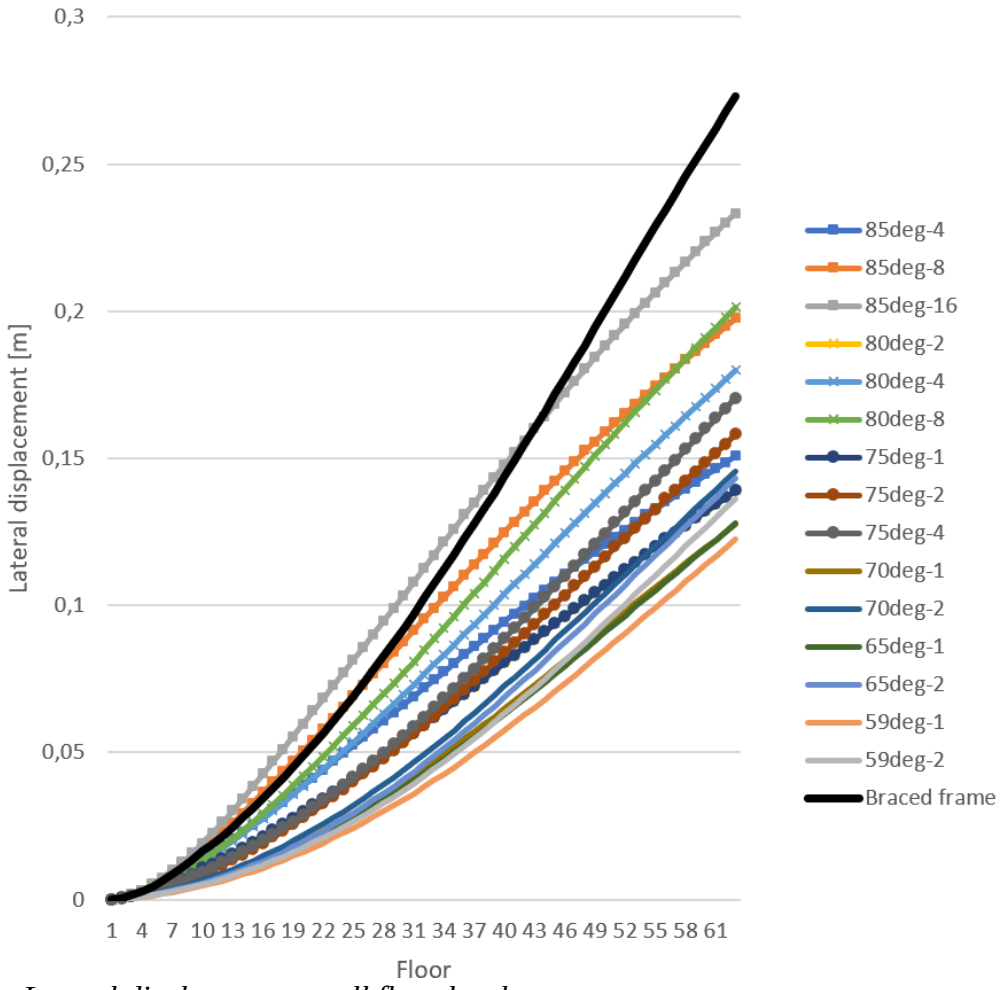

Figure 4.6 Lateral displacement at all floor levels

Compared to the braced frame structure all the diagrid structures have better performance in terms of lateral displacement. The lateral displacement for the braced frame structure is as large as 273mm, but even this is far from the required limitation of 400mm.

Another observation is that for the diagrid structures with the same angle, the smaller the size of the triangular module the smaller the horizontal displacement is. This reflects that denser structures provide larger structural stiffness globally.

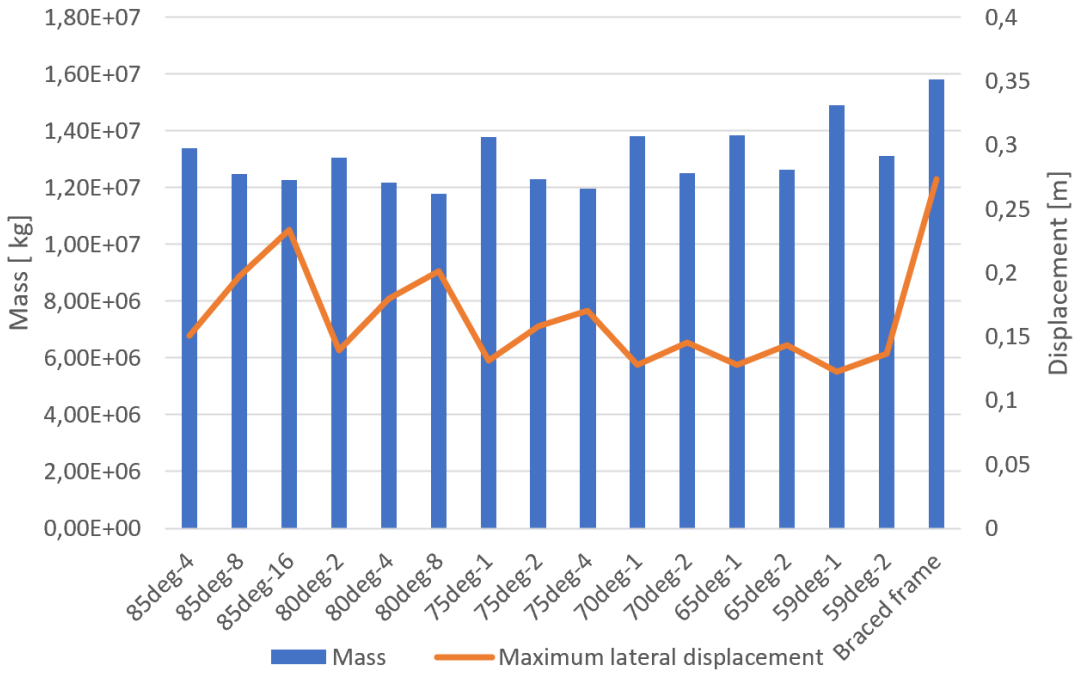

Figure 4.7 Mass of consumed material and maximum lateral displacement

4.5.2.2 Dynamic behavior

The natural frequencies of the lowest mode for these investigated timber structures vary between 0.3 to 0.5. The combination of eigenfrequencies and peak accelerations at the top floor are plotted in Figure 4.8 below. It is showed that all these proposals fulfill the comfort criterium for office buildings with regards to the dynamic behavior, where the braced frame structure has worst performance.

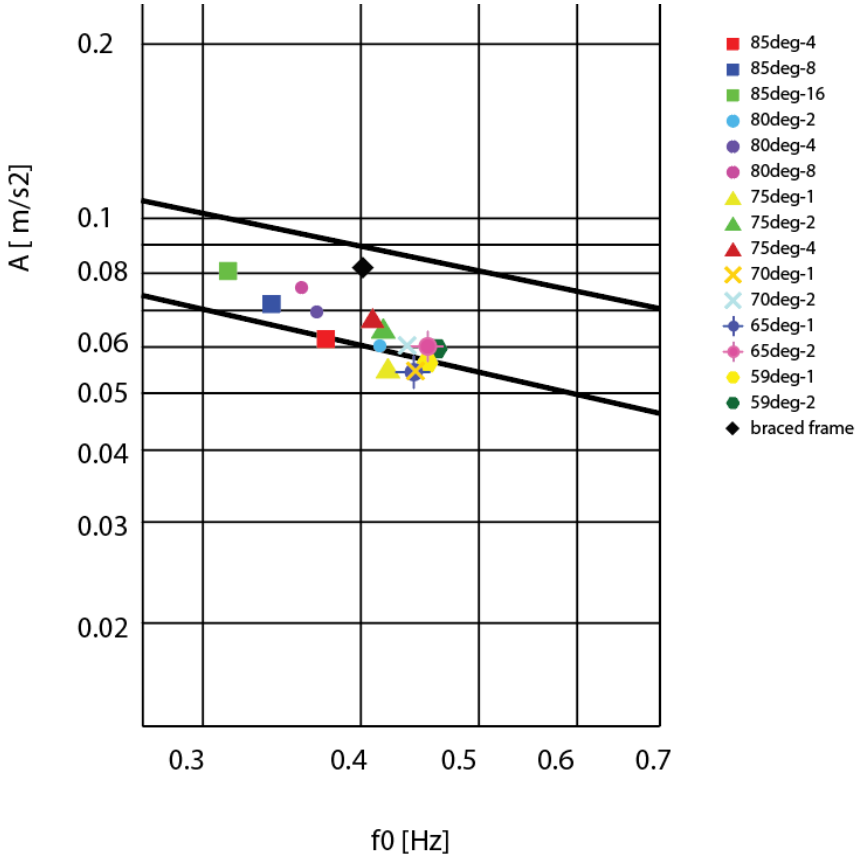

Figure 4.8 Eigenfrequency and peak acceleration for designs for the convex geometries.

For those with similar angle, the denser structures give a slightly better dynamic performance. This coincides with the result that denser structures are globally stiffer when it comes to the lateral displacement in Section 4.5.2.1. A lot of the convex structures are very close to satisfying the criterion for residential buildings as well. Several examples are the structures 85deg4, 80deg2 and 59deg1, which lie on the curve for residential buildings. The structures 75deg1, 65deg1 and 70deg1 are below the curve. Considering the uncertainty due to the joints, it is hard to draw the conclusion that they fulfill the requirement for residences.

4.5.2.3 Mass of consumed timber and Rental area

The rental area for all structural alternatives of the geometries fluctuates around 42 000 m^2 due to polygonization of plans near the corner when the density of trusses vary. However they can be regarded as at the same level. Therefore, its influence on the ratio of comsumed material per rental area can be almost neglectable.

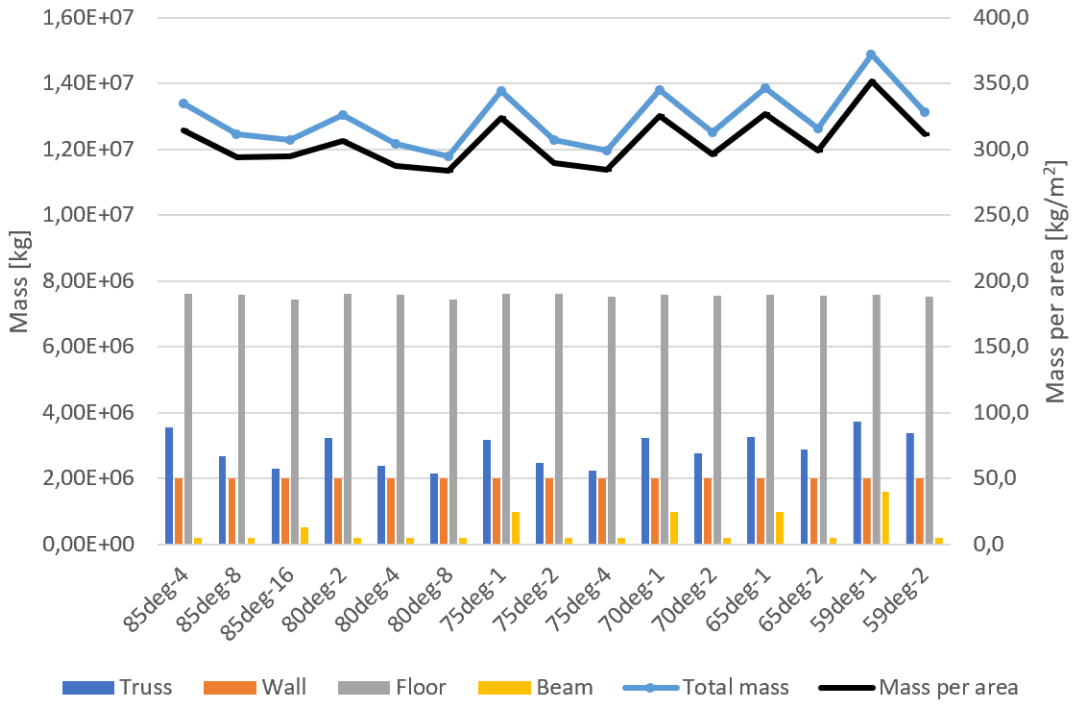

Figure 4.9 Mass of structural elements and the whole structure

The proposals that require least construction materials per unit rental area are 80deg8 and 75deg4, at 283kg/m^2 and 285kg/m^2, respectively. The material used for the diagrid truss systems are also lowest for these two alternatives. It is observed that the material consumption for truss systems has a great influence on the rankings regarding the total mass of the timber material and even the material amount per area. When it comes to the braced frame structure which provides a total rental area of 46 600 m^2, it consumes 374 kg/m^2, which is 6% more than one that needs most timber among all the convex structures, which is 59deg1. This is also 32% more than 80deg8, the best one among all convex ones.

4.5.2.4 Reaction force at foundation

Due to the difference in the geometries, the braced frame structure is subjected to more wind loads than the convex ones. Because of this, the bending moment and horizontal reaction force at the foundation are larger for the braced framed structure. For all the convex structures, the difference is not that clear since the building geometries are almost the same.

One observation is that the overturning moments are resisted mostly by the external structural systems, both for the diagrid structures and the braced frame structure. For the diagrids with angles 70 degrees or even smaller, more than 90% of the moments are resisted by the external structures. Apart from this, the denser structures have relatively stiffer external structures and these resists more moments than the sparse ones which has a same angle.

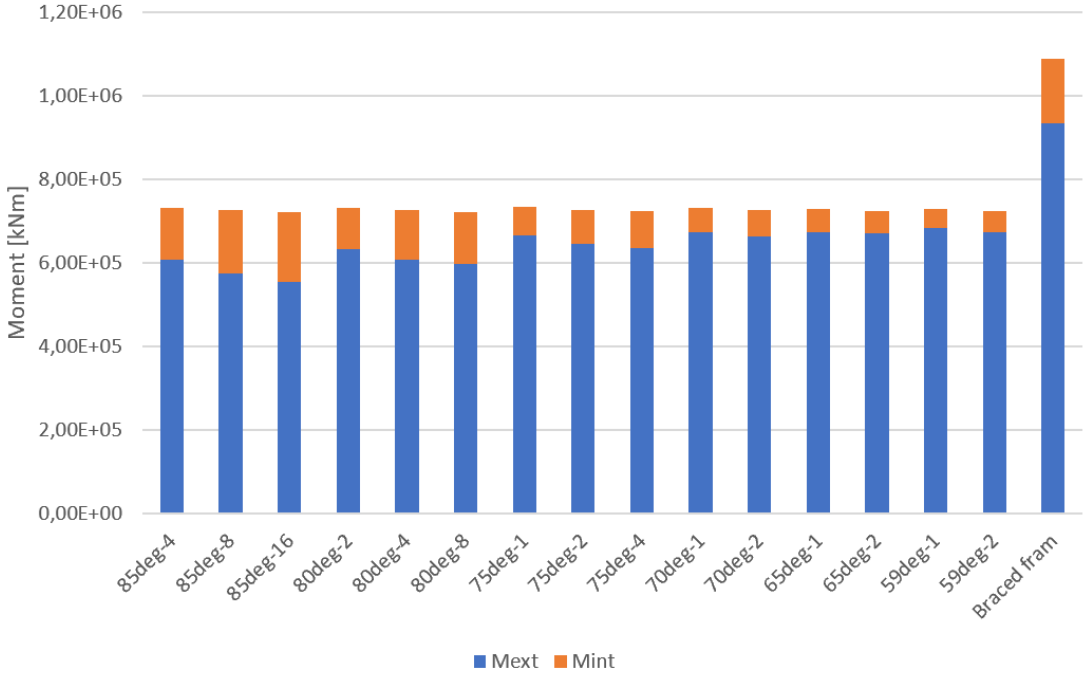

Figure 4.10 Distribution of overturning moment resisted by external structure and internal structure.

When it comes to shear resistance, the core walls play a more important role, especially for the diagrids with larger angles. This is because the more inclined columns, or trusses with smaller angles can resist also shear forces.

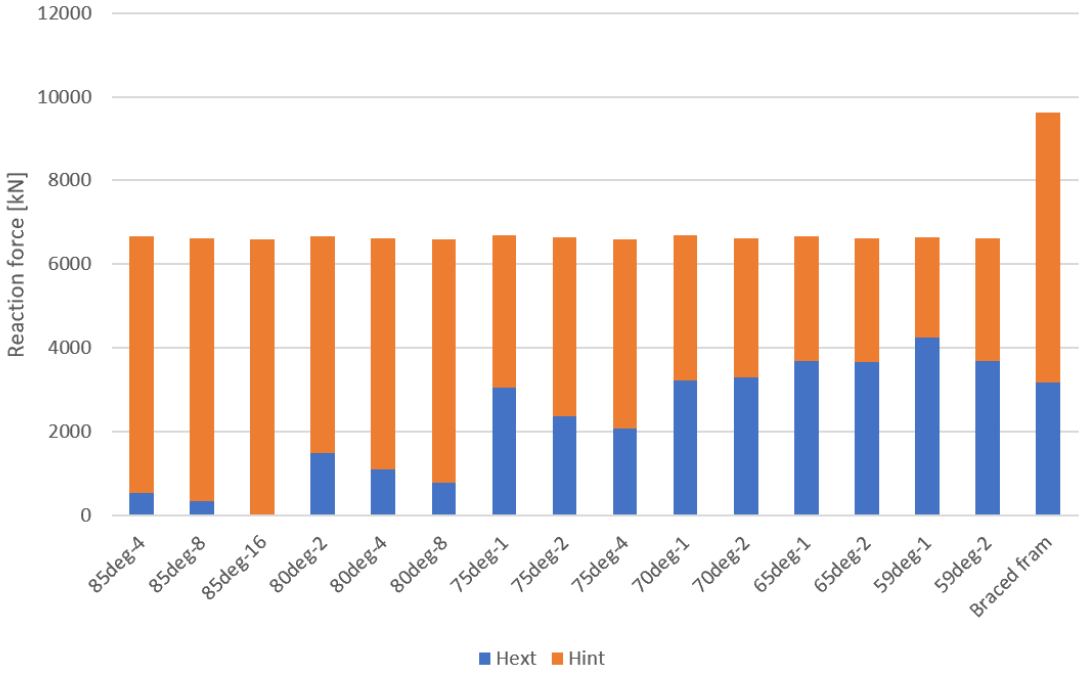

Figure 4.11 Distribution of horizontal force resisted by external structure and the internal structure.

4.6 Hyperboloid

One special feature of the hyperboloid geometry is that there are always straight paths down to the ground and a straight load path is considered as structurally efficient. In order to keep the continuous straight load path which makes the geometry efficient, the angles of trusses are fixed to the generation method of the geometry. Due to the limitation of the ground plan and the height, there is not much flexibility in choosing a hyperboloid geometry where it is still possible to make use of the floor areas. Therefore, only one shape is appropriate with regards to the floor area at each level and will be studied. In order to make it more practical, the geometry is scaled up by multiplying the radius of circles by 1.3, leading to an average width of 27.3m, which is lower than 30m. In the perspective of structure and visual impact, the structure has a similar slenderness as other geometries and is regarded as comparable.

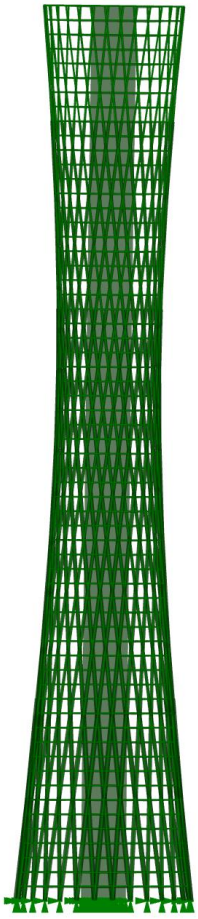

Figure 4.12 An example of the hyperboloid structure

4.6.1 Parameters

Since the angle is bound to the geometry, it is not possible to alter angles of the truss system without changing the geometries. Therefore, only the density of trusses will be studied. This is controlled by the number of dividing points, which determines how many triangular modules, or crossing joints, there are around one floor.

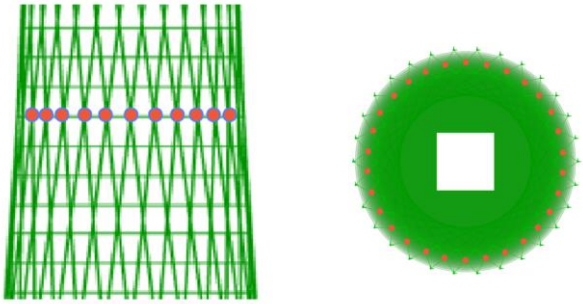

Figure 4.13 Parameters of hyperboloid structure

4.6.2 ULS design and optimization

The density of the trusses is controlled by the number of dividing points. Same as previously, the optimization algorithm *OptCroSec* was used to obtain the cross sections of trusses over floors. The outer beams are kept of the same dimension. The designs and stresses thereafter were verified according to Eurocode following procedures presented in Appendix E. The stresses of the trusses can be found in Appendix G.

The design for each case is presented in Table 4.7.

Table 4.7 Design of the structural members

Name	Number of Dividing points	Wall thickness	Cross section of beams	Optimized cross section of trusses for different floors	
hyp1	10	50cm	25x25cm	1-7: 8-24: 25-35: 36-46: 47-62:	100x100cm 85x85cm 70x70cm 55x55cm 40x40cm
hyp2	15			1-10: 11-31: 32-43: 44-52: 53-62:	85x85cm 70x70cm 55x55cm 40x40cm 25x25cm
hyp3	20			1-22: 23-41: 42-56: 57-62	70x70cm 55x55cm 40x40cm 25x25cm

hyp4	25			1-16: 17-38: 39-55: 56-62	70x70cm 55x55cm 40x40cm 25x25cm
hyp5	30			1-8: 9-36: 37-44: 45-62:	70x70cm 55x55cm 40x40cm 25x25cm

4.6.3 Result

4.6.3.1 Lateral displacement

The lateral displacement decreases as the density of trusses increases for the hyperboloid diagrids, all of which are below 200mm. The hyperboloids turn out to be better than the braced frame structure regarding lateral displacement.

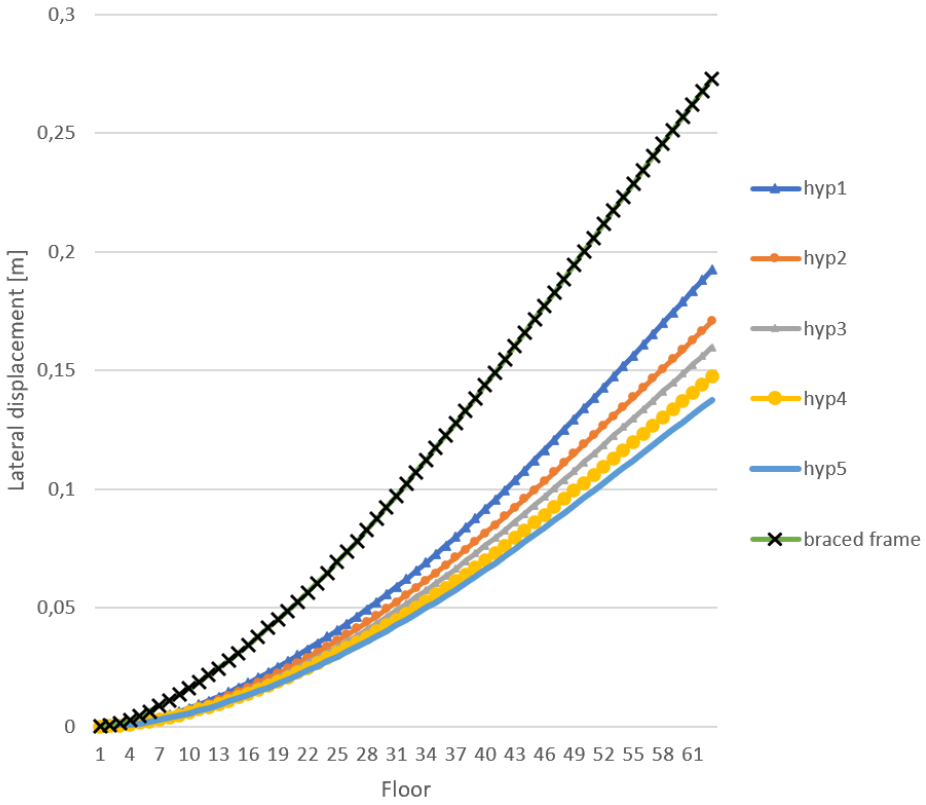

Figure 4.14 Lateral displacements for the hyperboloid structures and the braced frame structure for all stories

Due to the good shear resistance of diagrid structures, the bending deformation governs the structural behavior.

The displacement has a negative relationship to the mass of timbers for the hyperboloid structures. The more material consumed, the denser the structure is and the less the structure deforms. However, the braced frame structure deforms more, even though it's mass is higher than the hyperboloid structures. In terms of deformation, the hyperboloids are better solutions than the traditional braced frame structure.

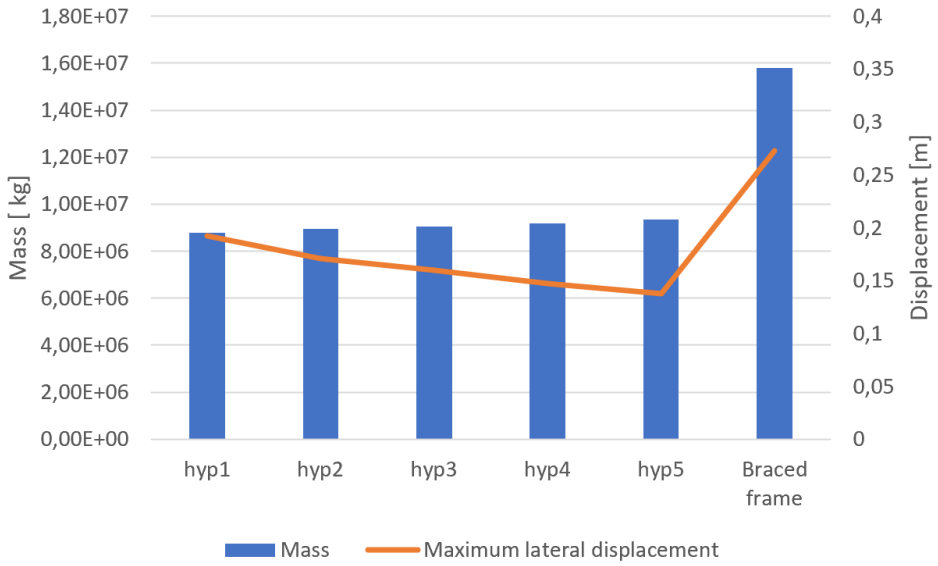

Figure 4.15 Mass of consumed material and maximum lateral displacement

4.6.3.2 Dynamic behavior

All the designs for the hyperboloid geometry show good dynamic performance. They all fulfill not only the comfort criteria for office buildings but also for residential buildings. The natural frequencies of the lowest mode for the hyperboloid diagrid systems vary in the range between 0.31 to 0.36 Hz.

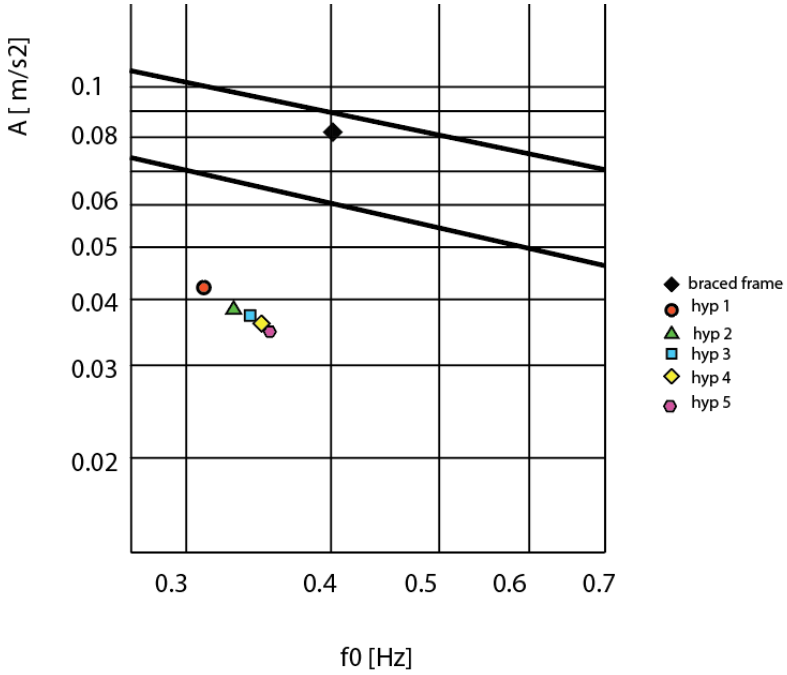

Figure 4.16 Eigenfrequency and peak acceleration for designs for the hyperboloid geometry

4.6.3.3 Mass and rental area

The difference of rental area is very minor, varying between 31516 m^2 and 31534 m^2, which can be neglected. The slight increase in material for trusses resulted in an increased mass per floor area. The change is around 19kg per square meter.

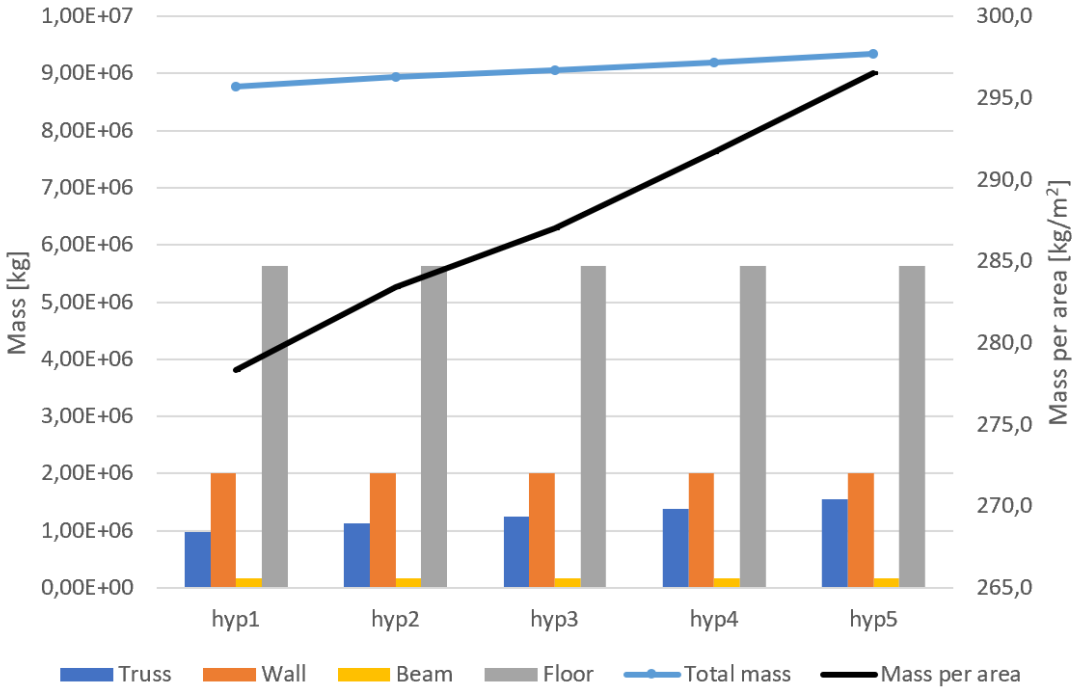

Figure 4.17 Mass of structural elements and the whole structure

By changing from the braced frame structure to hyperboloid diagrid structures, 77-97kg timber material can be saved for each unit floor area. The hyperboloid structures are more material efficient.

4.6.3.4 Base support force

Due to aerodynamics, all hyperboloid structures are subjected to relatively low horizontal loads and bending moment caused by wind. The bending moment at the connection with the foundation is about 36% compared to that of the braced frame structure in cuboid geometry. Over 80% of the moment is resisted by the external diagrid systems rather than the core wall for all hyperboloid structures. Therefore, the core can be significantly smaller in hyperboloid structures to increase the total rentable area specially on the levels where the building has its smallest waist.

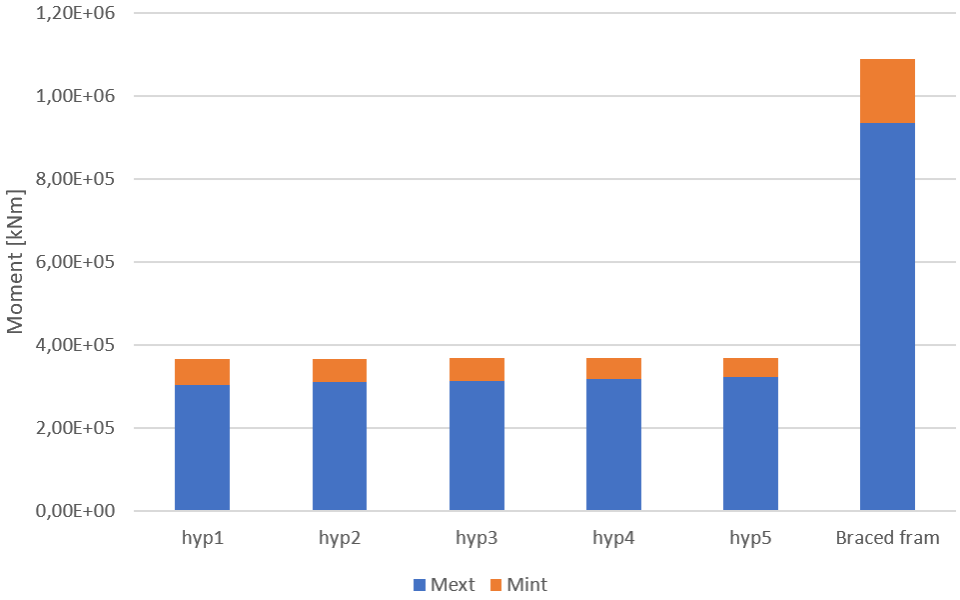

Figure 4.18 Distribution of overturning moment resisted by external structure and internal structure.

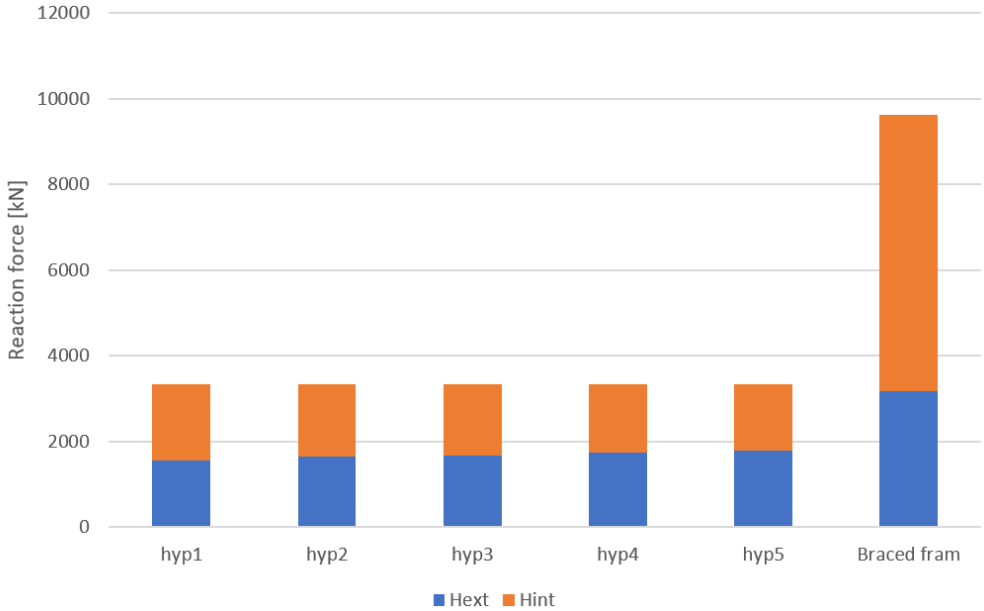

Figure 4.19 Distribution of horizontal force resisted by external structure and the internal structure.

Unlike the diagrid structure in convex forms, these in the hyperboloid form make a good contribution to resist shear forces as well. Nearly 50% of the horizontal reaction forces go to the external diagrid structures.

4.6.3.5 Discussion

Overall, all the candidates in this group of hyperboloid structures have stable performance. They show significantly better behavior in terms of dynamics compared to both the convex structures and the traditional frame structure. The material efficiency is quite high as well. The largest disadvantage is the decrease in the rental area.

For further design, the inclination of the trusses towards the center on the upper part over the waist might increase the risk for buckling of the floor slabs, which need to be carefully evaluated and designed if one of these candidates is chosen for further design.

4.7 Evaluation

All the structures in three different geometrical forms were evaluated together.

4.7.1 Criteria

The criteria used for the evaluation are presented in Table 4.8. They were compared to each other regarding the importance and a point between 1-3 was assigned to the criteria in each comparison.

Table 4.8 Evaluation criteria and the weighing factors

Evaluation criteria		1	2	3	4	Total points	Weighting factor
Lateral displacement	1		1	2	1	4	16%
Dynamic behaviour	2	3		3	2	8	32%
Mass/rentable area	3	2	1		2	5	20%
Base support force	4	3	2	3		8	32%
Total point						25	100%

Note: If one criterion is less important than another, it gets 1 point; If one criterion is of same importance it gets 2 point; If one criterion is more important than another, it gets 3

Since all models should fulfill the requirement of deflection smaller than 40 cm, lateral displacement is less important in this evaluation but still the smaller the lateral displacement the better the structural efficiency. Dynamics and base support force are more important because they are the requirements that should be fulfilled for every tall building. Mass and rentable area ratio affect the economic and sustainable aspect of the building. The smaller the mass per rentable area the less timber material that could be used and therefore the smaller impact on the environment.

4.7.2 Summarized results for evaluation

The values of the results for all the alternatives that were compared and evaluated are summarized in this section.

4.7.2.1 Lateral displacement

In general, denser diagrid structures, such as 75deg1, 70deg1, 65deg2, 65deg1, 59deg1, 59deg2 in convex form and hyp5 and hyp4 in hyperboloid has smallest lateral displacement, which is smaller than 150mm. The braced frame structure is significantly worse, with a lateral displacement approaching 300mm, see Figure 4.20.

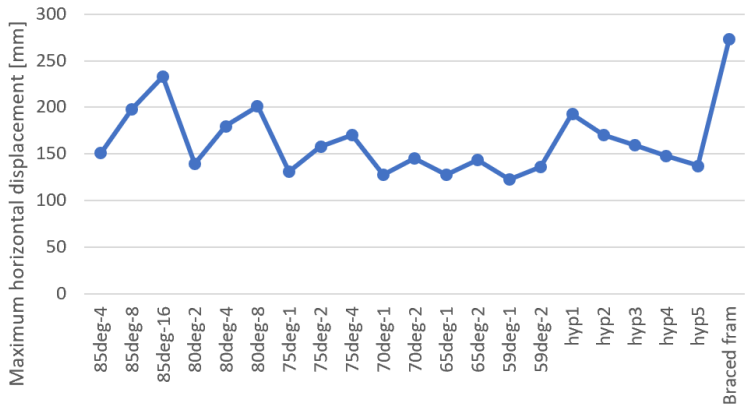

Figure 4.20 Maximum horizontal displacement for all proposals

4.7.2.2 Mass timber per unit area

Regarding mass timber for per unit area, the best solutions are 80deg8, 75deg4 and hyp1. There is a weak trend that between the alternatives with same angles, the more sparse the diagrid system is the less material is consumed per unit area. The brace frame structure consumes most material among all, see Figure 4.21.

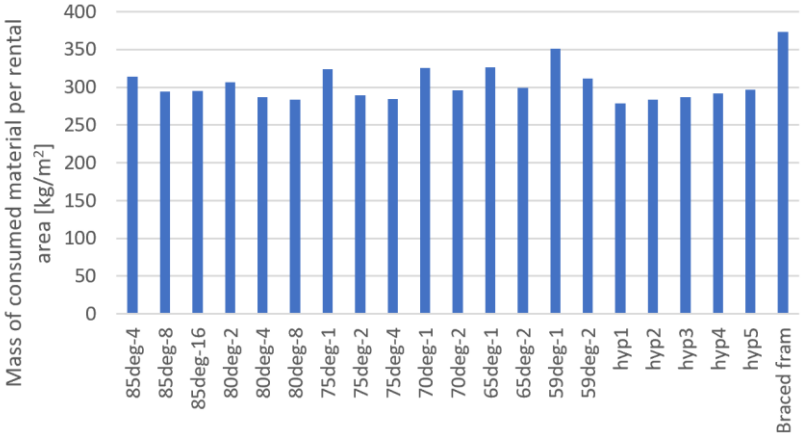

Figure 4.21 Mass of consumed material for unit rental area for all proposals

4.7.2.3 Base moment

The diagrid structures in hyperboloid form are subjected to the least overturning moment. The structures in convex form are subjected to overturning moments which are almost twice as large as that for the hyperboloids and the overturning moment for the braced frame structure is slightly more than 3 times as large as that for the hyperboloids, see Figure 4.22.

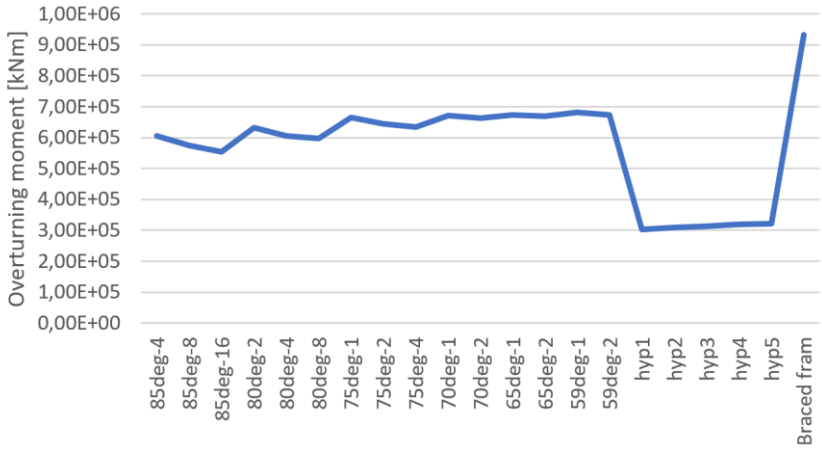

Figure 4.22 Overturning moment for all proposals

4.7.2.4 Dynamic behavior

The dynamic behavior for all the proposals is summarized in Figure 4.23. The peak acceleration-natural frequency points for all the hyperboloid structures lie far below the curve for residential buildings and some of the convex structures like 75deg1, 65deg1 and 70deg1 fulfill the requirement for residential buildings marginally. All other convex structures fulfill the requirement for the office building but not residential use. The braced frame has worse dynamic performance but still satisfies the comfort criterion for office buildings, see Figure 4.23.

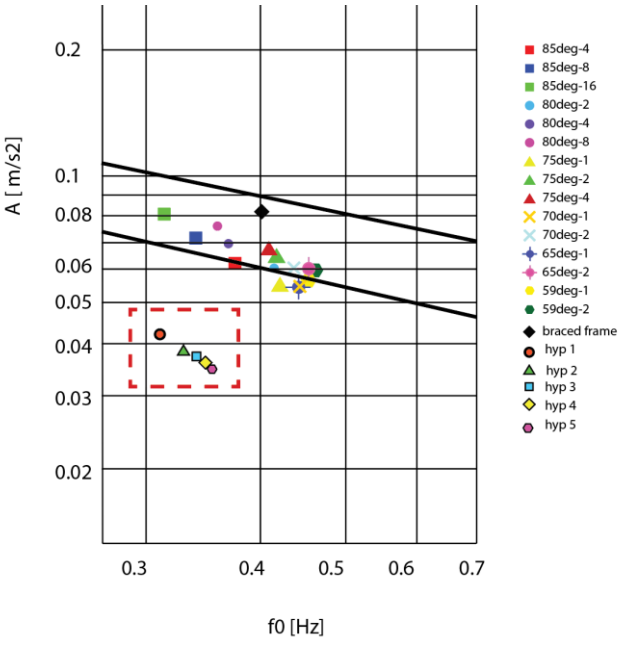

Figure 4.23 Dynamic performance for all proposals

4.7.3 Evaluation

The results shown in Section 4.7.2 were evaluated according to criteria and their weighting factors presented in Section 4.7.1. A scaling score between 1-3 was assigned to each alternative and the results for the evaluation are presented in Table 4.9. The grade scale from 1-3, where 1 means "not good", 2 means "Ok" and 3 means "better". Table 4.9 shows that the three models hyp2, hyp3, hyp4 and hyp5 have the highest score.

Table 4.9 Preliminary evaluation of designs

	Lateral displacement	Dynamic behavior	Mass/rental area	Base moment	Total
85deg-4	3	2	2	2	2.16
85deg-8	2	2	3	2	2.2
85deg-16	1	2	3	2	2.04
80deg-2	3	2	3	2	2.36
80deg-4	2	2	3	2	2.2
80deg-8	2	2	3	2	2.2
75deg-1	3	3	2	2	2.48
75deg-2	3	2	3	2	2.36
75deg-4	3	2	3	2	2.36
70deg-1	3	2	2	2	2.16
70deg-2	3	2	3	2	2.36
65deg-1	3	3	2	2	2.48
65deg-2	3	2	3	2	2.36
59deg-1	3	3	1	2	2.28
59deg-2	3	2	2	2	2.16
hyp1	2	3	3	3	2.84
hyp2	3	3	3	3	3
hyp3	3	3	3	3	3
hyp4	3	3	3	3	3
hyp5	3	3	3	3	3
Braced frame	1	2	1	1	1.32

To choose a final concept, another comparison between the three models was made. Since the limitation of lateral deformation and the dynamic comfort criterion were fulfilled by a large margin, they are less valuable to be included in the further evaluation. Instead, mass of timber consumed per unit rental area and the overturning moment acting on the structure are the two criteria deemed to be most important due to economic aspects. Less timber used means lower cost for the superstructure while a lower overturning moment means that the dimensions of the foundation can be smaller, also reducing costs. Among the four alternatives that have highest point, hyp2 consumes least timber per rental area and the overturning moment is smallest at the same time, see Table 4.9.

Table 4.10 Secondary evaluation of designs

	Mass/area [kg/m^2]	Base moment [kNm]
hyp2	283	309 438
hyp3	287	314 178
hyp4	292	319 036
hyp5	297	321 790

Therefore, hyp2 is the most promising proposal according to the evaluation. It is also the best one with regards to fire safety due to having the largest dimensions of the trusses.

5 Preliminary structural design

The proposal *Hyp2*, the diagrid structure in hyperboloid geometry with 25 dividing points, is according to the comprehensive evaluation in Chapter 4 the most promising.

5.1 Design of structural members

The geometrical features and design details are presented in Figure 5.1.

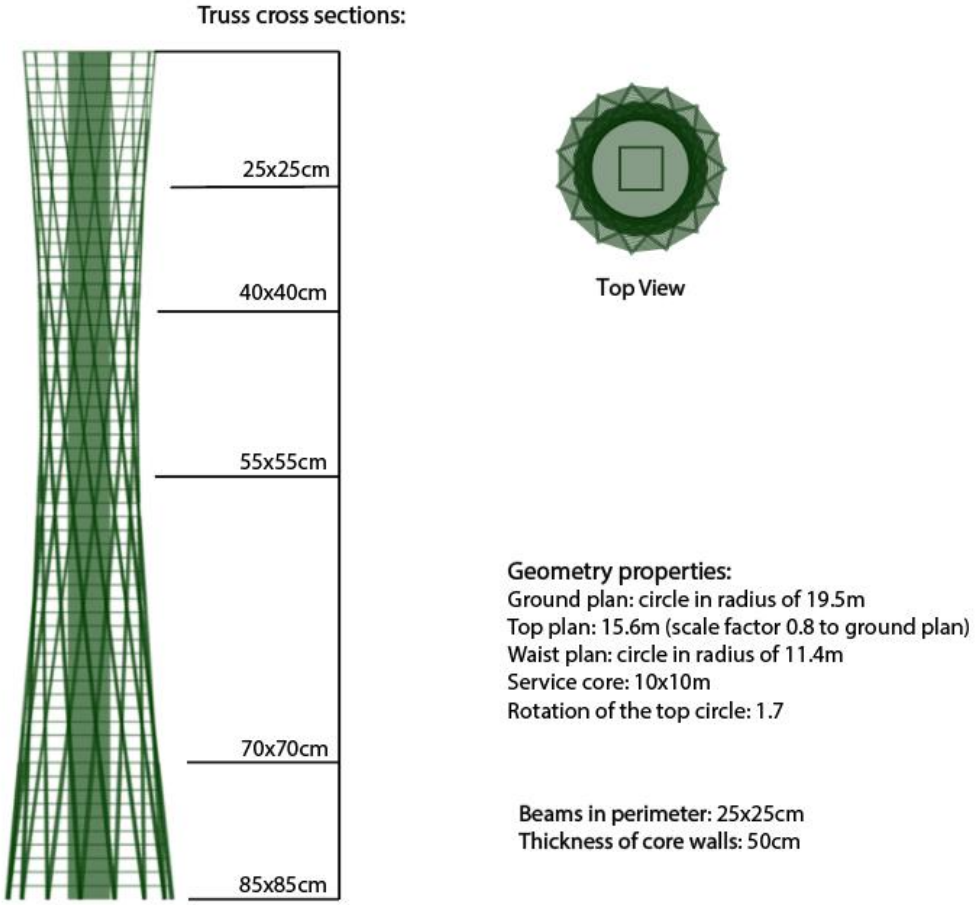

Figure 5.1 Review of the winning proposal

5.2 Joints

How the trusses are joined together in a diagrid system plays a dominant role with regards to the stiffness and how the structure behaves. The joints are aimed to be modelled as hinged at the crossing of two trusses while fixed or to great extent fixed at connections between floors within one triangular module. In earlier study the joints are modelled as fixed, truss elements modelled as beam elements, due to the complication of adjustments of joints in *Karamba 3D* and in order to make all the structures comparable. Furthermore, fixed joints give a lower horizontal displacement than the pinned joints, see chapter 5.2.1. In reality, rigid joints are very expensive to construct. On the other hand, modelling joints as totally fixed might lead to the design being on the unsafe side.

5.2.1 Deviations/risk due to joints

In order to get a perception of deviations and risks arising from joints, the study where all the truss members are modelled as bars, not transferring moment, was conducted for the winning proposal.

Under characteristic SLS load combination, the maximum displacement at the top and natural frequency of the lowest mode at top floor for Hyp2 with all joints fixed and all joints pinned are as in Table 5.1:

Table 5.1 *Maximum displacement and natural frequency for hyp3 with fixed joints respective pinned joints, in SLS*

	Maximum displacement [mm]	Natural frequency of the lowest mode [Hz]	Peak acceleration of the top floor [m/s^2]
Fixed joints	170.1	0.33	0.039
Pinned joints	203.3	0.3	0.042

With pinned joints, the structure exhibits a slightly lower natural frequency and slightly higher peak acceleration at the top floor. But the dynamic behaviors of both joints satisfy the requirement for even the residential buildings. The maximum displacement is increased by 26.8%, from 170mm to 203mm. The real displacement may lie somewhere in between in the real structure. Both values of lateral displacement are far below the comfort criteria of 400mm.

When it comes to the strength of the structure, the maximum utilization of the truss elements in both compression and tension decrease and the utilization of the core walls increase by contrast. This reflects the fact that the diagrid structure pinned together is less stiff than a fixed connected one and more loads are carried by the interior core. In the real case, thicker walls are required.

Table 5.2 Utilization of carrying capacity of truss elements and core walls when the joints are fixed respective pinned, in ULS

	Truss, Maximum utilization, tension	Truss, Maximum utilization, compression	Core walls, maximum compression
Fixed joints	23%	80%	68%
Pinned joints	4.6%	63%	80%

5.2.2 Design of joints

For the erection of truss elements, a certain amount of moment resistance of joints is needed during construction, even though the trusses are intended to carry loads by axial strength in design. To avoid splitting in timber joints, smaller dowels are preferred and the distance between dowels should be long enough according to Eurocode 5, otherwise brittle failure may occur in the connection. Splitting in wood is common and happens because timber has low strength perpendicular to the grain and the dowels are close to each other. To minimize splitting, dowels should also be mounted in a line parallel to the grain.

Table 5.3 Maximum sectional force of trusses in diagrid system, in ULS

Section	Floor	Truss Compression force [kN]
S1	1-10	5787.3
S2	11-31	4453.4
S3	32-43	2243.9
S4	44-52	939.6
S5	53-62	275.9

A proposal for the design for timber truss connections is slotted-in steel plates timber connection as shown in Figure 5.2, and the steel plates are protected from fire. From the result in Table 5.3 a hand calculation for timber truss connection in diagrid system was performed in Mathcad and Figure 5.3 and Figure 5.4 illustrates how it will look.

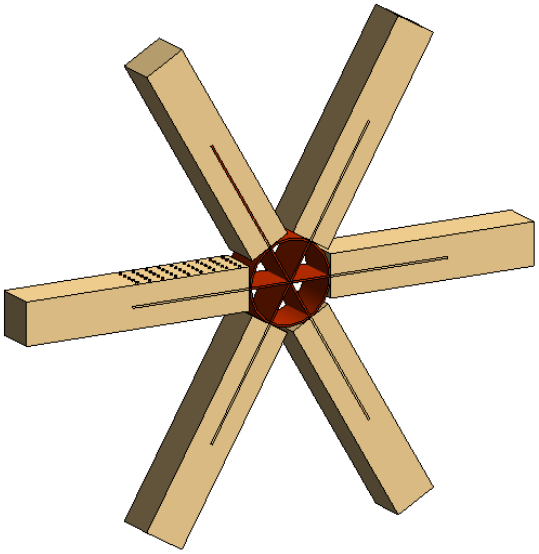

Figure 5.2 Conceptual design of joints

A steel tube is welded with steelplates and is connected with the timber trusses through bolts. The steel plates are hidden inside the timber trusses.

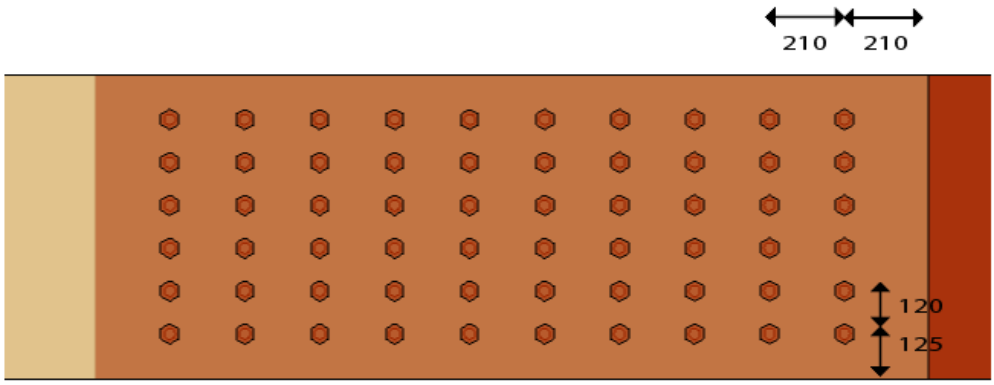

Figure 5.3 Design of the critical joints

The fasteners are chosen to be M30 and is the 30mm is the maximum bolt diameter for this connection according to Eurocode 5. Total there are 60 bolts in each connection. The number of steel elements inside the timber truss can also be increased to two depending on the thickness of the truss. The timber trusses are connected to the concrete element by a connection called a glued-in rod connection and this kind of connection can also be used for the connection between the timber truss in Figure 5.3.

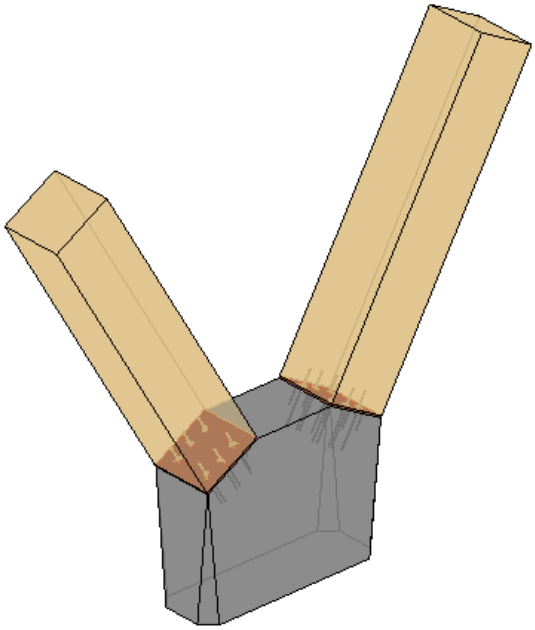

Figure 5.4 Details of the joints

5.3 Overview of structural performance

The overall structural performance of the proposal is summarized in Table 5.4.

Table 5.4 Overview performance of the winning structure

	Fixed jointed	**Pinned jointed**
Mass	8936 tons	
Rental area	31534 m^2	
Mass per area	283.4 kg/ m^2	
Footprint area	1195 m^2	
Building width	39 m	
Foundation moment	310 MNm	
Maximum vertical deformation	24.4 mm	27.7mm
Maximum horizontal deformation	170.1 mm	203.3mm
Eigenfrequency of structure	0.33Hz	0.30Hz
Peak acceleration	0.039m/s^2	0.042m/s^2

6 Discussion

The topic of this thesis is the study of geometries and feasibility of a 200m timber building. Though certain limitations about the building such as the location of the building etc. were made, however, the inclusion of a great number of criteria and perspectives and the complicated interface of the geometry and the structural systems made this research quite broad and complex. Due to limited time and knowledge in modelling some of the factors that might to some degree affect the results and conclusions might not have been included, leading to uncertainties. The final proposal that has been put forward was based on the investigations made in this thesis.

6.1 Slenderness and comparability

One of the most important issues in this project is the comparability and this ran through all the process. In order to make the alternatives as comparable as possible, one crucial limitation that was made from the very beginning is that the design will be limited to a space of 30x30x200m. On one hand, the approval of footprint land is usually the starting point of all the designs and the urban lands are usually planned in rectangular plan. The study of existing skyscrapers shows that 30 m is a common width of skyscrapers. On the other hand, having the same width and height means that all the investigated alternatives will have the same slenderness ratio, which is considered as a dominant factor in the structural view.

The slenderness ratio of a building is defined by the height of the building divided by the smaller base width. However, slenderness is only used to indicate the potential structure behavior and the real structural behavior is more based on the ratio of the height of the building to the smaller width of the stabilizing system (MPA & fib, 2014). When the footprint plan is fixed to a square, geometrically, the circular section already has a smaller second moment of area, which plays a key role for a slender structure where the bending behavior dominates. It is natural that the global lateral stiffness is inherently weaker than that with a square section. The possibility for the circular section to have a better lateral behavior lies in the aerodynamics. Therefore, a precise estimation of the decrease in the wind loads is more important in this case than the others. Also, the effect of variation of width over height is not really reflected by the notion of a slenderness ratio.

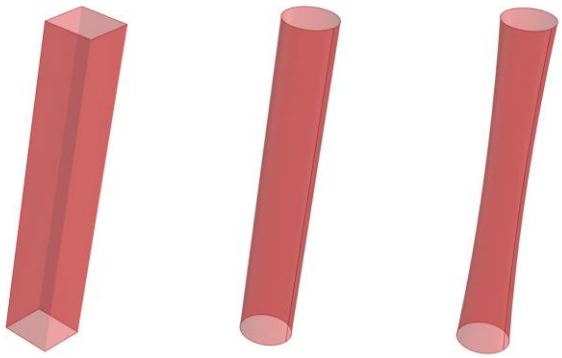

Figure 6.1 Three geometries with the same slenderness ratio but visually and structurally they differ in lateral stiffness.

The obtained results show also that the certain structural models of a same geometry might perform better than some of other geometries but not all of them. This means

that one geometry cannot be unconditionally better than another when it comes to the lateral deformation but depends very much on the specific structural designs, including dimensions of structural members, how densely they are placed etc. During the literature study it was also observed that due to the different limitations, for example a same total floor area or a same footprint area etc., and different design details, the comparison of two identical structural systems can lead to different conclusions.

6.2 Simplifications and design codes

Some simplifications were made during the calculations. The wind loads applied were calculated in line with Eurocode. However, for simplification, the force factor only considers the shapes of the section and the variation over the height is not included, where the base width was used through the calculation. This means that the loads on the geometries with narrowed sections over height were overestimated.

According to Eurocode, the reduction factor that decrease with the increase in the ratio of radius of roundness of corners for rectangular sections to the width of the section, decreases until r/b reaches 0.2 and remains unchanged after that. Meaning that when the radius of the roundness is larger than 6 m, the reduction of the wind loads will be the same as when the radius of the roundness of the corners is 6m. In reality, wind loads are likely to decrease gradually all the way with increasing roundness of corners, until the section became circular.

Apart from this, the calculation procedures for wind turbulence in Eurocode are valid only for structures designed up to 200m. The height of the studied structure in this thesis reaches exactly the upper limit. For design of skyscrapers the wind tunnel method is a common way to determine wind loads and their influence on building geometries. Usually, the results from wind tunnel test shows lesser wind than that calculated from Eurocode. Deeper study needs to be done to estimate difference in the aerodynamic effect on different geometries.

6.3 The three geometries

The study of the structural models of the three geometries, i.e., the braced frame structure in cuboid, truss structure in the convex form and the hyperboloid form with continuous truss down shows that they share both similar and different features. Figure 6.2 below illustrates the force patterns for each geometry when they are subjected only to the horizontal loads.

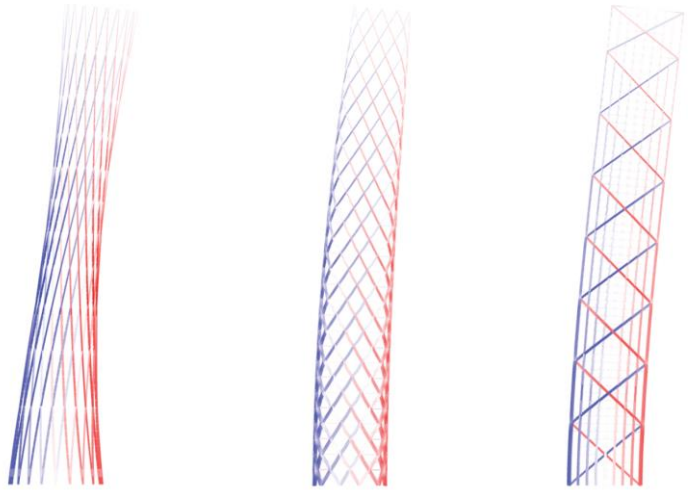

Figure 6.2 Force patterns for hyperboloid diagrid with continuous path, convex form with diagrid truss and braced frame structure

For the braced frame structure, the vertical columns are subjected to axial forces caused by bending while the mega diagonal bracing elements help to resist shear deformation. The diagrid structures applied for both the convex form and the hyperboloid form can carry both moment and shear force. One special behavior for the hyperboloid topology is that the loads can transfer straight down through the continuous path to the ground. In terms of material efficiency, it is preferred that the loads are transferred axially, which is also the case where vertical columns are subjected to bending. When the loads act on the truss in an angle which deviates from the direction parallel to the fibers, the strength of the cross section needs to be reduced.

It was observed that for all these designs the sizes of structural elements are governed by the capacity of cross sections for ULS load combinations rather than the control for lateral deflections. When the structural components were designed to provide enough resistance in ULS, the tip displacements for all alternatives are much lower than the required h/400 under SLS load combinations. All the hyperboloid structures have similar and much better behavior regarding lateral displacement and vibration.

When it comes to dynamic behavior, due to the uncertainties in the structural damping for slender timber buildings like this, it is hard to conclude whether all alternatives satisfied the requirements for comfort. In the calculations a 9% structural damping was applied, which is a recommended value for timber structures with mechanic connections according to the old Swedish handbook for snow and wind loads (Boverket, 1997). This recommended value coincides with the range 6%-12% for

timber bridges according to EN1991-1-4. The hyperboloid structures have the best dynamic behavior of all while the braced frame structure are the worst.

6.4 The hyperboloid

The hyperboloid form turned out to be the best solution according to the evaluation. One significant disadvantage of this form is the amount of usable volumes and areas. The form is strongly structure-dependent and not closely related to the enclosed space. In some cases, the decreased volume is not a problem and can even be preferred, because of, for example, less heating demand (Reid, 2013). The hyperboloid grid shell or shell structure are common for structures such as cooling towers in power stations, water towers that lifts mass on the top of the structure, TV towers, sightseeing towers etc. In the view of structural efficiency, when the maximum usable area is not a key factor, the hyperboloid form requires least material cost and decreases the self-weight to reach a certain height, which was also verified by this study. The mass of timber consumed for braced frame structure is about 32% more than that for hyperboloid form (type hyp1). Note that the hyperboloid geometry was scaled by 1.3, meaning that the diameter of all the floors is amplified by 30%, and this indicates that the gross material was increased and material per unit area might be decreased, compared to the hyperboloid that has the same base width as other geometries. The reason why the hyperboloid won depends highly on the remarkably better dynamic behavior.

The narrowest floor has a radius of 11.4 m, with a distance ranging from 4.3 to 6.4 m from the shaft to the façade. The limited floor plans might lead to difficulty in employing the waist floors. These floors can potentially be used for cafeterias, sightseeing etc. There is a possibility that the hyperboloid geometry can be scaled up even more. This might cause problems with daylight provision for the floors with largest width on the downside, but there is potential that these floors can be used as garages or shopping malls, which have low requirements on daylight. Also, the exact size of the geometries investigated are not that precise. For example, when checking the net floor areas, the thickness of the shaft walls was not considered.

As mentioned before, the hyperboloid geometry is structure-dependent, meaning that the properties of the geometry, for example how narrow the waist is, is governed by the properties such as rotation degrees of continuous paths. By fixation in both the height and width, the available hyperboloid geometries that can work as a building that aims at providing adequate rental floors rather than a tower, are quite limited. In this project only one workable case was investigated. The existing hyperboloid structures normally have a wider base and are stockier. The wider base is also one important factor that makes hyperboloid a stable structure. The curvature of the investigated hyperboloid geometry cannot vary significantly because of the limitation of the building width and the usability of the floors, which leads to a relatively narrower base. The benefit from the wide base is somehow not obvious in this geometry.

Due to the trusses that are inclined inward on the upper part, compression in the floor slabs cannot be avoided. Due to the detailed design of the floor slab, there is a risk of buckling of floor elements with large spans. On the perimeter, the truss elements are anchored at each floor and the buckling length is close to the floor height, which is

approximately 3.2 m. The dimensions of the trusses will not lead to buckling so far. Tensile forces will arise in some trusses when the imposed load does not act. Tensile forces are undesirable because the design of tension in timber trusses and the uplifting of the structure can be complicated and risky. Some measures that may be necessary to eliminate tensile forces are more masses on top floors which improves dynamic performance at the same time, concrete cover on floors to improve dynamic behavior of floors or concrete connections directly on the perimeter structure as what SOM did in its timber tower research project (SOM, 2013).

To increase the geometrical stiffness the lateral load is supposed to be resisted mostly by the external structure, i.e., the truss system in the perimeter, and a soft core was desired. In the study, core walls with constant thickness of 500mm over height for all models was studied. For the winning proposal hyp2 with fixed connections, the result shows that 85% of the overturning moment and 50% of the horizontal forces are resisted by the perimeter structure.

Due to the difficulty of modelling joints, the joints have been both fixed, when the truss elements were defined as beams, and pinned when the truss elements were modified to act as bars. The intention of modelling joints in connections of the triangular module as pinned and the trusses for one side of the triangular module as continuous has not been carried out. The real results of horizontal deformations lie between those obtained with fixed and pinned joints, between 170mm and 203mm.

6.5 Long term effect on structure

Both the strength and stiffness of timber can be influenced by moisture. The lower the moisture the material is exposed to, the higher the strength and stiffness are. Since timber is an anisotropic material, the mechanical properties are influenced in different degrees when loaded in different directions. All the structural members are supposed to be designed to carry load in the fiber direction. The changes of compression and tension strength parallel to the fiber direction is 5% respective 2.5% and 4% for bending, when the moisture content is changed by 1%. The modulus of elasticity parallel to the fiber direction changes by 1.5% (Svenskt Trä, 2016). Time is another factor that influence the mechanical material properties. The strength is weakened with increased loading time. For strength modification with regards to the combined effect of moisture and loading duration, the factor k_{mod} is denoted. Service class 2 with permanent loading was assumed, leading to a decrease in strength by 40%.

The long-term deformation or creep deformation is important to be considered in the design of timber structures. For engineered wood products (EWP), the creeping may be different for different types of products and some of the EWP may creep more than sawn timber. In a composite structure where different parts creeps to different degrees the creep is important for the stress analysis (Svenskt Trä, 2016). But this is especially important when it comes to the serviceability of the building. Creep factor is used to take this is into consideration, which shows the ratio of creep deformation to instantaneous deformation. The value of this is 0.8 for Glulam (glued laminated timber) and solid timber (EN1995-1-1, 2004).

For a 200m timber tower, apart from the vertical deformation of the floor slabs, the design of which is not included in this project, the vertical deformation of structural

members that carry gravity loads might influence the free height of the floors. The vertical deformation presented in Table 5.4 is the maximum nodal deformation in perimeter among all the floors, but the long-term effect has not been included yet. But even though the creep factor is considered, an increase of 20% of the deformation to approximately 3 cm due to long-term effects is not much. For a design like this, where the floors are supported by the trusses in the perimeter and the core walls, the vertical deformation of the core wall elements need to be considered in long-term as well because of the risk of inclination of floors which may make it hard in serviceability.

6.6 Joints

The performance of joints will greatly influence the global behavior of a slender timber structure, not only the stiffness but also dynamic response. For simplification, when comparing different solutions, the nodes were modelled as rigid, moment resistant and disregarding the slip in joints. This does not coincide with the realistic constructions. Moment resistant timber joints are expensive and might not be economic and at the same time it is not on the safe side in design to consider the joints as moment resistant especially to full degrees. Regarding the rigidity by fully filling the voids at joints can reduce some of the slip. One the other hand, a certain amount of ductility of the structure is desired. Since timber is a brittle material, the structure can fail without any obvious indication and a certain degree of ductility allows load redistribution and deformations before the structure collapses.

6.7 Potential error source

A series of simplifications were made throughout the study which may influence the reliability of the results. One of those is the stiffness and slip of joints as mentioned in Section 6.6. How much this simplification influences the results such as deflection and dynamic behavior is uncertain, especially for various geometries. If the slip in joint affects different geometries to the same extent the results of comparison of different geometries can still be regarded as reliable.

Another error source lies in the wind loads. Simplifications in the calculation of wind loads, discussed in Section 6.2, makes it differ slightly from the real case, especially for those geometries with variable width over heights. But this was estimated to be minor. The simplification of distributed load over the height to a point load on the top of the structure in the evolutionary design in geometry study by shell structures can be another potential error source related to assignment of winds. Table C4.2 in Appendix C4 shows that the ranking of geometries regarding horizontal displacement under distributed loads differs from that under one single point load. But it was observed also that the difference in ranking for each geometry is limited to usually the places in the adjacent region and those change place has almost close displacement. The consequence of this is that there might be some better geometries that is not selected. But considering that the optimizing process is evolutionary, and the good genes of those best solutions are inherited still to the next generation, the resulted geometry might be similar globally but minor difference in parameters. The optimized geometry from this evolutionary design will thereafter still be analyzed with distributed wind loads.

Some of the uncertainties comes from the assignment of material properties. During the geometry study with shell structures, it was observed that when the ratio of the modulus of elastic and shear modulus changes the results of ranking regarding to lateral displacement fluctuates marginally. For the evaluation, the results where elastic modulus and shear modulus of derived and equivalent to a triangular truss module over two floors with a height of approximate 6.4m where the trusses are inclined at an angle of 65 degrees with cross section area. In principle the material can be assigned to various combinations depending on how the trusses are constructed. The result might be different if different material properties are assigned.

In order to build diaphragm floor, the slabs are thin and have a large elastic modulus which is ten times that of the shell tubal structure. This is regarded as sufficient and has been verified by the equal nodal displacement for each slab. In the analysis with trusses where core walls are included as well, to simulate the real structural response to compare with the design criteria, the material properties are retrieved from prefabricated elements from market. In general, the floor behaves as diaphragm but the interaction between slabs and walls and even the concentrated stresses caused by the points load anchored on each floor slab might influence in some uncontrolled way. The precise mechanical properties of walls and slabs are dependent on the precise design of corresponding elements.

Apart from this, the strength of timber will be weakened when it is subjected to loads which is not parallel to the fiber direction. The effect of this was neglected. This may influence different structures to different degrees, especially for those where bending deformation is more dominant. For the winning hyperboloid structure, the horizontal loads are carried all the way down to the ground along the straight path, the decrease of strength raised in the angle between loading and fiber direction is minimized, caused only by the vertical loads.

At last, though regular verifications and checks have been made throughout the modelling and computation, there might still be some manual mistakes that have not been observed. The project covers a wide scope and a great number of models are involved, more time is needed to get rid of all unexpected mistakes and errors.

6.8 Improvement and future work

In the stage of preliminary design, a promising proposal has been put forward and the sizes of primary structural elements have been estimated according to the sectional forces. The structure can be improved through the following strategies:

- The ring beams can be optimized by grouping them into primary and secondary beams where the primary ring beams refer to those that connect inclined columns (trusses) and transfer them into triangle modules.
- Additional masses, concrete cover on the floors or as concrete joints to eliminate the probable occurrence of tensile forces in the truss elements.
- The structural elements can be replaced by stiffer products that exist in the market or specially constructed

For the detailed design and verification of individual structural elements and to make the proposal buildable, there are several works still left to be completed. For example:

- Calculate the detailed wind pressure on the enveloping façade surface
- Fire design for the structural elements
- Robustness of the load-carrying structural system
- Detailed design and verification of all or most critical members according to EN1995-1-1 in compression and combination compression and bending
- Verification of global deformation and deformation of individual elements in service limit state including long-term effect
- Detailed design and optimization of the joints with regards to strengths, stiffness, and ductility

6.9 Software

The software *grasshopper* is a flexible digital tool for building parametric models. New forms will be generated when the governing parameters varies. Together with its plug-in *Karamba 3D* it is quite easy to assemble FEM models and conduct FEA. The programs also provide a series of optimization algorithms, among which evolutionary design tool *Galapagos* and cross section optimizer *OptCroSec* were used. These tools make the optimization process more effective.

The *Python-component* is a very useful tool and makes it flexible to set loads who are closely related to the modelled geometries.

One inconvenience with *Karamba 3D* is that it uses another unit system that is used for the inputs and outputs, rather than the IS (International system of units) base units. Extra attention and care is needed when putting in important input data. It has happened that very wrong results were obtained due to the mix up of units and all the computation needed be repeated.

Finally, *Karamba 3D* is most applicable and easiest for analyzing steel structures since some algorithm such as *OptiCroSec* etc. are based on Eurocode 3 for steel structures. For timber structures, the design can be regarded only as a reference and the verification of capacity and risk for buckling is needed to be done manually. *Python-component* is a good supplement tool here to do the verification. In addition, it is currently not possible to give different strength in different direction for an anisotropic material such as timber.

7 Conclusion

The study shows that a 200m timber tower is probably possible to be built in terms of structural behavior, as long as the stiffness and cross sections of the structural elements are sufficient. The structural solutions for all the three geometries with optimized cross section, the requirements for serviceability are fulfilled, where the braced frame structure has relatively worse dynamic performance.

Due to the light self-weight, additional masses might be needed to hold down the structure and to avoid the tensile forces on the windward side of the building, if this is not desired.

There are uncertainties arising from the connections with stiffness and joint slip which was not modeled and included in the calculation. How this will influence these structuralized structures is uncertain. Further study is needed to draw a more precise conclusion.

The diagrid structures in convex and hyperboloid form are more material effective and stiffer per mass material compared to the straight braced frame structure for this 200m timber tower. The dynamic performance is dramatically better as well, especially for the hyperboloid form. Apart from the low self-weight, the winning proposal with its special hyperboloid forms have good aerodynamic features and the overturning moment is much smaller than for other geometries and have less requirements for the design of the foundation.

One significant disadvantage of this proposal is the large land use. The utilization ratio of the land is low. Though less construction material is consumed, whether the proposal is economical build is uncertain. The construction of a round building can be more complicated than a square section but the truss columns aligned in straight line makes this easier. However, the construction of a round floor slab is not common and is more complicated. To make the construction effective and cheap, further investigation of this kind floor slabs is needed and to find ways to make them able to be prefabricated and connected on site in an easy way.

In the initial geometry study with membrane tubal element, an observation is that for such a high building, compared to aerodynamic effect, the influence of the slight change in façade curvature on deformation is little. A more efficient way to design a high-rise building is to find a good geometry according to aerodynamics and thereafter to find the most efficient structural system for it. It is also proven that the depth of building has great influence in structural behavior, and it is a good way to improve the structural behavior for tall timber building by utilizing the external structure system around the façade.

8 Further research

To make it feasible to build a 200m timber, the joints need to be investigated more deeply. Rigid joints with tolerance for adequate ductility is necessary.

Structural damping rate for a 200m timber building is not certain. Underestimation of this may lead to overdesign if the dynamic issue is most critical for the design. For the optimization of a material effective structure, a more precise estimation and study in this is needed.

Apart from this uncertainty involved in the study, one potential topological design which is structural effective is that with angles of trusses aligned with one principal stresses, smaller on the top to resist shear deformation and changes successively to vertical which is more efficient to resist moment. Due to the time limitation this was not included in this study but is worth to be investigated.

9 References

Abd Samat, R., Khairudin, M.F, Din, M.H., Ali, G.G, Fadzil, A.B. & Bakar, S.A, *Comparative Structural Performance Of Diagrid and Bracing System in Mitigation of Lateral Displacement*, IOP Conf. Series: Earth and Environmental Science 220 (2019) 012025. IOP Publishing

Abrahamsen, R. (2017). *Mjøstårnet - Construction of an 81 m tall timber building,* 23 Internationales Holzbau-Forum IHF 2017

Alaghmandan, M & Elnimeiri, M. (2013). *Reducing Impact of Wind on Tall Buildings through Design and Aerodynamic Modifications (Architectural and Structural Concepts to Mitigate Wind Effect on Tall Buildings).* Architectural Engineering Conference 2013, State College, Pennsylvania

Ali M.M. & Moon, K.S. (2007). *Structural Developments in Tall Buildings: Current Trends and Future Prospects*, Architectural Science Review, 50:3, 205-223

Al-Kodmany, K. (2020): *Tall Buildings and the City: Improving the Understanding of Placemaking, Imageability, and Tourism*. Springer.

Awida, T.A. (2011). *Slenderness Ratio Influence on the Structural Behavior of Residential Concrete Tall Buildings*. Journal of Civil Engineering and Architecture, Volume 5, No. 6 (Serial No. 43), June 2011, pp. 527-534.

Balendra, T. (1993). Vibration of Buildings to Wind and Earthquake Load, Springer-Verlag, London

Boverket (2011). *BFS 2011:6. Boverkets byggregler: Föreskrifter och allmänna råd*, BBR. Karlskrona: Boverket.

Boverket (2013). *BFS 2013:14. Boverkets byggregler: Föreskrifter och allmänna råd*, BBR. Karlskrona: Boverket.

Boverket (2019). *BFS 2019-1-EKS-11. Boverkets byggregler: Föreskrifter och allmänna råd*, BBR. Karlskrona: Boverket.

Boverket. (1997). Snö- och vindlast, BSV 97.

Boake, T.M. (2014). *Diagrid Structures*, Birkhauser.

Cascone, F., Faiella, D., Tomei, V. & Mele, E. (2021). *Stress lines inspired structural patterns for tall buildings*. Engineering Structures 229 (2021) 111546

CEN (2005). *EN1991-1-4. Eurocode 1: Actions on structures- Part 1-4: General actions- Wind actions*.

CTBUH. (n.d). CTBUH Height Criteria for Measuring & Defining Tall Buildings. Retrieved 2021-03-14 from https://cloud.ctbuh.org/CTBUH_HeightCriteria.pdf

Elbakheit, A. R. (2018). Wind-Induced vibrations to tall buildings and wind turbines. *Vibration Analysis and Control in Mechanical Structures and Wind Energy Conversion Systems*.

Elshaer, A. (2017). *Aerodynamic Optimization and Wind Load Evaluation Framework for Tall Buildings* [PhD thesis, Lakehead University]

Engelmark, H. (2005) *Stabilisering av höga trähus: koncept och förskjutningskontroll.* [Master's thesis]. Luleå University

Feng, M.Q. & Mita, A. (1995). Vibration control of tall buildings using mega subconfiguration. J. Eng. Mech. 121 (10) (1995) 1082–1088.

Fu, F. (2018). *Design and analysis of tall and complex structures.* Butterworth-Heinemann.

Gyllensten, S. & Modig, A. (2020): *The 200 m timber tower: A study on the possibilities of constructing a 200 meter tall timber building.* [Master's thesis]. Chalmers University of Technology

Holmes. J.D. (2001). *Wind Loading of Structures*. Spon Press, London.

Ibrahim, N. & Hayman, S. (2005). Daylight Design Rules of Thumb. *Conference on Sustainable Building South East Asia*, *April 2005*, 11–13.

Irwin, P. (2009). *Wind challenges of the new generation of super tall buildings*. Journal of Wind Engineering and Industrial Aerodynamics, Vol. 97. Pages 328-334.

Johanneson, P & Vredblad, B. (2011l). Byggformler och tabeller (2nd edition). LiberAB

Kawai. H. (1998). *Effect of Corner Modifications on Aeroelastic Instabilities of Tall Buildings*. Journal of Wind Engineering and Industrial Aerodynamics, Vol. 74-76.

Moelven. (n.d). *Flervåningshus Trä8.* Retrieved 2021-03-07 from https://www.moelven.com/se/produkter-och-tjanster/allt-om-limtra/flervaningshus-tra8/

MPA & *fib.* (2014). *Tall buildings: Structural design of concrete buildings up to 300 m tall*. Fib Bulletin No. 73.

Preisinger, C. (2016). *Karamba user manual for version 1.2.2.* Retrieved 2021-03-21 from https://web.arch.virginia.edu/~km6e/arch721/docs/Karamba_1_2_2_Manual.pdf

Ramage, M., Foster, R., Smith, S., Flanagan, K. & Bakker, R. (2017). *Super Tall Timber: design research for the next generation of natural structure*, The Journal of Architecture, 22:1, 104-122

Ramage, M., Reynolds, T. & Foster, R. (2017a). *Proposal for Defining a Tall Timber Building*, July 2016, Journal of Structural Engineering 142(12):02516001

Ramage, M., Reynolds, T. & Foster, R. (2017b*): Rethinking CTBUH Height Criteria in the context of tall building, CTBUH research paper*, CTBUH Journal, 2017 Issue IV

Reid, E. (2016). *Understanding buildings: A multidisciplinary approach*. Routledge.

Shi, Q. & Zhang, F. (2019). *Simplified calculation of shear lag effect for high-rise diagrid tube structures*, Journal of Building Engineering 22 (2019) 486–495

Sidén, M. (2017). *KL-träbjälklag i kombination med stålstommar: Teknisk utvärdering och utveckling av lösningar för förband och längre spännvidder*. [Master's thesis]. Luleå University

SIS. (2016). *SS-EN 81-70*: *Säkerhetsregler för konstruktion och installation av hissar - Särskilda applikationer för person- och varupersonhissar - Del 70: Tillträde till hissar för personer inklusive personer med funktionsnedsättningar.*

SIS. (2008). *SS-ISO-10137-2008: Grundläggande dimensioneringsregler för bärverk - Byggnaders samt gång- och cykelbroars brukbarhet med hänsyn till svängningar och vibrationer.*

SIS. (2002). *SS-EN1990: Grundläggande dimensioner för bärverk.*

SIS. (2005). *SS-EN1991-1-4: Laster på bärverk - Del 1-4: Allmänna laster – Vindlast.*

SIS. (2002). *SS-EN1991-1-2*: *Laster på bärverk - Del 1-2: Allmänna laster - Termisk och mekanisk verkan av brand.*

SIS. (2009). *SS-EN1995-1-2: Dimensionering av träkonstruktioner - Del 1-2: Allmänt - Brandteknisk dimensionering.*

Skyscraper Center (n.d.a). *Burj Khalifa*. Retrieved 2021-02-15 from https://www.skyscrapercenter.com/building/burj-khalifa/3

Skyscraper Center (n.d.b). *Mjøstårnet*. Retrieved 2021-02-15 from https://www.skyscrapercenter.com/building/mjostarnet/26866

SOM. (2013). *Timber tower research project final report*, Skidmore, Owings & Merill, LLP.

Svenskt trä. (n.d.). Om trä. Retrieved 2021-02-03 from https://www.traguiden.se/om-tra/

Svenskt trä. (2019). The CLT handbook. Svenskt trä

Swedish Wood. (2016a). *Design of timber structures, Volume 1 EDITION 2:2016.* Swedish wood.

Swedish Wood. (2016b). *Design of timber structures, Volume 2 EDITION 2:2016*. Swedish wood

Thambirajah, B. (1993). *Vibration of Buildings to Wind and Earthquake Loads*, Springer-Verlag London Limited

Xie, J. (2014): *Aerodynamic optimization of super-tall buildings and its effectiveness assessment*. Journal of Wind Engineering and Industrial Aerodynamics.

Appendix A Estimation of force coefficient

The force coefficients for rectangular sections with sharp and rounded corners are calculated according to Section 7.6 in EN1991-1-4. The force coefficient for circular cylinders is calculated according to Section 7.9 in EN1991-1-4.

The width of the building is assumed to be uniform over height for all geometries. Terrain category IV is assumed. The location is assumed to be Gothenburg and the reference wind speed v_b was obtained from EKS11.

The surface of the structure was assumed to be planed timber, though it might probably be covered largely by glass. However, the results don't show significant differences.

Table A.1 Input: width and height of the building

b	30m
h/l	200m

The force coefficients for various geometries were calculated to:

Table A.2 Force coefficients for certain geometries

Rectangular sections			Circular cylinder
Sharp corners	r=3	r=6	
1.45	1.09	0.72	0.55

The values of force coefficients applied in the FEA models are:

Table A.3 Force coefficients applied in FEA

Roundness of sections of rectangles	Force coefficient c_f
Sharp corners: 0-3	1.4
Rounded corners:3-6	1
Rounded corners: 6-14	0.7
Circle: 14-15	0.5

The calculation procedures are attached below, where numbering of expressions and figures are referred to those in EN1991-1-4 and EKS11.

The height of the building: $l := 200m$

The width of the building: $b := 30m$

Calculation of force factor for rectangular section

$c_f = c_{f0} \cdot \psi_r \cdot \psi_\lambda$ (7.9)

$c_{f0} := 2.1$ when b=d (Figure 7.23)

For a square cross-section with rounded corners (Let b=30m in this case)

$r := 3$ $\psi_{r3} := 0.75$ (Figure 7.24)

$r > 6$ $\psi_{r6} := 0.5$

$\lambda := \min\left(\frac{1.4 \cdot l}{b}, 70\right) = 9.333$ for l>= 50m, rectangular (Table 7.16)

$\psi_\lambda := 0.69$ Assume solidity ratio 1 (Figure 7.36)

Therefore for a square section:

Without roundness of corners: $c_f := c_{f0} \cdot \psi_\lambda = 1.449$

With roundness r=3 $c_{f3} := c_{f0} \cdot \psi_\lambda \cdot \psi_{r3} = 1.087$

With roundness r=6 $c_{f6} := c_{f0} \cdot \psi_\lambda \cdot \psi_{r6} = 0.724$

Calculation of force factor for cylindral section

$c_f = c_{f0} \cdot \psi_\lambda$

$k := 0.0015mm$ for glass $\frac{k}{b} = 5 \times 10^{-8}$ (Table 7.13)

$v_b := 25\frac{m}{s}$ (Figure C-4 EKS 11)

$\rho := 1.25\frac{kg}{m^3}$ $q_b := \frac{1}{2} \cdot \rho \cdot v_b^{\,2} = 390.625Pa$

(Table 4.1)

$z_0 := 1m$ $z_{min} := 10m$ For terrain category IV

$z := l = 200m$

$k_r := 0.19 \cdot \left(\frac{z_0}{0.05m}\right)^{0.07} = 0.234$ (4.5)

$c_r := k_r \cdot \ln\left(\frac{z}{z_0}\right) = 1.242$ (4.4)

$c_0 := 1$ $v_m := c_r \cdot c_0 \cdot v_b = 31.039\frac{m}{s}$ (4.3)

$$I_v := \frac{1}{c_0 \cdot \ln\left(\frac{z}{z_0}\right)} = 0.189$$

Set $k_p := 3$

$q_p := \left(1 + 2 \cdot k_p \cdot I_v\right) \cdot \left(k_r \cdot \ln\left(\frac{z}{z_0}\right) \cdot c_0\right)^2 \cdot q_b = 1.284 \times 10^3\ \text{Pa}$ (7§ ESK 11)

$v_{ze} := \sqrt{\frac{2 \cdot q_p}{\rho}} = 45.325 \frac{m}{s}$ (NOTE2 for Figure 7.28)

$\nu := 15 \cdot 10^{-6} \frac{m^2}{s}$ $R_e := \frac{b \cdot v_{ze}}{\nu} = 9.065 \times 10^7$ (7.15)

$c_{f.0} := 0.68$ (Figure 7.28)

$\lambda := \min\left(0.7 \cdot \frac{l}{b}, 70\right) = 4.667$ For circular cylinder (Table 7.16)

$\psi_r := 0.67$ (Figure 7.36)

$c_f := c_{f.0} \cdot \psi_r = 0.456$

Appendix B Calculation of characteristic wind loads

The wind loads were calculated in line with EN1991-1-4 and ESK11 and programmed in Python-component in Grasshopper. All the expressions and figures in this Appendix are retrieved from EN1991-1-4 and ESK11. The method of discretization of the section was applied.

Force coefficients applied in the calculation was estimated in Appendix A.

The width of the building is assumed to be uniform over height for all geometries. Terrain category IV is assumed. The location is assumed to be Gothenburg.

The wind force acting on the structure or structural elements were calculated by the expression:

$$F_w = c_s c_d \cdot c_f \cdot q_p(z_e) A_{ref} \qquad \text{(B.1)}$$

By discretization:

$$F_w = c_s c_d \cdot \sum c_f \cdot q_p(z_e) A_{ref} \qquad \text{(B.2)}$$

where:

$c_s c_d$	is the structural factor
c_f	is the force coefficient, estimated according to Appendix A, simplified as uniform over the height
$q_p(z_e)$	is the peak velocity pressure at reference height z_e. z_e was defined according to Figure B.1
A_{ref}	is the reference area of the structure or structural elements, see Figure B.2.

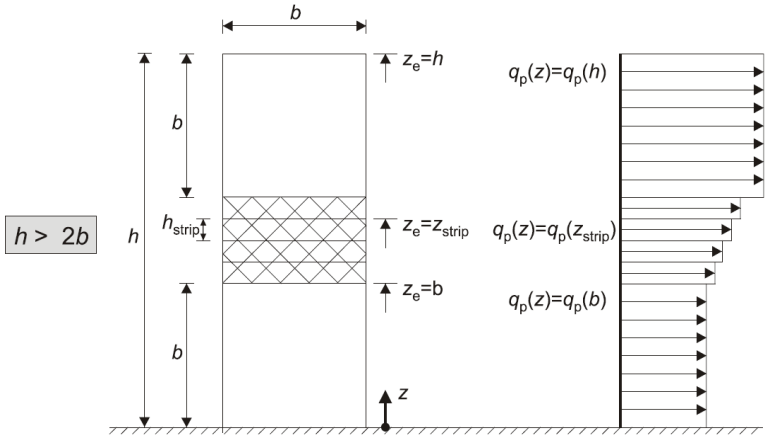

Figure B.1 Reference height z_e for structure when h>2b. In the calculation z_e=200 when h>170m; z_e=30 when h≤30m. z_e=the height of each floor when 30m<h≤170m. (EN1991-1-4)

The reference area was calculated by expression:

$$A_{ref} = \ell \cdot b \qquad \text{(C.3)}$$

where:

b	is the width of the structural elements, varying over height
ℓ	is the length of the structural elements, considered as the height of one floor

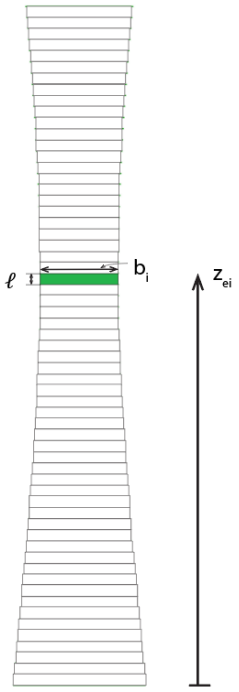

Figure B.2 Illustration of discretization of the reference area. The reference area was divided into subareas where the length of each is equal to the height of one floor. The peak velocity pressure acting on $A_{ref,I}$ has a reference height $z_{ei.}$

The peak velocity pressure was determined by:

$$q_p(z) = [1 + 2k_p(z) \cdot I_v(z)] \cdot {c_r}^2(z) \cdot {c_0}^2(z) \cdot \frac{1}{2} \cdot \rho \cdot v_b^2 \qquad \text{(B.4)}$$

where:

k_p	is the peak factor
$I_v(z)$	is the turbulence intensity at height z
$c_r(z)$	is the roughness factor at height z
$c_0(z)$	is the orography factor at height z, taken as 1
ρ	is the air density, taken as 1.25kg/m^3
v_b	is the reference wind speed, 25m/s for Gothenburg

Table B.1 Terrain parameters for category IV

$\boldsymbol{z_0}$	1m
$\boldsymbol{z_{min}}$	10m
$\boldsymbol{z_{max}}$	200m

Roughness factor

$$c_r(z) = k_r ln(\frac{z}{z_0}) \; z_{min} \leq z \leq z_{max} \quad \text{(B.5)}$$

$$c_r(z) = k_r ln(\frac{z_{min}}{z_0}) \; z \leq z_{min} \quad \text{(B.6)}$$

Peak factor

According to EKS11. For construction affected by dynamic effect:

$$k_p = \sqrt{2ln(\nu T)} + \frac{0.6}{\sqrt{2ln(\nu T)}} \quad \text{(B.7)}$$

or k_p=3 which is larger

where:

k_p	is the peak factor
ν	is the up-cross frequency
T	is the averaging time for the mean velocity, T=600s

$$\nu = n_{1,x} \cdot \sqrt{\frac{R^2}{B^2+R^2}} \geq 0.08Hz \quad \text{(B.8)}$$

where:

$n_{1,x}$	is the estimated natural frequency of structure
R^2	is the factor for resonate response
B^2	is the factor for background response

Estimation of the fundamental lateral frequency of multi-story buildings higher than 50m:

$$n_{1,x} = \frac{46}{h} \text{ Hz} \quad \text{(B.9)}$$

$$B^2 = e^{[-0.05(\frac{h}{h_{ref}})+(1-\frac{b}{h})(0.04+0.01(\frac{h}{h_{ref}}))]} \quad \text{(B.10)}$$

where:

h	is the height of the building
h_{ref}	is the reference height, h_{ref} =10m

$$R^2 = \frac{2\pi F \phi_b \phi_h}{\delta_s+\delta_a} \quad \text{(B.11)}$$

where:

F	is the Karman's wind energy spectrum
ϕ_b	is the size factor regarding the width of the building
ϕ_h	is the size factor regarding the height of the building

δ_s is the mechanical damping
δ_a is the aerodynamic damping

$$F = \frac{4y_C}{(1+70.8y_C^2)^{\frac{5}{6}}} \quad \text{(B.12)}$$

y_C is the unitless factor and:

$$y_C = \frac{150n_{1,x}}{v_m(h)} \quad \text{(B.13)}$$

$v_m(z)$ is the mean wind velocity at the height z and:

$$v_m(z) = c_r(z)c_0(z)v_b \quad \text{(B.14)}$$

$$\phi_h = \frac{1}{1+\frac{2n_{1,x}h}{v_m(h)}} \quad \text{(B.15)}$$

$$\phi_b = \frac{1}{1+\frac{3.2n_{1,x}h}{v_m(h)}} \quad \text{(B.16)}$$

When the modal deflections are constant for each height h and which is the most case, the logarithmic decrement of aerodynamic damping can be estimated by:

$$\delta_a = \frac{c_f \rho b v_m(z_s)}{2n_1 m_e} \quad \text{(B.17)}$$

where:

c_f is the force coefficient, from Appendix A
m_e is the equivalent mass per unit length for the upper third of the building, for floor 40- 62 in this calculation
n_1 is the estimated lowest eigenfrequency of the building
$v_m(z_s)$ is the mean wind velocity at height $z_s = 0.6 \cdot h \geq z_{min}$
ρ is the air density, 1.25kg/m^3

The value of δ_s was chosen as 0.09[2] out of the recommended value for timber construction with mechanical connection from the old handbook for snow and wind loads published by Boverket (1997). In EN1991-1-1, this value for timber bridges is between 0.06-0.12. There is much uncertainty about the precision but the underestimation of this value will lead to a larger end factor and larger wind loads, the design will be on the safe side.

TableC.2 Recommended values of the mechanical damping δ_s for differenct constructions, according to the old Swedish handbook for wind and snow loads (Boverket, 1997)

Typ av konstruktion	δ_m
Metallkonstruktioner, t. ex. stålskorstenar, utan installationer och sekundära delar utöver manteln	$0{,}015 \leq \delta_m \leq 0{,}02$
Metallkonstruktioner, t. ex. stålskorstenar, med installationer och sekundära delar utöver manteln	$0{,}02 \leq \delta_m \leq 0{,}03$
Fackverksmaster[1] med - svetsade förband eller friktionsförband - skruvförband	 0,015 $0{,}02 \leq \delta_m \leq 0{,}06$
Betongkonstruktioner, t. ex. betongskorstenar	$0{,}03 \leq \delta_m \leq 0{,}05$
Höga husbyggnader med stålstomme	$\delta_m \leq 0{,}06$
Höga husbyggnader med betongstomme	$\delta_m \leq 0{,}09$
Murverkskonstruktioner	$\delta_m \leq 0{,}20$
Träkonstruktioner utan mekaniska förband	$\delta_m \leq 0{,}06$
Träkonstruktioner med mekaniska förband	$\delta_m \leq 0{,}09$

Turbulence intensity

$$I_v(z) = \frac{k_l}{c_0(z) \cdot ln(\frac{z}{z_0})} \quad z_{min} \leq z \leq z_{max} \qquad \text{(B.18)}$$

$$I_v(z) = \frac{k_l}{c_0(z) \cdot ln(\frac{z_{min}}{z_0})} \quad z \leq z_{min} \qquad \text{(B.19)}$$

where:

k_l is the turbulence factor, 1

$c_0(z)$ is the orography factor, 1

Appendix C1 Geometry study: Perspective view of the 25 typical geometries

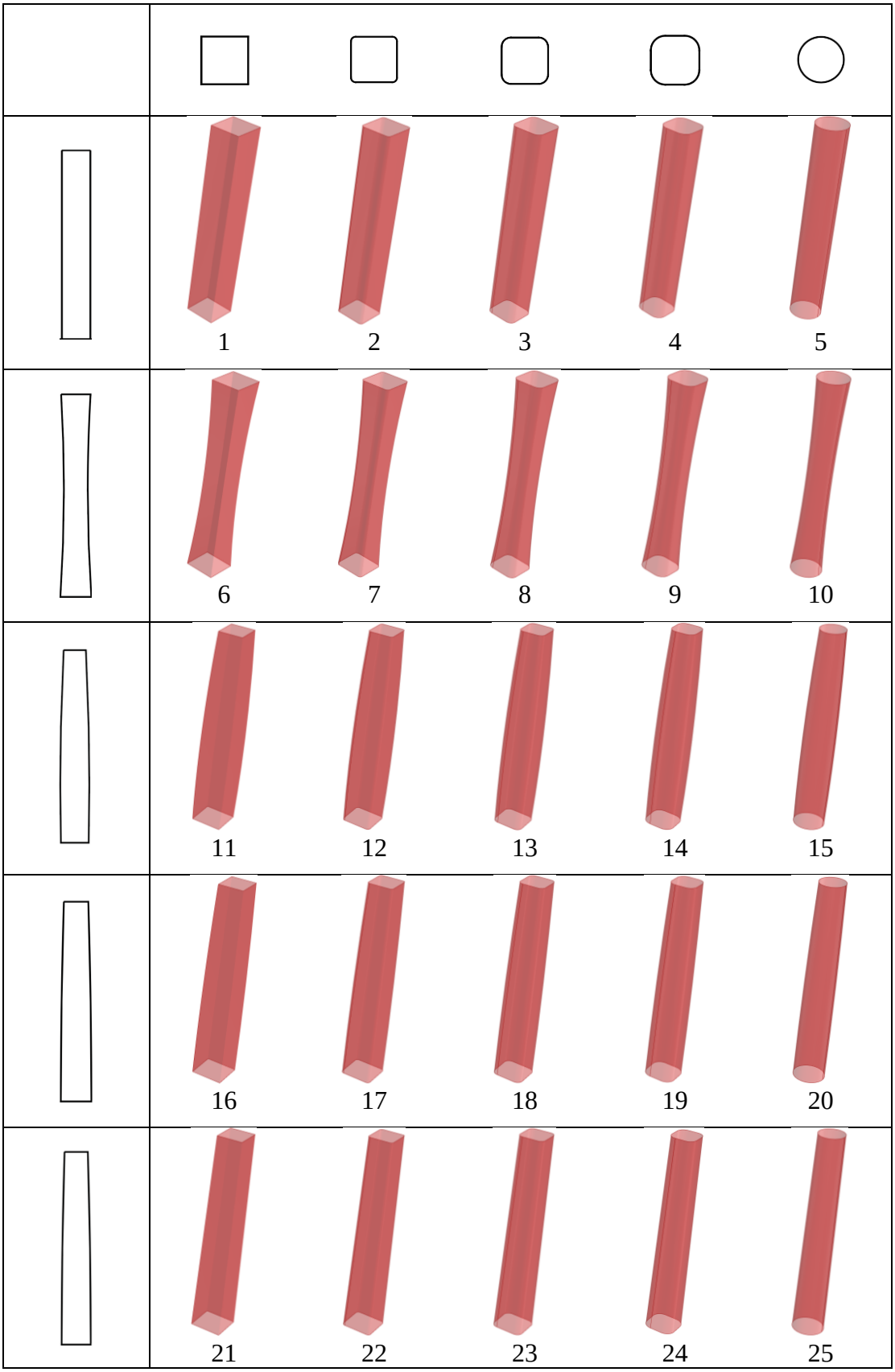

Appendix C2 Geometry study: Convergence study for FEM analysis

A convergence study with regards to the mesh sizes were conducted. For the models with only a single point on the top, the ratio of number of quads in vertical and peripheral direction was kept to 5/3 to keep the proportion of element sides to be 1. The resolution of slabs was chosen to be 1m.

Convergence studies for both the average nodal displacements for the whole structure and the top displacement in force-acting direction were conducted, with regards to the mesh resolution of the tube. The study shows that the convergence error for the top displacement is already lower than 5% with resolution around 8m while the average displacement begins to converge when the resolution is approaching 2m. For the mesh with resolution of 2m the errors drop down to lower than 1%. Meshes with size 2m is sufficient for the analysis. While the resolution changing from 1m to 0.5m there are almost no differences in the results for both average and maximal displacement. Meshes with size 1m (Number of quads 200 x 120) were chosen for the calculation.

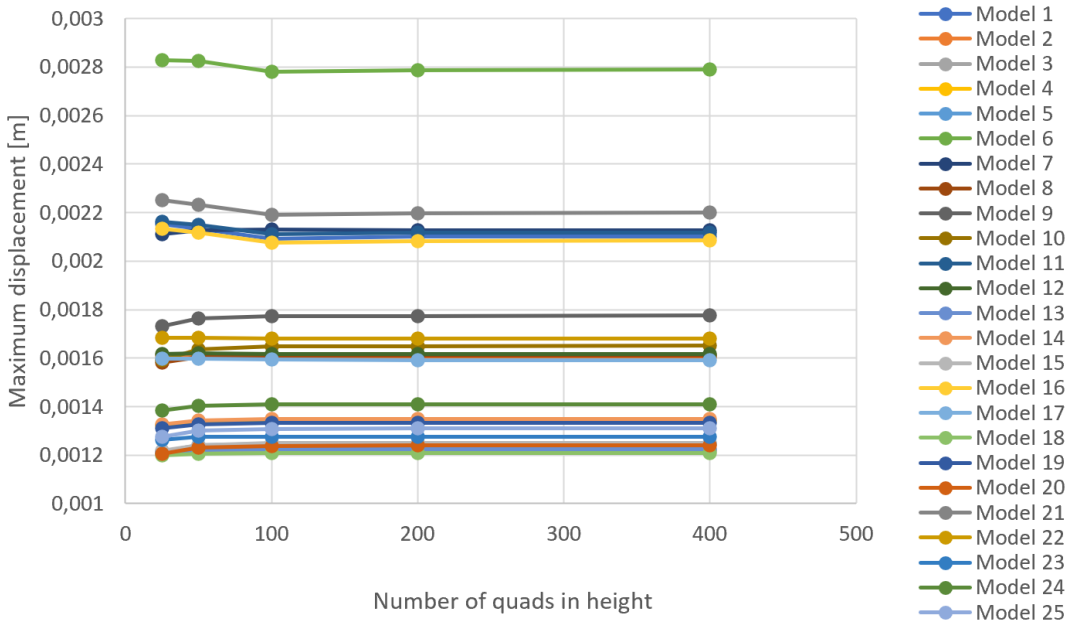

Figure C2.1 Convergence study for maximum displacement, for models with one single load on the top

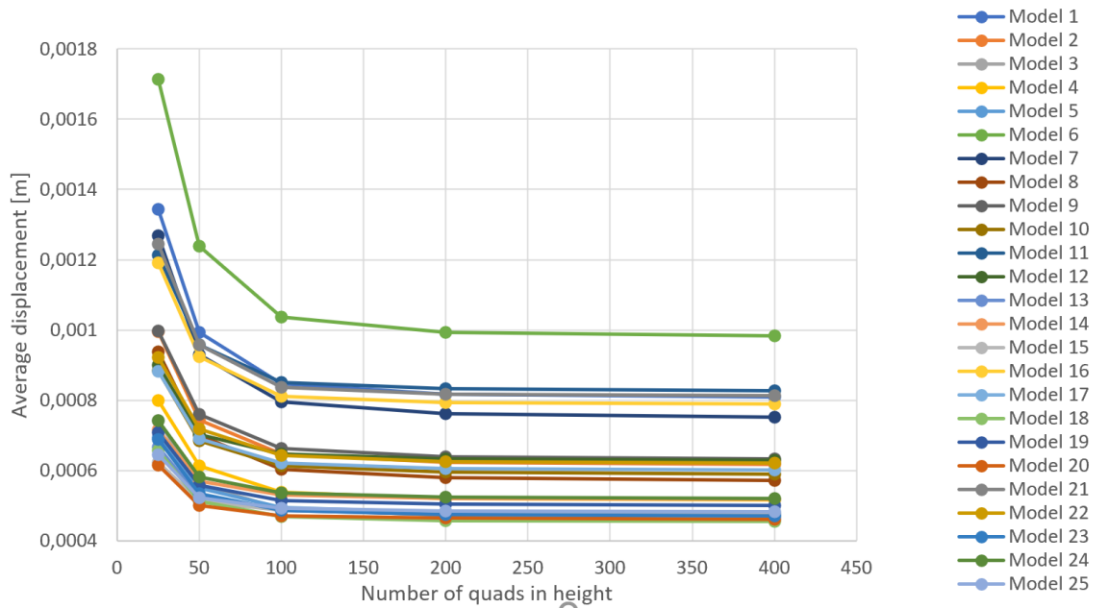

Figure C2.2 Convergence study for average displacement, for models with one single load on the top

For the structural models with distributed loads over the heights, where the slabs on all the floors are supposed to be modeled. Because all the nodes on the boundaries of the slabs need to be included in the element of the tube for full interaction, the meshes for the tube were generated by the component *Mesh breps*. Because of this the sizes of meshes on the tube are limited by the height of each floor level 3.2m. It was proved that a mesh resolution of 1m for both slabs and the tube is sufficient to get reliable results. Take model 25 for example, as shown in figure C2.3.

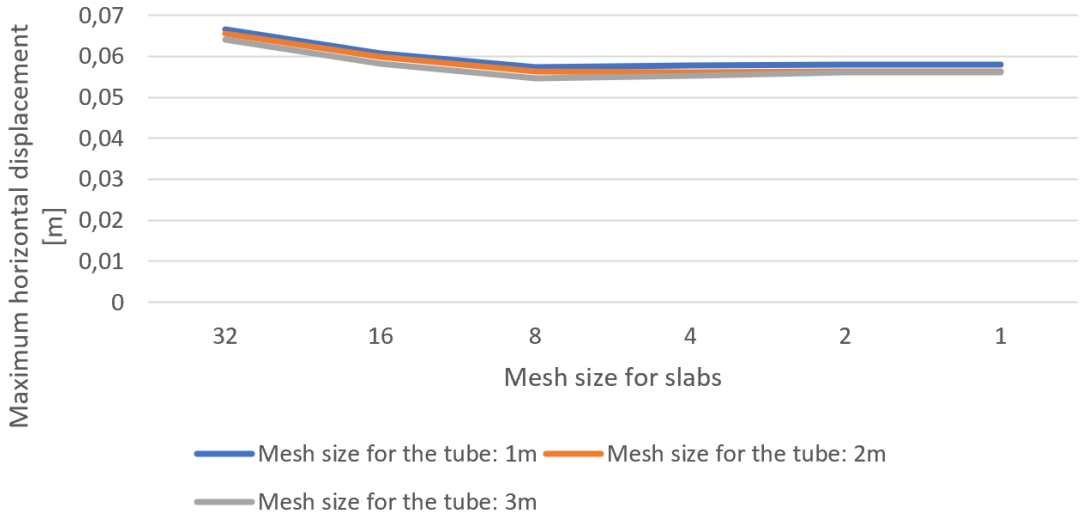

Figure C2.3 Convergence study for maximum displacement, for Model 25 with distributed loads over all stories regarding mesh size for slabs

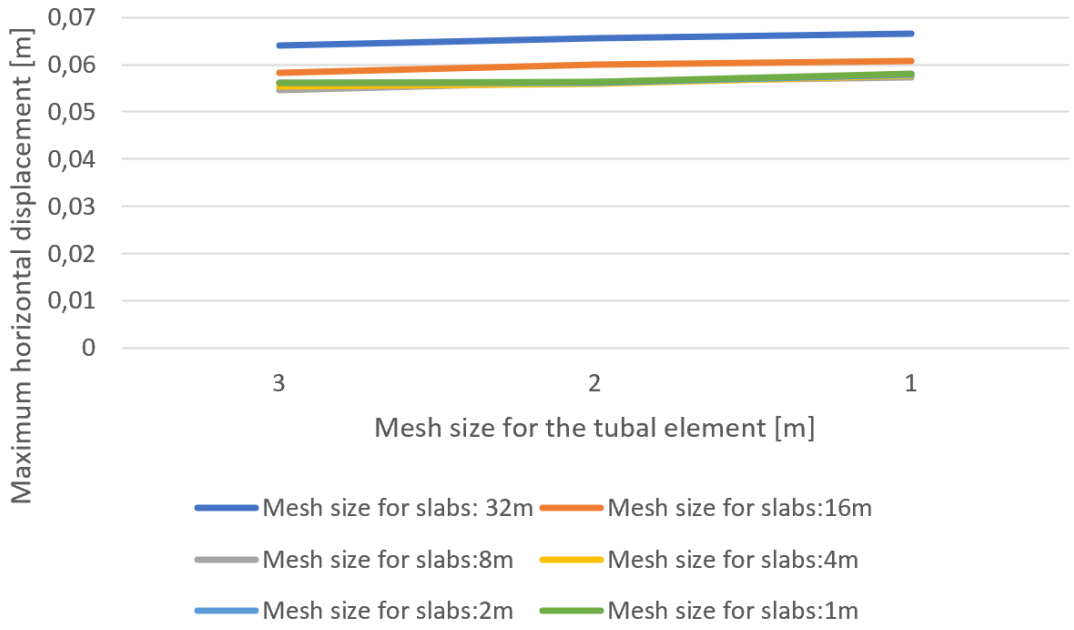

Figure C2.4 Convergence study for maximum displacement, for Model 25 with distributed loads over all stories regarding mesh size for the tube

From the example of Model 25 it is observed that when the mesh resolution for slabs is equal or smaller than 8m the results converge already. This is the same cases for all other models as well. In the FEM analysis, the mesh resolution for both slabs and the tube were set to 1m, which can be considered sufficient to get reliable results.

Appendix C3 Geometry study: Verification of FE models

Hand calculation was done to check whether the FE models are correctly built. The lateral displacements were calculated for building, regarded as a beam subjected to bending, with square respective circular cross section when they are subjected to a point load of 1400kN respective 500kN.

Table C3.1 Comparison of the results from hand calculation and FEA

	Cross section	F	I	u_beam	u_FEM	Difference
1. Square	30x30 m t: 50cm	1400	$9 \cdot 10^{3}$	$1.975 \cdot 10^{-3}$	$2 \cdot 10^{-3}$	-1.2%
2. Circle	d: 30m t: 50cm	500	$5 \cdot 310^{3}$	$1.198 \cdot 10^{-3}$	$1.25 \cdot 10^{-3}$	-4.2%

The differences of the results from hand calculation and FEM analysis are smaller than 5%. The results from hand calculation are slightly smaller in both cases. This can be explained by that in the hand calculation the shear deformation was ignored.

Other control like the reaction force and the loads acting on the structure has also been checked for both the models with one single point load and distributed loads.

The sum up of the reaction forces and the foundation moment from FE models and the hand calculation were compared as well to make sure the model were correctly built.

Appendix C4 Geometry study: Control of the validity of the simplified models in evolutionary design

In the evolutionary design, different structural models and different materials were applied. If the results differ too much from the general method, the optimization will not be as reliable as it supposed to be due to this further simplification in modelling. Since the optimized geometry from the evolutionary design process will thereafter be analyzed together with all other models in the general way again, the only consequence is that there might be other better geometries which are missed. How these factors affect the results of optimization is assessed in this appendix.

Table C4.1 Difference assignment in the loads and material properties for general analysis and evolutionary design

	Load	Material property	
		E	G
Modelling for general analysis	Distributed load acting on all stories	10480 MPa	2278MPa
Specific modelling for evolutionary design	Point load on the top story	210000MPa	80760MPa

Figure C4.1 shows how this difference in modelling leads to different results in maximum horizontal displacement. When the 25 typical models modeled in the same as for evolutionary design, the curve for displacement shifts downwards. This is probably because of the large modulus of elasticity that was assigned in the evolutionary design.

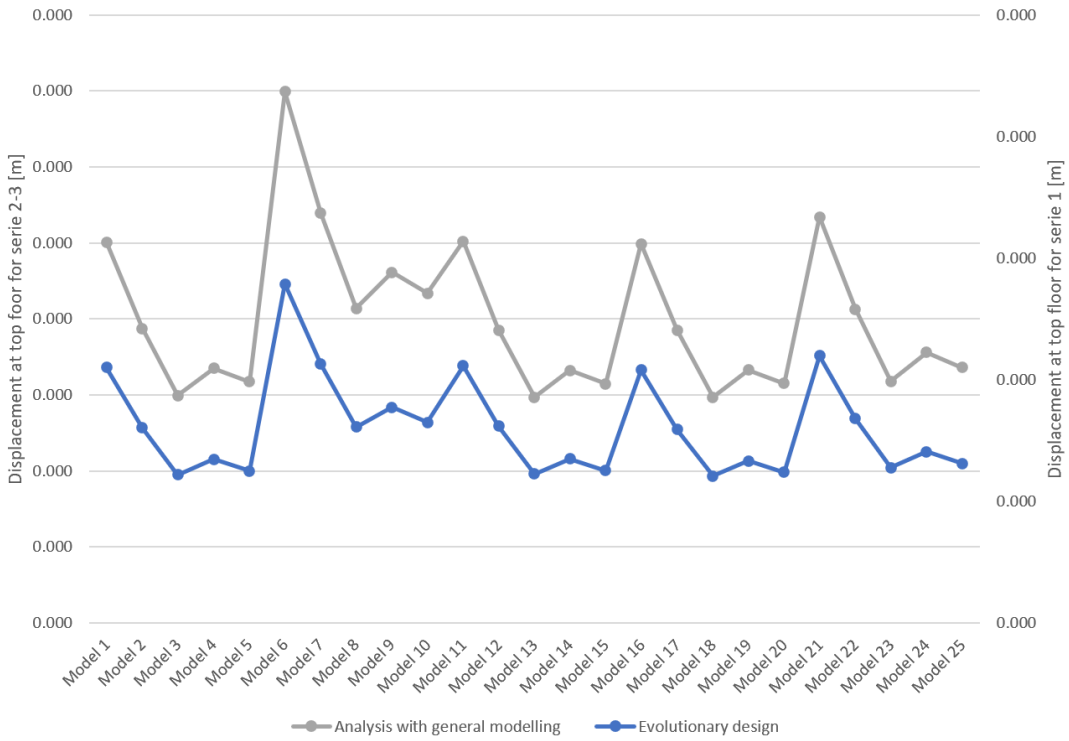

Figure C4.1 The maximum displacement for 25 typical models when they are modeled in the same way as the general analysis and when modeled in the same way as for the evolutionary design

Since it is the relative values of the lateral displacement, or the comparison between different geometries, that is more interesting, the 25 alternatives are ranked in Table C4.2 below.

Table C4.2 Ranking of 25 geometries with regards to the two different ways

Ranking	General analysis	Analysis for evolutionary design
1–5	Model 18	Model 13
	Model 3	Model 18
	Model 13	Model 3
	Model 20	Model 15
	Model 5	Model 20
6–10	Model 15	Model 5
	Model 23	Model 23
	Model 25	Model 14
	Model 19	Model 19
	Model 4	Model 4
11–15	Model 14	**Model 25**
	Model 24	Model 24
	Model 17	Model 12
	Model 2	Model 17
	Model 8	Model 2
16–20	Model 12	Model 22
	Model 10	Model 8
	Model 22	Model 10
	Model 9	Model 9
	Model 16	Model 16
21–25	Model 1	Model 1
	Model 11	Model 11
	Model 7	Model 21
	Model 21	Model 7
	Model 6	Model 6

The ranking in Table C4.2 shows that the different way to model in the evolutionary design can slightly influence the exact ranking places, but in general the influence is quite minor. Only the place for Geometry 25 changes equal or more than 3 places. Since during the process of the evolutionary design, the trend, the properties of good genes, rather than the exact parameters plays a more important role as well, this simplification and derivation in modelling for the evolutionary design can be accepted.

Appendix C5 Geometry study: Results for evolutionary optimization

Table C5.1 *Design examples from different generations*

Generation	Displacement				Area					Geometry-controling parameter			
	Top displacement	Normalized top displacement	Average displacement	Normalized average displacement	Rental area	Normalized rental area	Footprint area	Minimim Floor area	Maximum Floor Area	r	a	s1	s2
10	0,001209	1,000	0,000511	1,000	48164	1,00	848	559	866	6,309	44,0	1,01	0,80
	0,001209	1,000	0,000516	1,010	48423	1,01	848	572	866	6,316	43,0	1,01	0,81
	0,001212	1,002	0,000511	1,000	47847	0,99	847	546	867	6,309	44,0	1,01	0,79
	0,001212	1,002	0,000511	1,000	47832	0,99	847	546	865	6,418	43,0	1,01	0,79
	0,001212	1,002	0,000512	1,002	48103	1,00	847	559	865	6,414	45,0	1,01	0,80
	0,001213	1,003	0,000513	1,004	48097	1,00	847	559	865	6,416	43,0	1,01	0,80
	0,001214	1,004	0,000511	1,000	47770	0,99	860	565	864	6,436	42,0	1,00	0,80
	0,001215	1,005	0,000513	1,004	48069	1,00	846	558	864	6,465	44,0	1,01	0,80
	0,001218	1,007	0,000516	1,010	48178	1,00	831	550	865	6,411	44,0	1,02	0,80
	0,001283	1,061	0,000531	1,039	44213	0,92	865	561	865	6,409	44,0	0,96	0,80
4-9	0,001211	1,002	0,000511	1,000	47843	0,99	847	546	865	6,4	43,0	1,01	0,79
	0,001211	1,002	0,000512	1,002	48114	1,00	847	559	865	6,309	45,0	1,01	0,80
	0,001214	1,004	0,000518	1,014	48352	1,00	847	572	864	6,433	43,0	1,01	0,81
	0,001212	1,002	0,000512	1,002	48111	1,00	847	559	865	6,396	44,0	1,01	0,80
	0,001213	1,003	0,000518	1,014	48376	1,00	847	572	865	6,396	44,0	1,01	0,81
	0,001215	1,005	0,000519	1,016	48608	1,01	847	585	864	6,443	41,0	1,01	0,82
3	0,001427	1,180	0,000524	1,025	48943	1,02	831	589	865	6,385	45,0	1,02	0,83
	0,001427	1,180	0,000617	1,207	46300	0,96	648	505	848	7,818	43	1,11	0,86
2	0,001221	1,010	0,000524	1,025	48943	1,02	831	589	865	6,385	45	1,02	0,83
	0,002005	1,658	0,000844	1,652	37214	0,77	402	230	778	11,91	49	1,32	0,7
1	0,001262	1,044	0,000546	1,068	49095	1,02	794	604	860	6,842	55	1,04	0,86
	0,002415	1,998	0,001089	2,131	37275	0,77	283	240	836	8,664	163	1,36	0,84
0	0,001262	1,044	0,000546	1,068	49095	1,02	794	604	860	6,842	55	1,04	0,86
	0,003743	3,096	0,00137	2,681	27440	0,57	893	310	893	2,764	99	0,61	0,72
	0,022247	18,401	0,007689	15,047	29030	0,60	50	50	751	13,7	1	1,41	0,85
	0,002579	2,133	0,00174	3,405	37011	0,77	241	144	855	7,205	169	1,29	0,66
	0,002012	1,664	0,000768	1,503	29637	0,62	727	357	727	14,181	140	0,73	0,7
	0,001598	1,322	0,000689	1,348	42819	0,89	534	366	836	8,664	163	1,04	0,79

Examples from generation 0

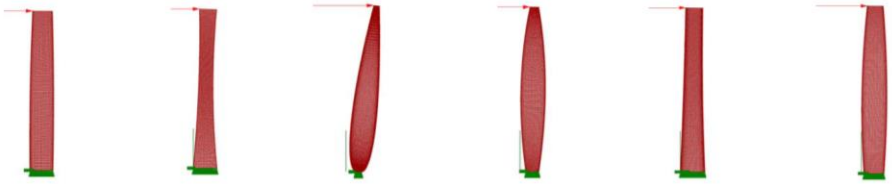

Smallest top displacent its generation Largest top displacement in its generation

Mesh size: U: 100 V:60 Resolution of meshes on slab:1

Table C5.2 The optimized geometry from evolutionary design done with help of Galapagos and the adjusted one based on it

	Parameter				**Result**		
	r [m]	**a[m]**	**s1[-]**	**s2[-]**	**u_av[m]**	**u_max[m]**	**A [m^2]**
The optimized geometry from optimization by Galapagos	6,32	43,0	1,01	0,8	0,000516	0,0012	48 423
The adapted geometry based on the optimized geometry	6	44	1	0,8	0,000457	0,0011	48 052

In the evolutionary design, sparser meshes of 2m are applied to save computation time. Convergence study shows that both the maximum displacement and the average displacement meshes are fine enough.

Appendix C6 Geometry study: Normalization and scaling of the results for primary evaluation

The values of the rental areas, masses of material consumed for unit area, structural stiffness per mass material and the lateral displacement for all alternatives were normalized by being divided by those of Geometry 1. Thereafter each geometry will be given a scale according to the corresponding normalized values. The scales for the normalized values and the scales given for each geometry are presented in Table C6.1 to Table C6.8 below.

Table C6.1 Scale factors for rental areas

Normalized rental area	Scale
0.4- 0.52	1
0.52 - 0.64	2
0.64 – 0.76	3
0.76 – 0.88	4
0.88 – 1	5

Table C6.2 Scales for all geometries related to the rental area

	Rental area [m^2]	Normalized value	Scale
Model 1	55 800	1	5
Model 2	55 321	0,99	5
Model 3	53 884	0,97	5
Model 4	51 489	0,92	5
Model 5	43 825	0,79	4
Model 6	39 477	0,71	3
Model 7	39 137	0,70	3
Model 8	38 119	0,68	3
Model 9	36 425	0,65	3
Model 10	31 003	0,56	2
Model 11	49 934	0,89	5
Model 12	49 505	0,89	5
Model 13	48 218	0,86	4
Model 14	46 075	0,83	4
Model 15	39 217	0,70	3
Model 16	49 070	0,88	4
Model 17	48 649	0,87	4
Model 18	47 385	0,85	4
Model 19	45 280	0,81	4
Model 20	38 540	0,69	3
Model 21	45 622	0,82	4
Model 22	45 231	0,81	4
Model 23	44 056	0,79	4
Model 24	42 098	0,75	3
Model 25	35 832	0,64	2
Hyperboloid	22 572	0,40	1
Optimized	48 245	0,86	4

Table C6.3 Scale factors for mass of material per unit area

Normalized mass of material per area	Scale
1.0-1.03	5
1.03-1.12	4
1.12-1.20	3
1.20-1.29	2
1.29-1.37	1

Table C6.3 Scales for all geometries related to the mass of material per unit area

	Mass per area [kg/m^2]	Normalized value	Scale
Model 1	129,1	1,00	5
Model 2	124,6	0,97	5
Model 3	122,2	0,95	5
Model 4	121,9	0,94	5
Model 5	129,1	1,00	5
Model 6	153,2	1,19	3
Model 7	147,9	1,15	3
Model 8	145,1	1,12	3
Model 9	144,7	1,12	3
Model 10	153,3	1,19	3
Model 11	135,8	1,05	4
Model 12	131,0	1,01	5
Model 13	128,5	1,00	5
Model 14	128,2	0,99	5
Model 15	135,8	1,05	4
Model 16	137,0	1,06	4
Model 17	132,2	1,02	5
Model 18	129,7	1,00	5
Model 19	129,4	1,00	5
Model 20	137,0	1,06	4
Model 21	142,1	1,10	4
Model 22	137,1	1,06	4
Model 23	134,5	1,04	4
Model 24	134,2	1,04	4
Model 25	142,1	1,10	4
Hyperboloid	177,4	1,37	1
Optimized	128,3	0,99	5

Table C6.5 Scale factors for stiffness per mass material

Normalized stiffness per mass material	Scale
1-1.17	5
1.17-1.36	4
1.36-1.56	3
1.56-1.75	2
1.75-1.95	1

Table C6.6 Scales for all geometries related to the stiffness per mass material

	Mass·displacement [·10^5kg·m]	Normalized value	Scale
Model 1	4,93	1,00	5
Model 2	4,98	1,01	5
Model 3	5,16	1,05	5
Model 4	5,47	1,11	5
Model 5	6,56	1,33	4
Model 6	6,52	1,32	4
Model 7	6,60	1,34	4
Model 8	6,84	1,39	3
Model 9	7,25	1,47	3
Model 10	8,64	1,75	1
Model 11	4,86	0,99	5
Model 12	4,92	1,00	5
Model 13	5,09	1,03	5
Model 14	5,40	1,10	5
Model 15	6,47	1,31	4
Model 16	4,80	0,97	5
Model 17	4,85	0,98	5
Model 18	5,03	1,02	5
Model 19	5,33	1,08	5
Model 20	6,39	1,30	4
Model 21	5,09	1,03	5
Model 22	5,15	1,04	5
Model 23	5,34	1,08	5
Model 24	5,65	1,15	5
Model 25	6,77	1,37	3
Hyperboloid	9,60	1,95	1
Optimized	4,98	1,01	5

Table C6.7 Scale factors for lateral displacement

Normalized maximum displacement	Scale
0.52-0.68	5
0.68-0.84	4
0.84-1.01	3
1.01-1.17	2
1.17-1.33	1

Table C6.7 Scales for all geometries related to the lateral displacement

	maximum displacement [m]	Normalized value	Scale
Model 1	0,096	1,00	3
Model 2	0,072	0,75	4
Model 3	0,055	0,57	5
Model 4	0,061	0,64	5
Model 5	0,058	0,60	5
Model 6	0,128	1,33	1
Model 7	0,096	1,01	2
Model 8	0,073	0,76	4
Model 9	0,081	0,85	3
Model 10	0,077	0,80	4
Model 11	0,088	0,92	3
Model 12	0,067	0,70	4
Model 13	0,051	0,53	5
Model 14	0,056	0,59	5
Model 15	0,053	0,56	5
Model 16	0,088	0,91	3
Model 17	0,066	0,69	4
Model 18	0,050	0,52	5
Model 19	0,056	0,58	5
Model 20	0,053	0,55	5
Model 21	0,093	0,97	3
Model 22	0,070	0,73	4
Model 23	0,053	0,56	5
Model 24	0,059	0,62	5
Model 25	0,056	0,59	5
Hyperboloid	0,083	0,87	3
Optimized	0,050	0,52	5

Appendix D Combination of loads

The design loads for ultimate limit state and serviceability limit state are calculated in principle of EN1990. The loads included are dead weight, imposed load and wind loads.

Fundamental combination in ULS

$\gamma_G G_k + \gamma_{Q,1} Q_{k,1} + \gamma_{Q,i} \psi_{0,i} Q_{k,i}$, where $i > 1$ (D.1)

Characteristic combination in SLS

$G_{k,j} + Q_{k,1} + \psi_{0,i} Q_{k,i}$, where $i > 1$ (D.2)

where G is permanent load and Q_1 is the main variable load and Q_i is other variable loads.

Table D.1 Partial safety factors γ for ULS and SLS

	ULS		SLS	
	Permanent action γ_G	Variable action γ_Q	Permanent action γ_G	Variable action γ_Q
Favorable	1	0	1	0
Unfavorable	1.35	1.5	1	1

Reduction factor ψ_0 for imposed loads for office Category B (office building) is 0.7.

Appendix E ULS design of structural elements of timber

The members are assumed to be designed to be subjected to only stresses in the direction parallel to the grain direction. The general design principle is that the design load should be smaller or equal to the design capacity. This can be checked by comparing the stresses caused by design load and the design material strength. The capacity of the structural members should be verified according to EN1995-1-1. The stresses are calculated from the sectional forces, such as moments, compressive forces and tensile forces, extracted from finite element analysis done by *Karamba 3D*. The calculation was done in *Grasshopper*.

E.1 Design strength

$$f_d = k_{mod} \frac{f_k}{\gamma_M} \qquad \text{(E.1)}$$

where:

f_d	is the design strength
f_k	is the characteristic value of the strength
k_{mod}	is the modification factor related to the load duration and moisture content
γ_M	Is the partial factor for material property

Table E.1 Recommended values for γ_M for solid timber and glued laminated timber according to Eurocode 5

Material	γ_M
Solid timber	1.3
Glued laminated timber	1.25

Service class 2 and permanent action is assumed.

Table E.2 Recommended values for k_{mod} for solid timber and glued laminated timber according to Eurocode 5

Material	**Service class**	**Load-duration class**
		Permanent action
Solid timber	**2**	0.6
Glued laminated timber	**2**	0.6

E.2 Design for trusses, beams and columns

Tension parallel to the grain

$$\sigma_{t,0,d} \leq f_{t,0,d} \qquad \text{(E.2)}$$

where:

$\sigma_{t,0,d}$ is the design tensile tress along the grain
$f_{t,0,d}$ is the design tensile strength along the grain

Compression parallel to the grain

$$\sigma_{c,0,d} \leq f_{c,0,d} \quad \text{(E.3)}$$

where:
$\sigma_{c,0,d}$ is the design compressive tress along the grain
$f_{c,0,d}$ is the design compressive strength along the grain

Combined bending and axial compression

$$\left(\frac{\sigma_{c,0,d}}{f_{c,0,d}}\right)^2 + \frac{\sigma_{m,y,d}}{f_{m,y,d}} + k_m \frac{\sigma_{m,z,d}}{f_{m,z,d}} \leq 1 \quad \text{(E.4)}$$

$$\left(\frac{\sigma_{c,0,d}}{f_{c,0,d}}\right)^2 + k_m \frac{\sigma_{m,y,d}}{f_{m,y,d}} + \frac{\sigma_{m,z,d}}{f_{m,z,d}} \leq 1 \quad \text{(E.5)}$$

where:
$\sigma_{c,0,d}$ is the design compressive stress along the grain
$f_{c,0,d}$ is the design compressive strength along the grain
$\sigma_{m,y,d}$, $\sigma_{m,z,d}$ are the design bending tresses about the principal axes
$f_{m,y,d}$, $f_{m,y,d}$ are the design bending strengths along the grain
k_m =0.7 for rectangular sections for solid timber, glued laminated timber and LVL
=1 for other cross sections or for other wood-based structural products

Shear

$$\tau_d \leq f_{v,d} \quad \text{(E.6)}$$

where:
τ_d is the design shear tress
$f_{v,d}$ is the design shear strength

For members in bending, the influence of cracks is taken into account by using effective width.

$$b_{ef} = k_{cr} b \quad \text{(E.7)}$$

k_{cr} =0.67 for glued laminated timber
=1 for other wooden products
b is the actual width of the cross sections of the members

Stability for columns and trusses subjected to either compression or combined compression and bending

$$\lambda_{rel,y} = \frac{\lambda_y}{\pi}\sqrt{\frac{f_{c,0,k}}{E_{0.05}}} \quad \text{(E.8)}$$

$$\lambda_{rel,z} = \frac{\lambda_z}{\pi}\sqrt{\frac{f_{c,0,k}}{E_{0.05}}} \quad \text{(E.9)}$$

where:

$\lambda_{rel,y}$, λ_y	are the slenderness ratios corresponding to bending about y-axis
$\lambda_{rel,z}$, λ_z	are the slenderness ratios corresponding to bending about z-axis
$f_{c,0,k}$	is the characteristic strength in the direction along the grains
$E_{0.05}$	is the modulus of elasticity parallel to the grains

When both $\lambda_{rel,y}$ and $\lambda_{rel,z}$ are smaller than 0.3, no check corresponding instability need to be checked. According to *Swedish Wood* (2016):

$$\lambda_y = \frac{l_e}{i_y} \quad \text{(E.10)}$$

$$\lambda_z = \frac{l_e}{i_z} \quad \text{(E.11)}$$

$$i_y = \sqrt{\frac{I_y}{A}} \quad \text{(E.12)}$$

$$i_z = \sqrt{\frac{I_z}{A}} \quad \text{(E.13)}$$

where:

λ_y, λ_z	are the slenderness ratios corresponding to bending about y- and z-axes
i_y, i_z	are the radius of gyration about y- and x-axes
l_e	is the effective buckling length in compression.
I_y, I_z	is the second moment of area about y- and z-axes
A	is the area of the cross section

The calculation shows that the relative slenderness ratio for all members about both y- and z-axes are smaller than 0.3 and therefore no member is subjected to the risk of instability. This is because large cross sections are required to resist the combined wind loads and gravity loads and at the same time the members are anchors at each floor levels, meaning a short buckling length. Therefore, no further verification due to instability is needed.

F.3 Design for core walls

The core walls are supposed to be constructed with CLT30 members, where the loads are considered to be borne by the directions parallel to the grains. (Swedish wood, 2019). For structural design of a CLT component, the compressive, tensile and bending stresses for layers in both directions need to be verified.

The core is subjected to the gravity loads and the wind loads, which are mainly carried by the layers with grain parallel to the vertical directions by bending and compression along the grain direction and shear resistance globally. Since the focus of

this study lies in the exterior structural system and the main purpose of the core is to carry the gravity loads, though it will contribute to the stabilizing. For simplification the wall members are treated as a homogenous component as a whole and no detailed design of the layers are included. An identical cross section of 500mm for diagrid structures and 800mm for the braced frame structure was chosen and the design in-plane compressive/tensile strengths was assumed to be 11.5MPa in both directions. The core walls were modeled as shell-element in *Karamba 3D* and as isotropic material. Because in a CLT member only layers with grains in the longitudinal direction are assumed to carry loads, the real design thickness might be twice as much as those mentioned.

The calculation of stresses and utilization of shell elements in *Karamba 3D* is based on the von Mises stresses, which is applicable for steel material and is not really the case for timber material, where the stresses in each direction need to be verified. However, this can give some insight in the magnitude of the stresses.

The sectional forces can be extracted from the results of FEM analysis conducted in *Karamba 3D*. For design the stiffness and the strength capacity can be influenced not only by the timber material, but also the total number of layers in the surface layer direction and the cross direction, as well as the thickness of them. These can be designed out of the sectional forces in each direction obtained from the finite element analysis. The design process for CLT element follows the procedures presented in Section 3.3.5 in *The CLT handbook* published by Swedish Wood (2017).

Check of buckling in walls

For the members subjected to the compression or combined compression bending there is risk for buckling. It is better to avoid occurrence of buckling during the design for higher utilization of the total capacity of the cross sections.

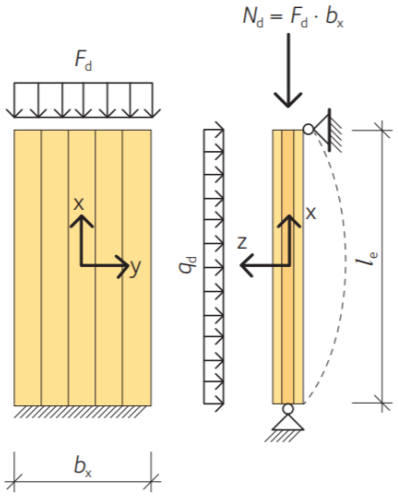

Figure E.1 CLT wall element subjected to axial compression and bending. Figure 3.27 in The CLT handbook (Swedish Wood, 2017)

No further check is needed to be done if the relative slenderness ratio $\lambda_{rel,y}$ is equal or smaller than 0.3.

$$\lambda_{rel,y} = \frac{\lambda_y}{\pi}\sqrt{\frac{f_{c,0,xlay,k}}{E_{0,x,05}}} \quad \text{(E.14)}$$

where:

$\lambda_{rel,y}$, λ_y	are the slenderness ratios corresponding to bending about y-axis
$f_{c,0,xlay,k}$	is the characteristic strength in the direction along the grains
$E_{0,x,05}$	is the modulus of elasticity parallel to the grains

$$\lambda_y = \frac{L}{i_{x,ef}} \quad \text{(E.15)}$$

$$i_{x,ef} = \sqrt{\frac{I_{x,ef}}{A_{x,net}}} \quad \text{(E.16)}$$

$$E_{0,x,05} = k \cdot E_{0,x,mean} \quad \text{(E.17)}$$

$$k = 1 - \frac{0.328}{\sqrt{\frac{2b_x}{0.15} - 1}} \quad \text{(E.18)}$$

where:

$i_{x,ef}$	is the effective radius of gyration about x- axis
L	is the buckling length
$I_{x,ef}$	is the effective moment of inertia about x- axis
$A_{x,net}$	is the net cross section area along x-axis
b_x	is in meter and as shown in Figure F.1

The connections between elements in vertical directions are supposed to be fixed and supposed to be supported by the floor slabs. The buckling length is assumed to be the floor height multiplied by a factor of 0.8. b_x is set to 10m. According to the calculation, the relative slenderness ratio is about 0.256. There is no risk of buckling.

Appendix F Calculation of peak acceleration

The calculation of the peak acceleration follows the procedures given by EKS11.

$$\ddot{X}_{max}(z) = k_p \cdot \sigma_{\ddot{X}}(z) \qquad \text{(F.1)}$$

where:

$\ddot{X}_{max}(z)$	is the peak acceleration
k_p	is the peak factor, calculated by expression B.7 in Appendix B
$\sigma_{\ddot{X}}(z)$	is the standard deviation of the acceleration

The standard deviation of the acceleration is calculated by expression:

$$\sigma_{\ddot{X}}(z) = \frac{3I_v(h)Rq_m(h)bc_f\phi_{1,x}}{m} \qquad \text{(F.2)}$$

where:

$I_v(h)$	is the wind turbulence intensity at the height h
R	is the factor for resonance response, see equation (B.11) in Appendix B
$q_m(h)$	is the mean wind velocity pressure at the height h
b	is the width of the building
c_f	is the force factor, see Appendix A
$\phi_{1,x}$	is the first mode shape
m	is the mass per unit length of the top 1/3 of the building

$$\phi_{1,x} = (\frac{z}{h})^{\xi} \qquad \text{(F.3)}$$

where:

z	is the height for the top floor, taken as 200m in calculation
h	is the height of the height of the building
ξ	is the exponent for mode shape for structure fixed to the ground

$$q_m(h) = \frac{1}{2}\rho {v_m}^2(h) \qquad \text{(F.4)}$$

where:

ρ	Is the air density, 1.25kg/m^3
$v_m(h)$	is the mean wind speed at the height h, see equation (B.14) in Appendix B

Appendix G Stresses for trusses/columns for structural proposals

G.1 The convex structures

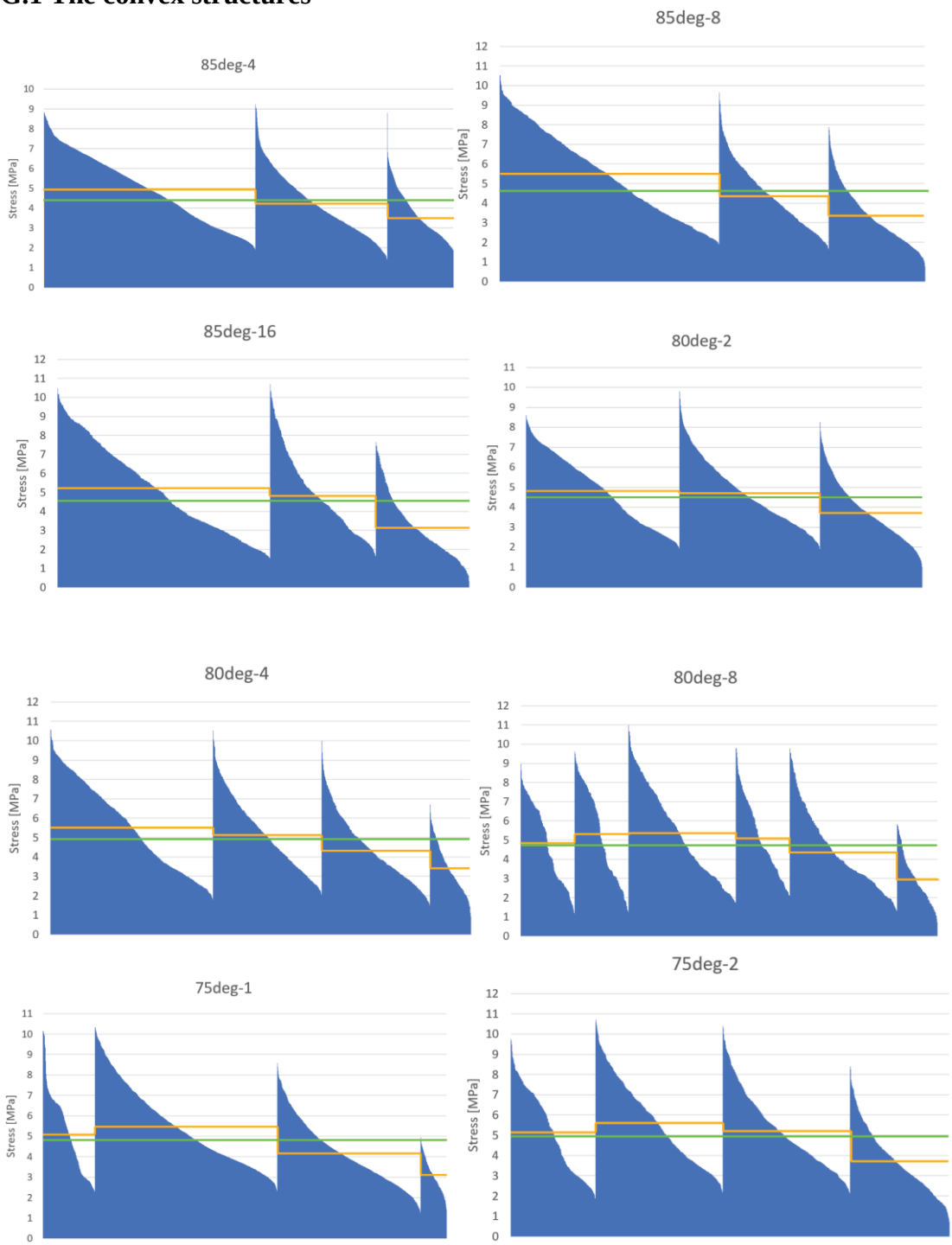

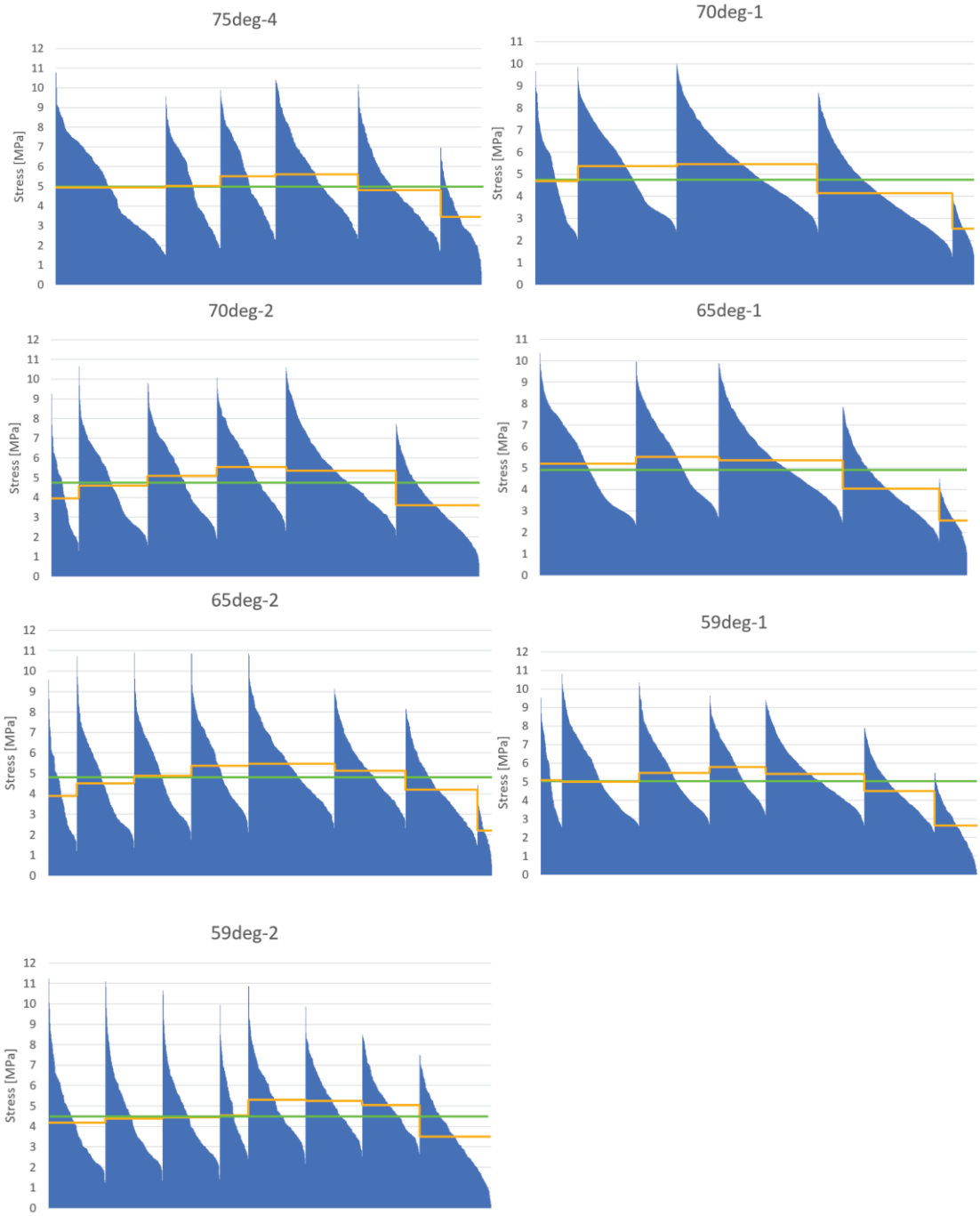
75deg-4
70deg-1
70deg-2
65deg-1
65deg-2
59deg-1
59deg-2
Stress [MPa]

G.2 The hyperboloid structures

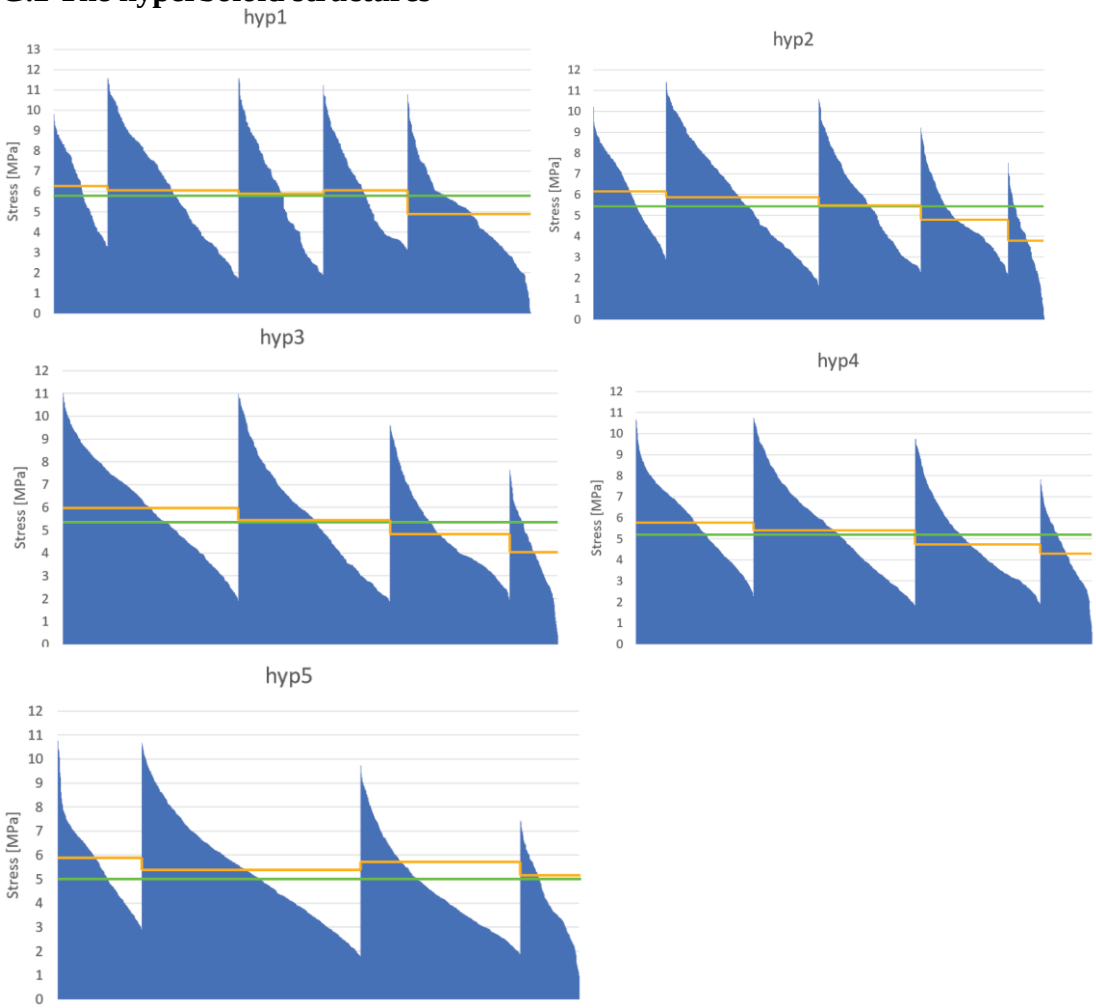

G.3 The braced frame structure

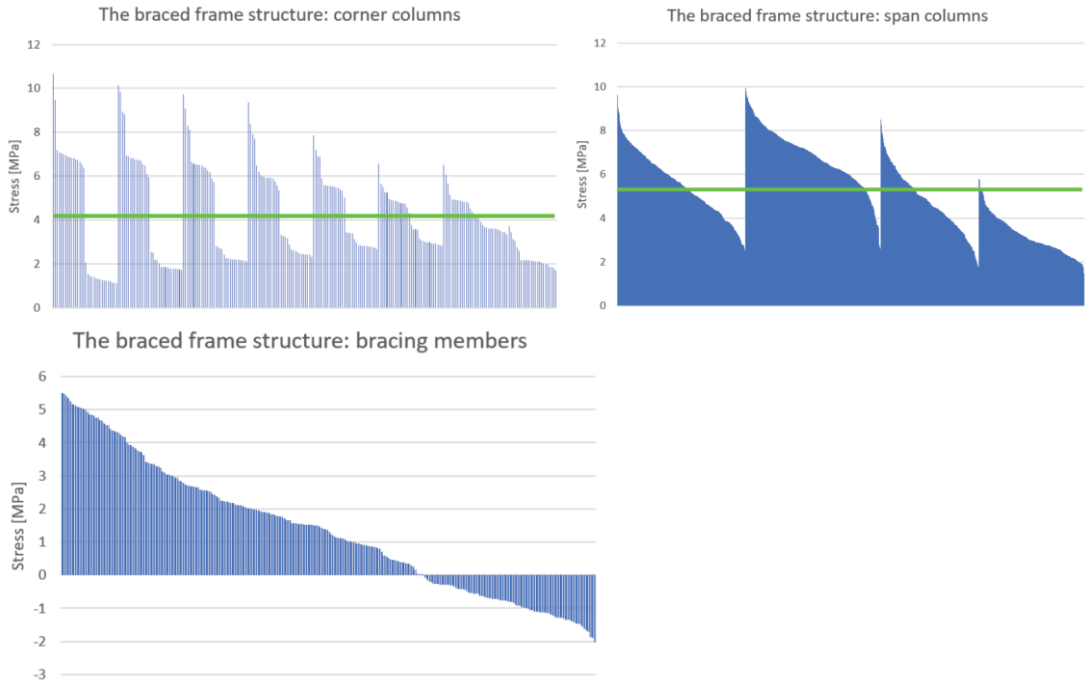

Appendix H Calculation of timber connection

The capacity for connection were calculated according to EN1995-1-1 and (Johannesson & Vretblad, 2011) and performed in Mathcad. All the expressions and figures in this Appendix are retrieved from EN1995-1-1 and (Johannesson & Vretblad, 2011)

Steel's plate tension strength compared with the tension strength for connection from the result.

$$N_t, Rd = A * \frac{f_y}{\gamma_{M0}} \quad \text{(H.1)}$$

where:

f_{yk}	is the yield strength of steel
N_t, Rd	is the tension strength
A	is the area of the plate thickness of the plate times width of the plate
γ_{M0}	is the partial factor for material properties

Steel's plate compression strength compared with the compression strength for connection from the result. The cross-section class was needed, see H.1

Table H1 Classification of steel members

Classification of steel members according to maximum width-to-thickness ratios				
Class	SANS 10162-1		EN 3-1-1	
	Flanges	Webs	Flanges	Webs
Members in axial compression – I, H, PFC & L sections				
1			$\frac{c_1}{t_f} \le 9\epsilon$	$\frac{c_2}{t_w} \le 33\epsilon$
2			$\frac{c_1}{t_f} \le 10\epsilon$	$\frac{c_2}{t_w} \le 38\epsilon$
3	$\frac{b_1}{t_f} \le \frac{200}{\sqrt{f_y}}$	$\frac{h-2t_f}{t_w} \le \frac{670}{\sqrt{f_y}}$	$\frac{c_1}{t_f} \le 14\epsilon$	$\frac{c_2}{t_w} \le 42\epsilon$
Members in flexural compression – I, H & PFC sections				
1	$\frac{b_1}{t_f} \le \frac{145}{\sqrt{f_y}}$	$\frac{hw}{t_w} \le \frac{1\,100}{\sqrt{f_y}\left(1-\frac{0.39C_u}{ØC_y}\right)}$	$\frac{c_1}{t_f} \le \frac{9\epsilon}{\alpha}$	$\frac{c_2}{t_w} \le 72\epsilon$
2	$\frac{b_1}{t_f} \le \frac{170}{\sqrt{f_y}}$	$\frac{hw}{t_w} \le \frac{1\,700}{\sqrt{f_y}\left(1-\frac{0.61C_u}{ØC_y}\right)}$	$\frac{c_1}{t_f} \le \frac{10\epsilon}{\alpha}$	$\frac{c_2}{t_w} \le 83\epsilon$
3	$\frac{b_1}{t_f} \le \frac{200}{\sqrt{f_y}}$	$\frac{hw}{t_w} \le \frac{1\,900}{\sqrt{f_y}\left(1-\frac{0.65C_u}{ØC_y}\right)}$	$\frac{c_1}{t_f} \le \frac{14\epsilon}{\alpha}$	$\frac{c_2}{t_w} \le 124\epsilon$
Angle in axial compression				
3	As per I, H and PFC sections		$\frac{h}{t_f} \le 15\epsilon : \frac{b+h}{2t_f} \le 11.5\epsilon$	
$\epsilon = \sqrt{\frac{235}{f_y}}$; α = proportion of section in compression (see EN 3-1-1 Table 5.2)				

where:

c	is the width of the steel plate
ε	is calculated as in the table H.1
f_{yk}	is the yield strength of steel

With embedded in steel connection therefore no requirement to check instability of the steel plate.
Steel plate compression strength:

$N_c, Rd = A * \frac{f_y}{\gamma_{M0}}$ for class 1,2,3 (H.2)

$N_c, Rd = A_{eff} * \frac{f_y}{\gamma_{M0}}$ for class 4 (H.3)

where:

f_{yk}	is the yield strength of steel
N_c, Rd	is the compression strength
A	is the area of the plate thickness of the plate times width of the plate
γ_{M0}	is the partial factor for material properties
A_{eff}	is the effective are

To check if the connection has enough capacity to withstand the tension force embedding strength and yield moment strength are needed

$M_y, Rk = 0{,}3 f_{u,k}\, d^{2,6}$ (H.4)

where:

M_y, Rk	is the characteristic value for the yield moment in Nmm
$f_{u,k}$	is the characteristic tensile strength in N/mm^2
d	is the bolt diameter in mm

$f_{h,0,k} = 0{,}082\ (1 - 0{,}01d)\rho_k$ (H.5)

$f_{h,0,k}$	is the yield strength of steel
ρ_k	is the characteristic timber density in kg/mm^3
d	is the bolt diameter in mm

Axial withdrawal capacity should be taken lower value of the bolt tensile capacity or the load bearing capacity of either the washer or the steel plate. The bearing capacity of a washer calculated assuming a characteristic compressive strength on the contact area of $3Af_{c,90,k}$ (H.6)

A	is the contact area of the washer if a washer is not used but rather a steel plate then the washer diameter assumes to be minimum of $12t\ and\ 4d$
$f_{c,90,k}$	characteristic compressive strength perpendicular to grain
$12t$	t is the plate thickness
$4d$	d is the bolt diameter

The shear capacity of steel to wood connection is calculated with the failure mode f,g,h, which are the failure modes fore steel plate with any thickness as central member of a double shear connection

$$F_{v,Rk} = min \begin{Bmatrix} f_{h,1,k} t_1 d \\ f_{h,1,k} t_1 d \left[\sqrt{2 + \frac{4 M_{y,Rk}}{f_{h,1,k} d t_1^2}} - 1 \right] + \frac{F_{axRk}}{4} \\ 2{,}3 \sqrt{M_{y,Rk} f_{h,1,k} d} + \frac{F_{axRk}}{4} \end{Bmatrix} \quad \text{(H.6)}$$

Where

$F_{v,Rk}$	is the characteristic load carrying capacity per plane per fastener
$f_{h,1,k}$	is the characteristic embedment strength in timber member
t_1	is the smaller of the thickness of the timber middle member
d	is the fastener diameter
M_{yRk}	is the characteristic fastener yield moment
F_{axRk}	is the characteristic withdrawal capacity of the fasterner

The design capacity of bolt

$$F_{v,Rd} = \frac{k_{mod} F_{v,Rk}}{\gamma_M} \quad \text{(H.7)}$$

Where

$F_{v,Rd}$	is the design load carrying capacity per plane per fastener?
k_{mod}	modification factor for duration load and moisture content
$F_{v,Rk}$	is the characteristic load carrying capacity per plane per fastener?
γ_M	is the partial factor for material properties

DEPARTMENT OF ARCHITECTURE AND
ENGINEERING
CHALMERS UNIVERSITY OF TECHNOLOGY
Gothenburg, Sweden 2021
www.chalmers.se

CHALMERS
UNIVERSITY OF TECHNOLOGY